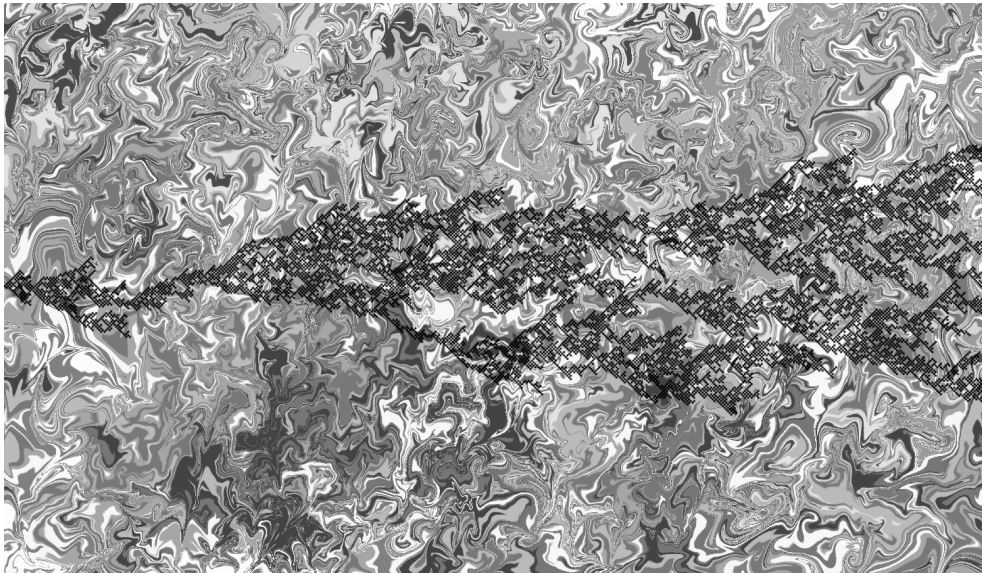# Critical Behaviour of Directed Percolation Process in the Presence of Compressible Velocity Field

Master's Thesis
(60 HE credits)

Author:

Viktor Škultéty†

Supervisors:

Juha Honkonen,
Thors Hans Hansson

Affiliation:

Fysikum, Stockholm University,
Nordic Institute for Theoretical Physics (NORDITA)

2017-04-21, Stockholm
†viktoroslavs@gmail.com

Abstract

Renormalization group analysis is a useful tool for studying critical behaviour of stochastic systems. In this thesis, field-theoretic renormalization group will be applied to the scalar model representing directed percolation, known as Gribov model, in presence of the random velocity field. Turbulent mixing will be modelled by the compressible form of stochastic Navier-Stokes equation where the compressibility is described by an additional field related to the density. The task will be to find corresponding scaling properties.

Acknowledgements

Contents

Introduction

The foundation of quantum field theory

In 1928 Paul Dirac postulated a relativistic equation of motion for the electron [1]. This led to an enormous development in theoretical physics and to the formulation of quantum field theory. Historically, the first theory to be constructed was quantum electrodynamics which describes the electromagnetic interactions between electrons, positrons and photons. A new theoretical framework became available for the perturbative calculation of particle scattering processes in high energy physics. Despite its early successes, quantum field theory was plagued by several serious technical difficulties. While the calculation of the low orders of perturbation theory was quite successful, higher order approximations were giving divergent contributions. These divergences, which arise from the large and small momentum scales, were clearly unphysical, since the measurements were showing finite results. It later also appeared that this is not only the problem of quantum electrodynamics, but the problem of quantum field theories in general. The problem of infinities was approached by many physicists and solved in the late 1940s mainly by Feynman, Schwinger, Tomonaga, Dyson [2]. They invented a method of eliminating these divergences without destroying the physical meaning of the theory. This method is known as *renormalization*.

After the divergences were successfully eliminated, the discovery of the running coupling constant was made. For example the electric charge e was no longer a constant but its exact value depended on the scale at which it was measured. This led to the important concept of the *renormalization group*, which was constructed in a solid form in the mid 1950s by Bogoliubov and Shirkov based on the work of previous authors [2, 3]. From a practical point of view, the renormalization group technique is an effective method of calculating correlation functions at large or small momentum scales (or equivalently at small or large spatial scales).

About the same time, a different field of physics was dealing with another unsolved problem related to scale invariance. Roughly speaking, scale invariance is a feature of objects or laws that do not change if length scales or other scales are multiplied by a common factor. These structures typically obey a non-trivial power-law scaling behaviour. In statistical physics, scale invariance is an important property of a system that undergoes certain phase transitions. Namely, so called second order phase transitions are characterized by a divergent correlation length which forces the system to be in a unique scale-invariant state. Measurements show [2] that various different systems have the same large-scale properties, while undergoing this type of phase transition. Properties such as power laws appear to be universal and independent of the microscopic structure of the system. This led to the concept of *universality classes*, which groups various systems with identical large-scale properties together, depending only on their general characteristics such as symmetry of the system, dimensionality of the space etc. In 1971 Wilson

introduced a systematic renormalization procedure based on eliminating the microscopic degrees of freedom [4, 5]. Starting from a path integral formulation of the quantum field theory he explained the existence of universality. This was the first appearance of path integral renormalization group in statistical physics.

Even though the renormalization group was initially developed for solving problems in particle physics and critical phenomena, it was later realized to be useful also for solving other problems, such as dynamical processes.

Field theory approach to dynamical processes

The term *dynamics* in a broad sense refers to any system evolving in time. General properties of macroscopic systems are almost impossible to describe rigorously due to large degrees of freedom. In order to avoid this complex construction, one introduces a random "noise" that mimics the microscopic properties of the system. Corresponding solutions are then non-deterministic and one is able to predict only the probabilistic evolution of the system. In 1973 Martin, Siggia and Rose [6] introduced the idea that an additional field related to the random force plays an important role in stochastic processes. This concept was later modified by De Dominicis and Janssen[7], which showed that the Martin-Siggia-Rose models can be reformulated in terms of path integrals. Here, methods from quantum field theory were particularly useful to study their universal properties. The path integral formulation also allows to forget about the quantum origin of the fields and treat them as classical objects. A quantum field operator then represents a classical fluctuating field and one can work in an euclidean rather than in a relativistic Minkowski metric. This allows us to investigate properties of different classical systems such as fully developed turbulence.

The problem of fully developed turbulence has puzzled physicists for more than four hundred years. An important aspect of fluid flow is that especially at high velocities, the flow may become unstable and the transition to a chaotic turbulent flow may occur. By considering large-scale high speed flow, the system seems to have scale-invariant properties. Measurements also show that the energy spectrum of the fully developed turbulence has a universal power-law behaviour that is independent from the origin of turbulence. These facts led to the stochastic formulation of turbulence. A significant progress in this field was made by Wyld [8]. Using a graphical representation of his calculations, Wyld showed that one can construct a perturbation series equivalent to Feynman diagrams from quantum field theory. Later Foster, Nelson and Stephen investigated the large scale and long time asymptotic properties using methods of renormalization group [9, 10].

The field-theoretic formulation of fully developed turbulence was first done by De Dominicis and Martin [11]. This allows us to use methods of quantum field theory to study universal properties of the turbulent fluid. Later, additional stochastic problems were approached using the field-theoretic renormalization group, e.g. stochastic magnetohydrodynamics and turbulent diffusion [12]. In the latter case for example, the path of the diffusing particle in a turbulent flow shows scale-invariant properties which do not agree with the dimensional analysis. This is also referred to as anomalous diffusion.

Another approach to stochastic processes was done by Doi and Peliti [13, 14]. Based on Doi's approach, Peliti showed that reaction-diffusion processes can also be reformulated in terms of field-theoretic models. One of these processes is also known as directed percolation. This process can generally describe various problems in nature from epidemic processes and forest fires to laminar-turbulent phase transitions. It can be easily imag-

ined as an agent spreading an infection among some species or fire spreading among trees. The important feature is that this process also shows a second-order phase transition, where the path of the agent shows scale-invariant properties. However, directed percolation represents a much wider universality class than just a reaction-diffusion system. It also describes the phase transition between active (fluctuating) phase to an inactive (absorbing) phase. This type of transition is observed in many different phenomena in physics, biology, chemistry and sociology. However, experimental results are inconsistent with theoretical predictions of directed percolation. It is believed that this might be due to additional external effects such as impurities or defects of the environment that are not taken into account in the original formulation of this process. Therefore various different modifications have been done, such as taking into account effects of long-range interactions[15], immunization[16] or mutation[17]. Another way to study external influences on the directed percolation phase transition is to consider the influence of a random environment. This can be done by considering the directed percolation process as a reaction-diffusion process advected by a turbulent velocity field, which is the motivation for our work. Several attempts have already been made [18, 19, 20] some of which we will discuss in this thesis.

Outline

The main aim of this thesis is to study universal properties of the directed percolation process advected by a compressible turbulent fluid using methods of the perturbative field-theoretic renormalization group. The problem of compressible turbulence is however even less understood than the incompressible one. Our approach is based on the model derived by Antonov [21] which represents the simplest known field-theoretic model based on the compressible form of Navier-Stokes equation. The physical relevance of this model is still however questionable, since it suffers from certain mathematical difficulties. The solution to this model is also known only to the first order of perturbation theory. The aim is therefore to study its influence on the directed percolation phase transition and compare the results with already known results obtained previously in the literature.

The outline of this thesis goes as follows: In Chapter 1 we introduce all the mathematical methods necessary for our calculation. Due to the complex structure of our model, we describe perturbative renormalization group using a simple Landau-Ginzburg ϕ^4 model. This is later generalized to the case of dynamical models. The field-theoretic models for reaction-diffusion processes using the Doi-Peliti approach are described in the end. Chapter 2 is devoted to the directed percolation phase transition. Here, all properties necessary to our problem are described and the field-theoretic formulation is then derived using methods from the first Chapter.

Since we are interested in the turbulent advection of directed percolation process, in Chapter 3 we will describe the properties of fully developed turbulence. The incompressible and compressible cases are discussed independently and the field-theoretic formulation is given at the end. In the following Chapter 4 we investigate the influence of compressible turbulent mixing on the directed percolation process. The large-scale properties are found using the field-theoretic renormalization group and finally, we conclude and discuss our results in Chapter 5.

Chapter 1

Field-Theory approaches to stochastic processes

The aim of this Chapter is to describe all the methods used in this thesis. They involve various different fields that have been developed in the last decades. However, since they are technically very complex, we are not going to describe them in detail, but rather give the reader a brief explanation. For more detailed description we recommend the reader to see [2, 16, 22, 23, 24, 25] and the references cited therein.

The renormalization group is a powerful tool for investigating the large-scale and long time properties of various scale invariant systems. These methods, originally developed for particle and condensed matter physics later appeared to have a more universal character. In this thesis we will work with the field-theoretic renormalization group approach to stochastic systems such as fully developed turbulence and reaction-diffusion systems. However, this approach has a very complex structure and therefore a description in terms of a simplified model is necessary. In these sections we start by discussing the simplest known - Ginzburg-Landau ϕ^4 model. This model, originally introduced for investigating the properties of continuous phase transitions, represents one of the simplest field-theoretic models. However, it is not solvable analytically and therefore a perturbative approach is necessary. Based on that, tools of renormalization group will be introduced. In the section 1.3 this approach will be generalized for the case of stochastic dynamical systems.

The general description of stochastic processes is given in terms of the Langevin equation that describes the stochastic dynamical evolution of a particle or a field of particles[1][26]. In section 1.3 we will show that these systems are completely equivalent to field-theoretic models in which the methods of field-theoretic renormalization group can be easily applied. An alternative way of constructing a model of stochastic systems is given in terms of a Master equation which describes the probabilistic time evolution of the systems which can be in various states [26]. This description is especially useful for studying the reaction-diffusion processes. In section 1.4 we show an alternative approach based on Doi's formalism, which allows us to construct field-theoretic models directly from the Master equations. This point is crucial to our work, since the field-theoretic description of both models allows us to study both processes simultaneously, which is the purpose of this thesis.

It should be stated that this chapter is purely technical and requires some knowledge of field-theoretic approach to condensed matter physics.

---

[1]Or equivalently in terms of Fokker-Planck equation, that describes the evolution of the probability distribution of the system.

1.1   Scaling in the theory of static critical phenomena

Phase transitions are a phenomena that can be observed in many different occurrences of nature. Typical examples are solid-liquid, superfluid He4 or para-ferromagnetic phase transitions. Qualitatively phase transitions can be divided into two groups, depending on the behaviour of the *order parameter* (e.g. density, magnetization) near the *critical point* (e.g. critical temperature). The order parameter can change either continuously or discontinuously. In the first case, the correlation length diverges, which is causing the system to be in a certain *universal state.* The behaviour of the order parameter arround the critical point is described by *critical exponents* and measurements show [2] that they are *universal* for various systems, i.e. they are independent of microscopic properties of the systems and they depend only on few parameters (e.g. the dimension of the space).

A significant progress in developing the theory of continuous phase transitions was done by Lev Landau [27]. His theory was based on the assumption, that the free energy can be expanded as a Taylor series in terms of the order parameter, Φ

$$\mathcal{F}(\Phi) - \mathcal{F}(0) = \tau \Phi^2/2 + g\Phi^4/4! + \cdots , \tag{1.1.1}$$

where $\tau \propto T - T_c$ is the deviation from the critical temperature, g is a positive constant and the absence of odd powers of Φ reflects the $\Phi \leftrightarrow -\Phi$ symmetry[2]. By looking at the minimum of (1.1.1) one can find that the order parameter behaves as

$$\Phi \propto \begin{cases} (T_c - T)^\beta, & T < T_c \\ 0, & T > T_c \end{cases} , \tag{1.1.2}$$

where $\beta = 1/2$ is the corresponding critical exponent. Although Landau's theory gave a good qualitative description of the phase transitions, quantitatively it was inconsistent with experiments [2]. The problem with models such as (1.1.1) is, that they neglect fluctuations of the order parameter field Φ. This approximation is not valid for continuous phase transitions, since the correlation length ξ generally diverges. Approximations such as this are usually referred to as *mean-field* approximations and they are valid only a above certain *critical dimension* d_c. It can be shown in the case of Landau's theory of magnetic phase transition $d_c = 4$ [2]. Below this dimension, these fluctuations cannot be neglected and a different approach has to be taken.

Field theory gives us tools for investigating properties of second order phase transitions. The celebrated field-theoretic model is the Ginzburg-Landau ϕ^4 model with a given (static) action functional[3] [22, 28]

$$\mathcal{S}[\phi] = \int \mathrm{d}^d x \ \left(\frac{1}{2}(\partial\phi(\boldsymbol{x}))^2 + \frac{\tau}{2}\phi^2(\boldsymbol{x}) + \frac{g}{4!}\phi^4(\boldsymbol{x}) \right) , \tag{1.1.3}$$

where $\phi(\boldsymbol{x})$ represents the space dependent order parameter scalar field, $(\partial\phi)^2 = \partial_i\phi\partial_i\phi$ is the squared gradient, $\partial_i = \partial/\partial x_i$, repeated indices are always summed over and g is a *coupling constant* describing the magnitude of the quartic interaction. The partition function is defined as[4]

$$\mathcal{Z}[h] = \mathcal{N}^{-1} \int \mathcal{D}\phi \ \exp\{-\mathcal{S}[\phi] + h\phi\} , \tag{1.1.4}$$

---

[2]Inversion symmetry is the direct consequence of for example spin inversion in Ising spin model.

[3]In standard literature, (1.1.3) is referred as an effective Hamiltonian. In order to be consistent with later convention, we will refer to it as an action functional.

[4]We have rescaled parameters and field in order to eliminate the factor $\beta = 1/k_B T$ from the integrand exponential [29].

where $\mathcal{N}$ is the normalization constant to be determined, $h\phi = \int \mathrm{d}\boldsymbol{x}\, h(\boldsymbol{x})\phi(\boldsymbol{x})$, h is an external magnetic field that acts as a source of perturbation and $\int \mathcal{D}\phi$ represents integration over all possible configurations of fields. The reason of introducing h will become clear in the next section when we will talk about perturbation theory. In statistical physics field $\phi(\boldsymbol{x})$ can be interpreted as a classical random field with a probability distribution in the space of fields

$$\mathcal{D}\phi \ \exp\{-\mathcal{S}[\phi]\} \ . \tag{1.1.5}$$

The *functional integral* formulation (1.1.4) includes fluctuations of the order parameter field ϕ which were absent in Landau's theory. In order to obtain mean-field results, one just neglects these fluctuations by taking the minimum of (1.1.4) (and assuming spatial hommogenity with $h = 0$).

We can use simple dimensional analysis to study the critical exponents themselves [29]. For example, let us take the two point correlation function

$$G(\boldsymbol{x} - \boldsymbol{x}') \equiv \langle \phi(\boldsymbol{x}')\phi(\boldsymbol{x}) \rangle \ , \tag{1.1.6}$$

where the mean value $\langle \cdots \rangle$ is taken over all possible configurations of fields ϕ. Since the exponential of (1.1.4) must be dimensionless, straightforward dimensional analysis of (1.1.3) and (1.1.6) tells us that

$$[\phi] = L^{(2-d)/2}, \quad [\tau] = L^{-2}, \quad [g] = L^{d-4}, \quad [G(\boldsymbol{x} - \boldsymbol{x}')] = L^{2-d} \implies [G(\boldsymbol{k})] = L^2 \ , \tag{1.1.7}$$

where L is the unit of length and $G(\boldsymbol{k})$ is a Fourier transformation of $G(\boldsymbol{x} - \boldsymbol{x}')$. Thus, if we make a change of the units of length by factor of λ from L to $L' = \lambda L$, then G should transform according to the rule that $G'L'^2 = GL^2$ which in the vicinity of the critical point $\tau \approx 0$ implies that[5]

$$G'(\boldsymbol{k}') = \lambda^{-2}G(\boldsymbol{k}) \ , \tag{1.1.8}$$

where $\boldsymbol{k}' = \lambda \boldsymbol{k}$. This result must always be true - it follows simply from definition of the two point function. It will be shown later, that in the zeroth order of perturbation theory (represented by subscript 0) the two point correlation function is

$$G_0(\boldsymbol{k}) = \frac{1}{k^2 + \tau} \ . \tag{1.1.9}$$

It is easy to see, that this correlation function satisfies (1.1.8) if we rescale lengths, namely $\boldsymbol{k}$ as $\boldsymbol{k}' = \lambda \boldsymbol{k}$, and τ according to (1.1.7) as $\tau' = \lambda^2 \tau$. In contrast to Eq. (1.1.8), direct measurements [2] show that in the vicinity of the critical point $\tau \approx 0$ the large scale behaviour $\boldsymbol{k} \to 0$ of the correlation function behaves as

$$G_0(\boldsymbol{k}) \propto \boldsymbol{k}^{-2+\eta} \ , \tag{1.1.10}$$

where η is in general nonzero exponent. It can be clearly seen from the derivation above, that the general dimensional considerations must be augmented, unless $\eta = 0$. Another

---

[5]We are using the convention that a physical quantity Q_p represented by the symbol Q is actually given by $Q_p = Q \times [Q]$. Under a change of units, Q changes, while Q_p is, of course, invariant.

such example is the correlation length ξ. From the dimensional analysis it can be shown that $\xi \propto \tau^{-1/2}$ ($[\xi] = L$), but experiments [2] show $\xi \propto \tau^{-\nu}$ where $\nu \neq 1/2$.

The results above appear to be incorrect. Any value for the critical exponents other than one given by a mean-field (or Landau) theory seems to violate the dimensional analysis. There is, however, another length scale, which we did not take into account. The only other length scale in the problem apart from the correlation length is the microscopic length scale – the lattice spacing a ($[a] = L$). The correlation length can, in principle, at critical temperature take the following form

$$G(\boldsymbol{k}) \propto \boldsymbol{k}^{-2} f(a\boldsymbol{k}) \ , \tag{1.1.11}$$

where $f(\boldsymbol{z})$ is some function of a dimensionless variable $\boldsymbol{z}$. Since the lattice spacing is small and we are looking at the large scale behaviour ($a\boldsymbol{k} \to \boldsymbol{0}$) (1.1.11) can be approximated as

$$f(\boldsymbol{z}) \approx \boldsymbol{z}^{\eta} \implies G(\boldsymbol{k}) \propto a^{\eta} \boldsymbol{k}^{-2+\eta} \ , \tag{1.1.12}$$

and therefore it satisfies both (1.1.8) and (1.1.10). Similarly, for the correlation length we conclude that

$$\xi = \tau^{-1/2} f(\tau a^2) \propto a^{2\theta} \tau^{-1/2+\theta} \ , \tag{1.1.13}$$

if $\tau a^2 \to 0$. Thus the critical exponent governing the divergence of the correlation length is $\nu = \frac{1}{2} - \theta$. The difference between this result and that of mean-field theory is the *anomalous dimension* θ. In the case of (1.1.11), the existence of a nonzero value of η can be considered to come from the fact that ϕ has acquired an anomalous dimension $\eta/2$.

Since classical dimensional analysis gives us incorrect results in our scale-invariant system, the anomalous dimension in fact reveals the *fractal structure* of our model. These dimensions can be computed in a controllable fashion by the *Renormalization group* (RG) techniques.

1.2   Perturbation theory, Renormalization group

Here we will give a schematic description of the perturbation theory and Renormalization group that have been employed in this thesis. A detailed description can be found in [2, 22, 24, 28].

In classical field theory, statistical averages can be calculated from the generating functional (1.1.4). All Green's functions, i.e. averaged products of any number of fields at different points, are expressed as functional derivatives of the partition function $\mathcal{Z}$ with respect to the source h at $h = 0$

$$G^{(n)}(\boldsymbol{x}_1, \cdots, \boldsymbol{x}_N) \equiv \langle \phi(\boldsymbol{x}_1) \cdots \phi(\boldsymbol{x}_N) \rangle = \left. \frac{\delta^n \mathcal{Z}[h]}{\delta h(\boldsymbol{x}_1) \cdots \delta h(\boldsymbol{x}_n)} \right|_{h=0} . \tag{1.2.1}$$

Unfortunately, the only path integral that can be easily evaluated exactly is Gaussian, and therefore in most cases these calculations have to be treated perturbatively. Perturbation theory then goes as follows. The action functional can be written as a sum of the quadratic

(free, Gaussian) and the interaction part $\mathcal{S} = \mathcal{S}_0 + \mathcal{S}_\mathrm{I}$. The partition function (1.1.4) will then have the form

$$\mathcal{Z}[h] = \mathcal{N}^{-1} \int \mathcal{D}\phi \ \exp\{-\mathcal{S}_0[\phi] - \mathcal{S}_I[\phi] + h\phi\} \ . \tag{1.2.2}$$

The main idea of the perturbation theory is to expand the interaction part $\mathcal{S}_\mathrm{I}$ in terms of small parameters (coupling constants) and evaluate path integrals in the free theory

$$\mathcal{Z}[h] = \mathcal{N}^{-1} \int \mathcal{D}\phi \ \sum_{n=0}^{\infty} \frac{(-\mathcal{S}_I[\phi])^n}{n!} \exp\{-\mathcal{S}_0[\phi] + h\phi\} \ . \tag{1.2.3}$$

Since the interaction term is usually a product of fields, it can be formally re-expressed as an operator containing functional derivatives with respect to the external field h. For example in the case of model (1.1.3) the interaction part is

$$\mathcal{S}_I[\phi] = \int \mathrm{d}^d x \ \frac{g}{4!} \phi^4(\boldsymbol{x}) \to \mathcal{S}_I\left[\delta/\delta h\right] \equiv \int \mathrm{d}^d x \ \frac{g}{4!} \frac{\delta^4}{\delta h^4(\boldsymbol{x})} \ , \tag{1.2.4}$$

where this transformation holds only inside of the integrand (1.2.3). The term $S_I[\delta/\delta h]$ can be taken out from the functional integral (1.2.3) and re-summed into the exponential operator. The resulting functional integral is then quadratic and therefore it can be integrated out [28]

$$\mathcal{Z}[h] = \mathcal{N}^{-1} \exp\{-\mathcal{S}_I[\delta/\delta h]\} \times$$
$$\times \int \mathcal{D}\phi \exp\left\{ -\frac{1}{2} \int \mathrm{d}^d x \mathrm{d}^d x' \ \phi(\boldsymbol{x}) D(\boldsymbol{x}, \boldsymbol{x}') \phi(\boldsymbol{x}') + \int \mathrm{d}^d x \ h(\boldsymbol{x}) \phi(\boldsymbol{x}) \right\} \tag{1.2.5}$$
$$= \mathcal{N}^{-1} \exp\{-\mathcal{S}_I[\delta/\delta h]\} \exp\left\{ \frac{1}{2} \int \mathrm{d}^d x \mathrm{d}^d x' \ h(\boldsymbol{x}) G_0(\boldsymbol{x}, \boldsymbol{x}') h(\boldsymbol{x}') \right\} \ , \tag{1.2.6}$$

where $D(\boldsymbol{x}, \boldsymbol{x}')$ is the quadratic operator of the action functional $\mathcal{S}_0$ and $G_0(\boldsymbol{x}, \boldsymbol{x}')$ is a corresponding *Green's function* defined as

$$\int \mathrm{d}^d x' \ D(\boldsymbol{x}, \boldsymbol{x}') G_0(\boldsymbol{x}', \boldsymbol{x}'') = \delta(\boldsymbol{x} - \boldsymbol{x}'') \ . \tag{1.2.7}$$

Eq. (1.2.6) represents the general expression for calculating perturbative corrections in the interacting field theory. In order to calculate correlation functions, one expands the interaction operator into the required order and performs functional derivatives (1.2.1). The calculation of two-point correlation function in the zero-th order of perturbation theory (in the free theory) shows that up to normalization it is equal to the Green's function

$$G_0(\boldsymbol{x}, \boldsymbol{x}') \equiv G_0^{(2)}(\boldsymbol{x}, \boldsymbol{x}') = \langle \phi(\boldsymbol{x}) \phi(\boldsymbol{x}') \rangle_0 \ . \tag{1.2.8}$$

In the statistical field-theoretic models, translation invariance is usually satisfied, and therefore the correlation functions depend only on the difference of its arguments $G(\boldsymbol{x}, \boldsymbol{x}') = G(\boldsymbol{x} - \boldsymbol{x}')$. For example the quadratic part and the Green's function in the Fourier space for the model (1.1.3) is

$$D(\boldsymbol{x}, \boldsymbol{x}') = (-\partial_{\boldsymbol{x}}^2 + \tau) \ \delta(\boldsymbol{x} - \boldsymbol{x}') \implies G_0(\boldsymbol{k}) = \frac{1}{k^2 + \tau} \ , \tag{1.2.9}$$

This proves Eq. (1.1.9). Function G_0 is called a *propagator* in most of the literature. One may notice another very important property. Statistical averages calculated from (1.2.6) are expressed as a sum off all possible products of Green's functions $G_0(\boldsymbol{x}_1, \boldsymbol{x}_2)$ (propagators) calculated in the free (Gaussian) theory. This property is called *Wick's theorem*[6]. For example the first order contribution to the two point correlation function of (1.1.3) involves evaluating

$$\int \mathrm{d}^d y \; \frac{g}{4!} \langle \phi(\boldsymbol{x}_1)\phi(\boldsymbol{x}_2)\phi^4(\boldsymbol{y}) \rangle \;. \tag{1.2.10}$$

The expression (1.2.10) is due to Wick's theorem expanded into the sum of all possible products of propagators including the integration over the interaction variable $\boldsymbol{y}$. This can be schematically represented by *Feynman diagrams* using the following diagramatic technique. In (1.2.10), the interaction argument $\boldsymbol{y}$ that is integrated out is called an *internal point* whereas the arguments of the two point correlation function $\boldsymbol{x}_1$ and $\boldsymbol{x}_2$ are called the *external points*. After the Wick's expansion, propagators are represented by a solid line, where endings correspond to its arguments. An internal point, connecting four propagators with integration over the corresponding variable is represented by a dot (vertex)

$$G_0(\boldsymbol{x}_1, \boldsymbol{x}_2) = \boldsymbol{x}_1 \text{———} \boldsymbol{x}_2 \;, \quad -g \int \mathrm{d}^d y = \underset{\boldsymbol{y}}{\times} \;. \tag{1.2.11}$$

Wick's expansion of (1.2.10) will then require an evaluation of the following diagrams:

$$\frac{1}{2} \; \boldsymbol{x}_1 \underset{\boldsymbol{y}}{\text———} \boldsymbol{x}_2 = \frac{-g}{2} \int \mathrm{d}^d y \; G_0(\boldsymbol{x}_1, \boldsymbol{y}) G_0(\boldsymbol{y}, \boldsymbol{y}) G_0(\boldsymbol{y}, \boldsymbol{x}_2) \;, \tag{1.2.12}$$

$$\frac{1}{8} \; \boldsymbol{x}_1 \underset{\boldsymbol{y}}{\text———} \boldsymbol{x}_2 = G(\boldsymbol{x}_1, \boldsymbol{x}_2) \frac{-g}{8} \int \mathrm{d}^d y \; G(\boldsymbol{y}, \boldsymbol{y})^2 \;. \tag{1.2.13}$$

Numerical factors in (1.2.12) and (1.2.13) are called the *symmetry* factors and they arise due to the numerical factor $1/4!$ in the interaction term of the action functional, the order of perturbation theory and from the fact, that diagrams can be constructed in several ways by permuting propagators.

These mathematical tools allows us to calculate corrections to correlation functions in any order of perturbation theory. The full calculation can be technically difficult and therefore a simplification is necessary.

1.2.1   Connected correlation function

Perturbation expansion described in the last section involves calculation of many Feynman diagrams. Therefore it is convenient to perform some simplifications of the calculation.

Internal mathematical structure of the diagram (1.2.12) does not allow us to separate it as a product of two independent products of propagators. Diagrams of this type are called *connected diagrams*. On the other hand, the mathematical structure of the diagram (1.2.13) can be separated. These diagrams are called *disconnected diagrams* and they can be always expressed as a product of connected parts. For example the diagram (1.2.13) can be schematically expressed as

$$\underline{\text———} = \text———} \times \text———} \;, \tag{1.2.14}$$

---

[6]A more general idea in probability theory is called the *Isserlis' theorem*.

where we have suppressed the explicit variable dependence. The last diagram in (1.2.14) is not connected to any external point and therefore it is often called a *vacuum diagram*. Multiplicative properties of disconnected diagrams lead to a significant simplification of correlation functions. For example the two point correlation function can be schematically expressed as (symmetry factors are suppressed):

$$G(\boldsymbol{x}_1, \boldsymbol{x}_2) = \underline{\qquad} + \underline{\quad} + \underline{\quad} + \underline{\quad \quad} + \underline{\quad} + \cdots \quad (1.2.15)$$

$$= \left(\underline{\qquad} + \underline{\quad} + \underline{\quad \quad} + \cdots \right) \times$$

$$\times \left(\bigcirc\!\!\bullet\!\!\bigcirc + \bigcirc\!\!\bullet\!\!\bigcirc\!\!\bullet\!\!\bigcirc + \bigcirc\!\!\bullet\!\!\bigcirc + \cdots \right) , \quad (1.2.16)$$

where the first bracket contains the sum of all diagrams that are connected to the external points and the second bracket contains the sum of all vacuum diagrams. In the case of the two point correlation function the first bracket contains only the connected diagrams. One should note however, that the higher order correlation functions might contain disconnected diagrams connected to the external points. For example one diagram for the four point correlation function might be

$$\frac{1}{4} \; {}^{\boldsymbol{x}_2}\!\!\!\underset{\boldsymbol{x}_1}{\searrow}\!\!\!\bullet\!\!\bigcirc_{\boldsymbol{y}_1} \quad \bigcirc\!\!\bullet\underset{\boldsymbol{y}_2}{}\!\!\!\overset{\boldsymbol{x}_3}{\nearrow}_{\boldsymbol{x}_4} = \frac{-g}{2} \int \mathrm{d}^d y_1 \; G_0(\boldsymbol{x}_1, \boldsymbol{y}_1) G_0(\boldsymbol{x}_2, \boldsymbol{y}_1) G_0(\boldsymbol{y}_1, \boldsymbol{y}_1) \times$$

$$\times \frac{-g}{2} \int \mathrm{d}^d y_2 \; G_0(\boldsymbol{x}_3, \boldsymbol{y}_2) G_0(\boldsymbol{x}_4, \boldsymbol{y}_2) G_0(\boldsymbol{y}_2, \boldsymbol{y}_2) . \quad (1.2.17)$$

Due to the mathematical structure of Feynman diagrams, sums of all possible connected and disconnected diagrams can be re-summed into exponentials containing only connected diagrams. This is a direct result of the *linked-cluster theorem*[24]. The general form of the n-point correlation function is then

$$G^{(n)}(\boldsymbol{x}_1, \cdots, \boldsymbol{x}_n) = \exp \left\{ \sum \begin{matrix} \text{Connected diagrams} \\ \text{with } n \text{ external lines} \end{matrix} \right\} \times \exp \left\{ \sum \begin{matrix} \text{Connected} \\ \text{vacuum diagrams} \end{matrix} \right\} . \quad (1.2.18)$$

Eq. (1.2.6) implies, that the sum of all vacuum diagrams is equal to $\mathcal{Z}[0]$ and the proper normalization is then $\mathcal{N} = \mathcal{Z}[0] = 1$. In order to obtain the sum of all connected diagrams with n external lines, one introduces the *generating functional of connected correlation functions* [7] as

$$\mathcal{W}[h] = \ln \mathcal{Z}[h] , \quad (1.2.19)$$

where the n-point *connected correlation functions* $G_c^{(n)}$ can be obtained in the usual way by taking the functional derivatives with respect the the external field at zero field

$$G_c^{(n)}(\boldsymbol{x}_1, \cdots, \boldsymbol{x}_n) = \left. \frac{\delta^n \mathcal{W}[h]}{\delta h(\boldsymbol{x}_1) \cdots h(\boldsymbol{x}_n)} \right|_{h=0} . \quad (1.2.20)$$

---

[7]Quantity analogous to the free energy from statistical mechanics.

1.2.2   Saddle-point approximation, vertex functions

Another simplification can be made by finding the Gaussian approximation of the model under consideration and then calculating corresponding leading corrections. This procedure is known as a *saddle-point approximation.* The general idea is the following [2, 22, 28].

Consider a general form of the partition function

$$\mathcal{Z}[h] = \int \mathcal{D}\phi \exp\{-\mathcal{S}[\phi] + h\phi\} . \tag{1.2.21}$$

The integrand can be approximated by the leading contribution of the saddle point of exponential, i.e. around the field Φ

$$h(\boldsymbol{x}) = \left.\frac{\delta\mathcal{S}[\phi]}{\delta\phi(\boldsymbol{x})}\right|_{\phi=\Phi} \implies \phi(\boldsymbol{x}) = \Phi(\boldsymbol{x}) + \phi'(\boldsymbol{x}) . \tag{1.2.22}$$

Using this formula, one can approximate the exponential in (1.2.21) in the following way

$$-\mathcal{S}[\phi] + h\phi = -\mathcal{S}[\Phi] + h\Phi - \frac{1}{2}\iint \mathrm{d}^d x \mathrm{d}^d x' \left.\frac{\delta^2\mathcal{S}[\phi']}{\delta\phi'(\boldsymbol{x})\phi'(\boldsymbol{x}')}\right|_{\phi'=\Phi} \phi'(\boldsymbol{x})\phi'(\boldsymbol{x}') + \cdots \tag{1.2.23}$$

The remaining integral in (1.2.21) is then Gaussian, and can therefore be easily evaluated

$$\mathcal{Z}[h] \approx \left(\det \boldsymbol{\mathcal{S}}_\Phi^{(2)}\right)^{-1/2} \exp\{-\mathcal{S}[\Phi] + h\Phi\}, \quad \boldsymbol{\mathcal{S}}_\Phi^{(2)} = \left.\frac{\delta^2\mathcal{S}[\phi']}{\delta\phi'(\boldsymbol{x})\phi'(\boldsymbol{x}')}\right|_{\phi'=\Phi} . \tag{1.2.24}$$

By introducing the generation functional of connected correlation functions (1.2.19), one finds

$$\mathcal{W}[h] = -\mathcal{S}[\Phi] + h\Phi - \frac{1}{2}\operatorname{Tr}\ln \boldsymbol{\mathcal{S}}_c^{(2)} + \mathcal{O}[(\phi')^3] , \tag{1.2.25}$$

where we have neglected irrelevant constants. One can see that the classical field Φ can be obtained from (1.2.25) as

$$\Phi(\boldsymbol{x}) \equiv \left.\frac{\delta\mathcal{W}[h]}{\delta h(\boldsymbol{x})}\right|_{h=0} . \tag{1.2.26}$$

This is suggesting that we should define the *effective potential*[8] Γ as a Legendre transformation of $\mathcal{W}$

$$\mathcal{W}[h] = \Gamma[\Phi] + h\Phi , \tag{1.2.27}$$

and so we find a relation between effective potential and action functional

$$\Gamma[\Phi] = -\mathcal{S}[\Phi] - \frac{1}{2}\operatorname{Tr}\ln \boldsymbol{\mathcal{S}}_\Phi^{(2)} + \cdots . \tag{1.2.28}$$

In order to give an interpretation of the effective potential Γ we need to make some definitions. As mentioned before, Feynman diagrams can be connected to the external points. Lines connecting these points are called *external lines* and the rest of them are called *internal lines.* Any diagram that can not be separated by cutting one internal line is called *one-particle irreducible* (1-PI) diagram. Typical examples can be seen on

Fig. 1.1. The second term in (1.2.28) represents the first order contribution in the *loop expansion*, i.e. the contribution from 1-PI diagrams. The general form is then[9]

$$\Gamma[\Phi] = -\mathcal{S}[\Phi] + (\text{1-PI loop diagrams}) . \tag{1.2.29}$$

This effective potential Γ is also the generating function of the *vertex functions*. They can be found as functional derivatives with respect to the field $\Phi(\boldsymbol{x}_i)$

$$\Gamma^{(n)}(\boldsymbol{x}_1, \cdots, \boldsymbol{x}_n) = \frac{\delta^n \Gamma[\Phi]}{\delta \Phi(\boldsymbol{x}_1) \cdots \delta \Phi(\boldsymbol{x}_n)} . \tag{1.2.30}$$

An interpretation of vertex function can be seen from the factorization of the n-point correlation function in the case of one field. It can be shown that [2]

$$G^{(n)}(\boldsymbol{x}_1, \cdots, \boldsymbol{x}_n) = \int \mathrm{d}^d x_{1'} \cdots \mathrm{d}^d x_{n'} \ G_c(\boldsymbol{x}_1, \boldsymbol{x}_{1'}) \cdots G_c(\boldsymbol{x}_n, \boldsymbol{x}_{n'}) \Gamma^{(n)}(\boldsymbol{x}_{1'}, \cdots, \boldsymbol{x}_{n'}) +$$
$$+ Q^{(n)}(\boldsymbol{x}_1, \cdots, \boldsymbol{x}_n) , \tag{1.2.31}$$

where $Q^{(n)}(\cdots)$ stands for a one-particle reducible function. Since only the first term represents the 1-PI contributions, we can imagine the vertex function as the loop corrections that are constructed from 1PI diagrams by cutting the external lines (cutting all $G_c(\boldsymbol{x}_i, \boldsymbol{x}_{i'})$). Moreover, from (1.2.29) we find

$$\Gamma^{(n)}(\boldsymbol{x}_1, \cdots, \boldsymbol{x}_n) = -\frac{\delta^n \mathcal{S}[\Phi]}{\delta \Phi(\boldsymbol{x}_1) \cdots \delta \Phi(\boldsymbol{x}_n)} + \begin{pmatrix} \text{loop corrections} \\ \text{from amptutated diagrams} \end{pmatrix} . \tag{1.2.32}$$

The last formula tells us how to calculate the n-point vertex functions directly from the action functional.

1.2.3 Renormalization

In field-theoretic lattice models, the translational invariance is usually assumed, and therefore in order to simplify our calculations we can perform a Fourier transformation. For example the action (1.1.3) becomes

$$\mathcal{S}[\phi] = \int \mathrm{d}^d k \ \phi(\boldsymbol{k})(\boldsymbol{k}^2 + \tau)\phi(-\boldsymbol{k})$$
$$+ g \int \mathrm{d}^d \boldsymbol{k}_1 \mathrm{d}^d \boldsymbol{k}_2 \mathrm{d}^d \boldsymbol{k}_3 \mathrm{d}^d \boldsymbol{k}_4 \ \delta(\Sigma_i \boldsymbol{k}_i)\phi(\boldsymbol{k}_1)\phi(\boldsymbol{k}_2)\phi(\boldsymbol{k}_3)\phi(\boldsymbol{k}_4) . \tag{1.2.33}$$

---

[8]Analogical quantity to the Gibbs free energy in the statical mechanics.

[9]Different authors use different conventions. For example in [22] authors define partition function as $\mathcal{Z} = \int \mathcal{D} \exp\{\mathcal{S}\}$, where the minus sign is inside the action functional. This results in the redefinition of the Legendre transformation (1.2.27) and the Eq. (1.2.29) still holds, but with a plus sign in front of $\mathcal{S}$.

Figure 1.1: On the left - 1PI diagram, i.e. diagram that cannot be separated by cutting one internal line. On the right - non 1PI diagram. This diagram can be separated by cutting the middle internal line connecting two vertexes (represented by the crossed line).

In Fourier space, the calculation of Feynman diagrams is different. Propagators are no longer described by points $\boldsymbol{x}_1, \boldsymbol{x}_2$ but by a single momentum $\boldsymbol{k}$. Delta function $\delta(\Sigma_i \boldsymbol{k}_i)$ at the interaction term (1.2.33) ensures the momentum conservation at each vertex. Integration over variables $\boldsymbol{x}_i$ is replaced by the integration over internal momenta – loops. These loops are generally divergent and in order to eliminate these divergences, one has to *renormalize* the theory.

Let us now analyze the two point correlation function $G(\boldsymbol{k})$. The sum of all two point 1PI diagrams is called *self energy* $\Sigma_0(\boldsymbol{k})$. Diagrams that are not 1PI are not interesting, since they can always be written as a product of some 1PI diagrams. The two point correlation function can be written as a geometric series of products of propagators G_0 and 1PI diagrams (represented by the blob)

$$G(\boldsymbol{k}) = \text{———} + \text{———}\oslash\text{———} + \text{———}\oslash\text{———}\oslash\text{———} + \cdots \tag{1.2.34}$$

$$= G_0(\boldsymbol{k}) + G_0(\boldsymbol{k})\Sigma_0(\boldsymbol{k})G_0(\boldsymbol{k}) + G_0(\boldsymbol{k})\Sigma_0(\boldsymbol{k})G_0(\boldsymbol{k})\Sigma_0(\boldsymbol{k})G_0(\boldsymbol{k}) + \dots \tag{1.2.35}$$

$$= \frac{1}{G_0^{-1}(\boldsymbol{k}) - \Sigma_0(\boldsymbol{k})} \tag{1.2.36}$$

$$= \frac{1}{(\text{———})^{-1} - \oslash} \ . \tag{1.2.37}$$

In the denominator we identify the two point vertex function

$$-\Gamma(\boldsymbol{k}) \equiv G^{-1}(\boldsymbol{k}) = G_0^{-1}(\boldsymbol{k}) - \Sigma_0(\boldsymbol{q}) \ , \tag{1.2.38}$$

which can be easily seen from (1.2.32). As mentioned above, the self energy function $\Sigma_0(\boldsymbol{k})$ contains divergences from loop integrals. For example, the ϕ^4 theory (1.1.3) in one loop level gives

$$\Sigma^{(1)}(\boldsymbol{k}) = \frac{1}{2} \ \underset{}{\overset{q}{\bigcirc\!\!\!-\!\!\!-}} \ = \frac{-g}{2} \int \frac{\mathrm{d}^d q}{(2\pi)^d} \frac{1}{\boldsymbol{q}^2 + \tau} \propto \int_0^\infty \mathrm{d}q \frac{q^{d-1}}{\boldsymbol{q}^2 + \tau} \ . \tag{1.2.39}$$

There are two types of divergences. First, one notices that the integral is infinite at the lower limit $q \to 0$ for $d \leq 2$ if $\tau = 0$ ($T = T_c$). Such a divergence is called *infrared* (IR) and this is the reason why we cannot simply put $\tau = 0$ even if we are studying the behaviour around the critical point. Another way how to avoid this divergence is to introduce an IR cutoff m in the integration domain $\int_m^\infty$ as will be explained later in Chapter 3.4. The integral (1.2.39) also clearly diverges for $d \geq 2$ as $q \to \infty$. This is called *ultraviolet* (UV) divergence. Since we are not interested in physics beyond the atomic scale a, we introduce UV cut-off $\Lambda = a^{-1}$ in momentum space so the integral becomes $\int_0^\Lambda \mathrm{d}k$. This process of eliminating divergences is called *regularization*. There are several ways how to regularize a theory but this one has a clear physical interpretation. In this case, divergences will be stored in terms containing Λ. One now has to modify the theory in such a way, that the theory will become finite after taking the limit $\Lambda \to \infty$, but without changing the physical properties of the model. This process is called *renormalization* and it can be done by renormalizing parameters and fields of the model. It can be shown [2], that the ϕ^4 model (1.1.3) can be renormalized by introducing the *renormalization constants* Z_i such that[10]

$$\phi_0 = Z_\phi \phi_R, \quad \tau_0 = Z_\tau \tau_R, \quad g_0 = Z_g g_R \ , \tag{1.2.40}$$

---

[10]Note that this choice of renormalization differs from the usual convention. In classical literature Z_ϕ is a normalization constant for correlation function and therefore the field is renormalized as $\phi_0 = Z_\phi^{1/2}\phi_R$.

where the τ_0 is the deviation from the criticality and, from now on, we will use subscripts R and 0 to denote *renormalized* and *unrenormalized* quantities. Note, that constants Z_i are naturally dimensionless. If we write normalization constants as $Z_i(\Lambda) = 1 + \delta_i(\Lambda)$, the two point correlation function (1.2.36) for ϕ^4 model can be then written as

$$G_R(\mathbf{k}) = \frac{1}{Z_\phi^2} G_0(\mathbf{k}) \approx \frac{1}{1 + 2\delta_\phi} \frac{1}{\mathbf{k}^2 + (1 + \delta_\tau)\tau_R - \Sigma_0(\mathbf{k})} \tag{1.2.41}$$

$$\approx \frac{1}{\mathbf{k}^2 + \tau_R - \Sigma_R(\mathbf{k})} = \frac{1}{\Gamma_R(\mathbf{k})} \ , \tag{1.2.42}$$

where we have introduced renormalized self-energy $\Sigma_R(\mathbf{k}) = \Sigma_0(\mathbf{k}) - 2\delta_\phi \mathbf{k}^2 - (2\delta_\phi + \delta_\tau)\tau_R$. We are free to choose *renormalization conditions* [2, 22, 28]. We take them to be

$$\Gamma_R(\mathbf{0}) = \tau_R, \quad \partial_{\mathbf{k}^2} \Gamma_R(\mathbf{k})|_{\mathbf{k}^2=0} = 1 \ . \tag{1.2.43}$$

Using these conditions we see directly from (1.2.42) that

$$\Sigma_0(\mathbf{0}) = (2\delta_\phi + \delta_\tau)\tau_R, \quad \partial_{\mathbf{k}^2} \Sigma_0(\mathbf{k})|_{\mathbf{k}^2=0} = 2\delta_\phi \ . \tag{1.2.44}$$

In order to have a physical theory, we need to eliminate all divergences. They can be found from the loop corrections of vertex functions (1.2.32). In momentum space, n-point correlation and vertex functions can be renormalized as

$$G_R^{(n)}(\{\mathbf{k}_i\}) = Z_\phi^{-n} G_0^{(n)}(\{\mathbf{k}_i\}), \tag{1.2.45}$$

$$\Gamma_R^{(n)}(\{\mathbf{k}_i\}) = Z_\phi^{n} \Gamma_0^{(n)}(\{\mathbf{k}_i\}) \ . \tag{1.2.46}$$

For example the four point vertex function for model (1.1.3) is

$$\Gamma_0^{(4)}(\{\mathbf{k}_i\}) = -g_0 + \frac{3}{2} \underset{q}{\overbrace{\bowtie}} + \begin{pmatrix} \text{higher loop} \\ \text{corrections} \end{pmatrix} = -g_0 + \Pi_0(\{\mathbf{k}_i\}) \ , \tag{1.2.47}$$

where $\Pi_0(\mathbf{k})$ is some function containing a divergence in Λ. Considering the normalization of the four point vertex function $\Gamma_R^{(4)} = Z_\phi^4 \Gamma_0^{(4)}$ one can show that

$$\Gamma_R^{(4)} = -g_R + \Pi_R(\{\mathbf{k}_i\}), \quad \Pi_R(\{\mathbf{k}_i\}) = \Pi_0(\{\mathbf{k}_i\}) - (4\delta_\phi + \delta_g)g_R \ , \tag{1.2.48}$$

and furthermore by imposing the normalization condition we find that

$$\Gamma_R^{(4)}(\{\mathbf{0}\}) = -g_R \implies \Pi_0(\{\mathbf{0}\}) = (4\delta_\phi + \delta_g)g_R \ . \tag{1.2.49}$$

Now, one has to rewrite the action functional in terms of renormalized quantities. Eq. (1.1.3) then becomes

$$\mathcal{S}_R[\phi_R] = \int \mathrm{d}^d x \ \left(Z_{\phi_R}^2 \frac{1}{2}(\partial\phi_R(\mathbf{x}))^2 + Z_\tau Z_{\phi_R}^2 \frac{\tau_R}{2}\phi_R^2(\mathbf{x}) + Z_g Z_{\phi_R}^4 \frac{g_R}{4!}\phi_R^4(\mathbf{x}) \right) \tag{1.2.50}$$

$$= \int \mathrm{d}^d x \ \left(\frac{1}{2}(\partial\phi_R(\mathbf{x}))^2 + \frac{\tau_R}{2}\phi_R^2(\mathbf{x}) + \frac{g_R}{4!}\phi_R^4(\mathbf{x}) \right) + \tag{1.2.51}$$

$$+ \int \mathrm{d}^d x \ \left(2\delta_{\phi_R} \frac{1}{2}(\partial\phi_R(\mathbf{x}))^2 + (\delta_\tau + 2\delta_{\phi_R})\frac{\tau_R}{2}\phi_R^2(\mathbf{x}) + (\delta_g + 4\delta_{\phi_R})\frac{g_R}{4!}\phi_R^4(\mathbf{x}) \right) \ .$$

The action (1.2.51) represents *renormalized perturbation theory*. From the last row, one can identify counterterms that have to be added to the original action in order to renormalize it. Their structure is obtained from the renormalization conditions (1.2.43) and (1.2.49)

$$\delta_\phi = \partial_{\boldsymbol{k}^2}\Sigma_0(\boldsymbol{k})|_{\boldsymbol{k}=0}/2 \ , \tag{1.2.52}$$

$$\delta_\tau = \partial_{\boldsymbol{k}^2}\Sigma_0(\boldsymbol{k})|_{\boldsymbol{k}=0} + \Sigma_0(\boldsymbol{0})/\tau_R \ , \tag{1.2.53}$$

$$\delta_g = 2\partial_{\boldsymbol{k}^2}\Sigma_0(\boldsymbol{k})|_{\boldsymbol{k}=0} + \Pi_0(\{\boldsymbol{0}\})/g_R \ . \tag{1.2.54}$$

In fact, these normalization conditions tell us that the corrections we are looking for are in the case of two point correlation function proportional to $\boldsymbol{k}^2$ and τ_R, and in the case of four point vertex function proportional to g_R. An alternative way of finding counterterms is to introduce renormalization constants such as

$$Z_1 = Z_\phi^2, \quad Z_2 = Z_\tau Z_\phi^2, \quad Z_3 = Z_g Z_\phi^4 \ , \tag{1.2.55}$$

in the action functional (1.2.52), calculate corresponding corrections and then invert them to find Z_ϕ, Z_τ, Z_g.

Although cut-off regularization is very intuitive for statistical field theory, it is technically difficult. Another way to regularize the theory is to use *dimensional regularization* [2, 28, 30, 31]. In this case, instead of dealing with a momentum cut-off, we set $\Lambda \to \infty$ (continuum limit) and store divergences in the Laurent series of the parameter $\varepsilon = 4 - d$ which describes the deviation from the upper critical dimension d_c. It is also convenient to introduce a renormalized coupling constant g_R dimensionless, introducing arbitrary *mass scale* μ

$$g_0 = \mu^\varepsilon g_R \ , \tag{1.2.56}$$

The exact form of the normalization constants also depends on the scheme that we choose. For practical calculations it is also convenient to use a *minimal subtraction* (MS) scheme, where the counterterms would contain only the divergent part of the diagrams. In such case, the normalization constants would have the form

$$Z_i = 1 + \sum_{n=1}^\infty \frac{A_{in}(g_R(\mu))}{\varepsilon^n} \ , \tag{1.2.57}$$

where A_{ni} are some finite dimensionless functions that depend only on $g_R(\mu)$. Correlation and vertex functions attain then the following form

$$G_R^{(n)}(\{\boldsymbol{k}_i\}; \tau_R(\mu), g_R(\mu), \mu) = Z_\phi^{-n}(g_R(\mu))G_0^{(n)}(\{\boldsymbol{k}_i\}; \tau_0, g_0) \ , \tag{1.2.58}$$

$$\Gamma_R^{(n)}(\{\boldsymbol{k}_i\}; \tau_R(\mu), g_R(\mu), \mu) = Z_\phi^n(g_R(\mu))\Gamma_0^{(n)}(\{\boldsymbol{k}_i\}; \tau_0, g_0) \ , \tag{1.2.59}$$

with[11]

$$\tau_R(\mu) = \tau_0 Z_\tau^{-1}(g_R(\mu)), \quad g_R(\mu) = g_0\mu^{-\varepsilon}Z_g^{-1}(g_R(\mu)) \ . \tag{1.2.60}$$

---

[11]One should always keep in mind the convention. For example in [16], the author introduces massless τ_R via $\tau_0 = \tau_R\mu^2 Z_\tau$. Here we are still assuming that $[\tau_R] = 2$. This convention can be found for example in [2, 22, 28].

The only question now is how to find out which vertex functions have to be renormalized. This can be done by the means of dimensional analysis. We introduce a formal *UV exponent* d_Γ of a vertex function Γ. In momentum space it is defined as [2, 22, 28]

$$d_\Gamma = d - n_\phi d_\phi \; . \tag{1.2.61}$$

Divergences that need to be eliminated are present in those vertex functions, for which

$$\delta_\Gamma \equiv d_\Gamma|_{\varepsilon=0} \geq 0 \; . \tag{1.2.62}$$

This formal UV exponent needs to be sometimes modified due to the presence of derivatives in the interaction terms $\mathcal{S}_I$. Let us for example consider interactions of the form $(\partial\phi)^4$. Since the field ϕ enters the vertex together with its derivative, there must be a ∂ on each external field ϕ in the all 1-irreducible functions Γ. The *real UV exponent* is then reduced by the number of fields ϕ that enter Γ (or number of external fields ϕ)

$$\delta'_\Gamma = \delta_\Gamma - n_\phi \; , \tag{1.2.63}$$

and the vertex functions that need renormalization must have $\delta'_\Gamma|_{\varepsilon=0} \geq 0$.

1.2.4 Anomalies in scale invariance

The elimination of divergences will create anomalies in scale invariance. To give quantitative description, we start with the definition of *generalized homogeneity* for an arbitrary function F

$$F(\lambda^{d_1} e_1, \ldots, \lambda^{d_n} e_n) = \lambda^{d_F} F(e_1, \ldots, e_n) \; , \tag{1.2.64}$$

where e_i are all parameters of the function F and d_i are corresponding dimensions. By taking the derivative with respect to λ and setting $\lambda = 1$ one finds a differential equation equivalent to (1.2.64)

$$\left(\sum_e d_e \mathcal{D}_e - d_F \right) F(\{e_i\}) = 0, \quad \mathcal{D}_e = e\partial_e \; . \tag{1.2.65}$$

Using this property, one can derive a differential equation describing scale invariance of any quantity of a scale invariant model. For example let us consider the model (1.1.3). As already mentioned above, canonical dimensional analysis is insufficient since there is an additional relevant length scale – a microscopic length scale. In dimensional regularization and MS scheme, this is represented by an scale-setting parameter μ. Dimensional analysis of renormalized theory yields

$$\left(\mathcal{D}_\mu + \mathcal{D}_{\boldsymbol{k}} + 2\mathcal{D}_{\tau_R} - nd_\phi^k \right) G_R^{(n)}(\{\boldsymbol{k}_i\}; \tau_R, g_R, \mu) = 0 \; , \tag{1.2.66}$$

where d_ϕ^k stands for the canonical dimension in the momentum space (Notice that there is no contribution from g_R since it was rescaled to be dimensionless in (1.2.56)). The existence of the anomalous dimension mentioned in the Chapter 1.1 is due to first term $\mathcal{D}_\mu$. Without it, classical dimensional analysis would be valid. In order to get rid of this term, one has to consider the following.

Correlation functions of the non-renormalized theory, i.e. $G_0^{(n)}$ in (1.2.58) clearly do not depend on the arbitrarily introduced mass scale μ. Performing the derivative with respect to $\ln \mu$, while holding g_0 and τ_0 fixed, we find the *renormalization group equation*

$$\left(\mathcal{D}_\mu + \beta_g \partial_{g_R} - \gamma_\tau \mathcal{D}_{\tau_R} + n\gamma_\phi\right) G_R^{(n)}(\{\boldsymbol{k}_i\}; \tau_R, g_R, \mu) = 0 \ , \tag{1.2.67}$$

with

$$\beta_g \equiv \tilde{\mathcal{D}}_\mu g_R, \quad \gamma_{\phi,\tau} \equiv \tilde{\mathcal{D}}_\mu \ln Z_{\phi,\tau} \ , \tag{1.2.68}$$

where $\mathcal{D}_\mu = \mu \partial_\mu|_{g_R, \tau_R}$ represents the derivative with holding renormalized parameter fixed and $\tilde{\mathcal{D}}_\mu = \mu \partial_\mu|_{g_0, \tau_0}$ the derivative with holding un-renormalized parameters fixed. The first formula in (1.2.67) is usually called the *beta function* and it describes how the *running coupling constant* g_R changes with the change of the scale. Since it depends on μ via (1.2.60), it can be calculated as

$$\beta_g = -g_R(\varepsilon + \gamma_g) \ . \tag{1.2.69}$$

In order to calculate the beta functions, it is useful to rescale the renormalization mass as $\tilde{\mu}(l) = \mu l$, so it becomes

$$\beta_g = \mathcal{D}_l g_R \ . \tag{1.2.70}$$

For the large scale behaviour $l \to 0$ the running coupling constant will approach the *IR fixed point* g_R^* if $\beta_g(g_R^*) = 0$ and if $\partial_{g_R} \beta_g|_{g_R = g_R^*} > 0$. The purpose of the second term in (1.2.68) is obvious if we express $\mathcal{D}_\mu$ in (1.2.67) and put it back into (1.2.66). By looking at the large scale behaviour $(\beta_{g_R}(g_R^*) = 0)$ one gets

$$\left(\mathcal{D}_{\boldsymbol{k}} + (2 + \gamma_\tau^*)\mathcal{D}_{\tau_R} - n(d_\phi^k + \gamma_\phi^*)\right) G_R^{(n)}(\{\boldsymbol{k}_i\}; \tau_R, g_R, \mu) = 0 \ , \tag{1.2.71}$$

where $\gamma_i^* = \gamma_i(g_R^*)$. As we can see here, γ_i functions are modifying canonical dimensions of our theory and are therefore called *anomalous dimensions*[12]. They can be calculated from the normalization constants (1.2.57)

$$\gamma_i = \beta_g \partial_{g_R} \ln Z_i \tag{1.2.72}$$

$$\approx -g_R(\varepsilon + \gamma_{g_R}) \partial_{g_R} \sum_{n=1}^{\infty} \frac{A_{in}(g_R)}{\varepsilon^n} \tag{1.2.73}$$

$$\approx -\mathcal{D}_{g_R} A_{i1}(g_R) \ , \tag{1.2.74}$$

providing the fact that the anomalous dimensions must be UV finite [22]. It is also important to mention, that vertex functions with negative UV exponent (1.2.62) do not influence the IR behaviour of the system and therefore can be neglected [22].

1.3 Critical dynamics

Since this thesis is about non-equilibrium critical phenomena, we will turn our attention to dynamical systems. An intuitive generalization of the static systems can be done

---

[12]The existence of anomalous dimensions is a direct consequence of the thermodynamic limit [2].

as follows [22, 29]. In equilibrium, the saddle point spatial configuration of the order parameter is given by

$$\frac{\delta \mathcal{S}^{\text{Stat}}[\phi]}{\delta \phi(\boldsymbol{x})} = 0 \ , \tag{1.3.1}$$

where $\mathcal{S}^{\text{Stat}}$ is some static functional, for example (1.1.3). If the system is slightly out of equilibrium, it is not unnatural to guess that the rate at which the system relaxes back to equilibrium is proportional to the deviation from equilibrium. This assumption of linear response is purely phenomenological, and leads to the following equation for the rate of change of the order parameter:

$$\partial_t \phi(\boldsymbol{x}, t) = -\overline{D} \frac{\delta \mathcal{S}^{\text{Stat}}[\phi]}{\delta \phi(\boldsymbol{x})}\bigg|_{\phi(\boldsymbol{x}) \to \phi(\boldsymbol{x}, t)} \ , \tag{1.3.2}$$

where $\overline{D}$ is some proportionality constant. This equation might not give the correct description of the equilibrium state, because the equilibrium state is actually a global minimum of $\mathcal{S}^{\text{Stat}}[\phi]$. In order to ensure that the system does not evolve into the local minimum, we must remember that the order parameter dynamics might exhibit fluctuations that arise from the microscopic degrees of freedom. To ensure this, we introduce a noise term $\eta(\boldsymbol{x}, t)$ into (1.3.2) such that

$$\partial_t \phi(\boldsymbol{x}, t) = -\overline{D} \frac{\delta \mathcal{S}^{\text{Stat}}[\phi]}{\delta \phi(\boldsymbol{x})}\bigg|_{\phi(\boldsymbol{x}) \to \phi(\boldsymbol{x}, t)} + \eta(\boldsymbol{x}, t) \ , \tag{1.3.3}$$

where the random force is usually taken as a Gaussian variable that is δ-correlated in time

$$\langle \eta(\boldsymbol{x}, t) \rangle = 0, \quad \langle \eta(\boldsymbol{x}', t') \eta(\boldsymbol{x}, t) \rangle = \delta(t - t') D(\boldsymbol{x}', \boldsymbol{x}) \ . \tag{1.3.4}$$

Eq. (1.3.3) is a more general form of the *Langevin equation* describing stochastic processes [26]. The main difference is that the description above is given in terms of the field $\phi(\boldsymbol{x})$ instead of the single variable $\boldsymbol{x}$. In dynamical systems, the objects of interests are the correlation functions (as in the case of static systems) and the *response functions* describing the response to an external force, i.e. the quantities

$$G^{(n, n')}(\{\boldsymbol{x}_i, t_i\}) = \left\langle \frac{\delta^n \phi(\boldsymbol{x}_1, t_1) \cdots \phi(\boldsymbol{x}_n, t_n)}{\delta \eta(\boldsymbol{x}_{1'}, t_{1'}) \cdots \eta(\boldsymbol{x}_{n'}, t_{n'})} \right\rangle \ , \tag{1.3.5}$$

where the symbol $\langle \cdots \rangle$ denotes the average taken over all possible configurations of the random field η.

It is also worth mentioning, that dynamical critical systems are generally described by two "correlation lengths". For example the Langevin equation for the ϕ^4 theory (1.1.3) (also known as model A [22]) has the following form in the Gaussian approximation

$$\partial_t \phi(\boldsymbol{x}, t) = -\overline{D}(-\partial^2 + \xi^{-2}) \phi(\boldsymbol{x}, t) + \eta(\boldsymbol{x}, t) \ , \tag{1.3.6}$$

where we have identified the correlation length $\xi_0 \propto \tau^{-1/2}$. The solution for the classical field $\Phi(\boldsymbol{k}, t) = \langle \phi(\boldsymbol{k}, t) \rangle$ can be found in the $\boldsymbol{k}, t$ representation as

$$\Phi(\boldsymbol{k}, t) \sim e^{-t/\tau_{\boldsymbol{k}}}, \quad \tau_{\boldsymbol{k}} = \frac{1}{\overline{D}(k^2 + \xi^{-2})} \ , \tag{1.3.7}$$

where $\tau_{\boldsymbol{k}}$ is the *relaxation time* (second correlation length). At the critical point $T \to T_c$ for the large scale behaviour $\boldsymbol{k} \to 0$ one obtains the following relation

$$\tau_{\boldsymbol{k}=0} \propto \xi^z \ , \tag{1.3.8}$$

where z is called the *dynamical exponent*. The value of this exponent is 2 in the mean-field approximation and corrections might be calculated using RG methods. There are, of course, other values for different models [22].

1.3.1   Iterative solution to the Langevin equation

One of the reasons why equations such as (1.3.3) cannot be solved analytically is due to nonlinearities on the right hand side. In order to treat nonlinearities perturbatively, Wyld introduced an iterative diagrammatic method [8]. Here we will give a schematic description of his approach.

First, we will rewrite (1.3.3) into more compact form

$$\partial_t \varphi(\boldsymbol{x}, t) = U(\varphi; \boldsymbol{x}, t) + \eta(\varphi; \boldsymbol{x}, t), \quad \langle \eta(\varphi; \boldsymbol{x}', t')\eta(\varphi; \boldsymbol{x}, t) \rangle = D(\varphi; \boldsymbol{x}', t'; \boldsymbol{x}, t) \ , \tag{1.3.9}$$

where $\varphi(\boldsymbol{x}, t)$ can represent a whole set of fields, $\eta(\varphi; \boldsymbol{x}, t)$ is a (Gaussian) random force and $U(\varphi; \boldsymbol{x}, t)$ is a given t-local functional not containing time derivatives of φ with a structure

$$U(\varphi; \boldsymbol{x}, t) = L\varphi(\boldsymbol{x}, t) + n(\varphi; \boldsymbol{x}, t) \ . \tag{1.3.10}$$

Here, $L\varphi(\boldsymbol{x}, t)$ is linear in $\varphi(\boldsymbol{x}, t)$ and all the nonlinear contributions are stored in $n(\varphi; \boldsymbol{x}, t)$. The linear problem (1.3.9) can be solved exactly, while the nonlinear part $n(\varphi; \boldsymbol{x}, t)$ has to be solved perturbatively by iterating the equation (1.3.9). To do this, we rewrite it into (we will now skip writing explicit variable dependencies)

$$\varphi = \Delta_{12}[n(\varphi) + \eta], \quad \Delta_{12} = (\partial_t - L)^{-1} \ , \tag{1.3.11}$$

where $\Delta_{12} = \Delta_{12}(\boldsymbol{x}', t'; \boldsymbol{x}, t)$ is the retarded Green's function (meaning $\Delta_{12}(\boldsymbol{x}', t'; \boldsymbol{x}, t) = 0$ for $t < t'$) of the linear operator $\partial_t - L$.

As a simple example, let us consider the case $n(\varphi) = g\varphi^2/2$ where g is a coupling constant. The solution to (1.3.11) can then be represented graphically as

$$\tag{1.3.12}$$

$$\tag{1.3.13}$$

where φ is represented by the wavy external line (tail), η by the cross, and Δ_{12} by the straight line with marked end corresponding to the argument $(\boldsymbol{x}', t')$. In QFT language this marks propagator and physically it represents the propagation of the perturbation due to the random force η. The point where the three graphical elements are joined is associated with the vertex factor $g/2$. In order to obtain correlation functions we have to multiply the corresponding number of fields φ together and average them over all possible realizations of the random force η. Graphically this leads to contracted pairs creating the

correlator D in all possible ways. Therefore we will obtain a new element - pair correlation functions of the field φ in the lowest approximation $\langle \varphi \varphi \rangle_0$

$$\Delta_{11} \equiv \langle \varphi \varphi \rangle_0 = \Delta_{12} \langle \eta \eta \rangle \Delta_{21} = \Delta_{12} D \Delta_{21} \tag{1.3.14}$$

$$= \left\langle \bullet\!\!-\!\!\times \quad \times\!\!-\!\!\bullet \right\rangle = \bullet\!\!-\!\!\sim\!\!-\!\!\bullet = \text{————} \;, \tag{1.3.15}$$

where the wavy line represents the correlator D from (1.3.9) and

$$\Delta_{21}(\boldsymbol{x}', t'; \boldsymbol{x}, t) = \Delta_{12}^T(\boldsymbol{x}', t'; \boldsymbol{x}, t) = \Delta_{12}(\boldsymbol{x}, t; \boldsymbol{x}', t') \;, \tag{1.3.16}$$

where T denotes the shift of variables with primed variables together with vector indexes. Physically the propagator can be (1.3.14) interpreted as a propagation of perturbation towards both sides from the "two point vertex" in the middle. Corrections to this correlation function are constructed from the graphical elements of (1.3.12) that contain triple vertices and the lines Δ_{11} and Δ_{12}

$$\left\langle \bullet\!\!-\!\!\!\prec\!\!\!\succ\!\!-\!\!\bullet \right\rangle = \bullet\!\!-\!\!\prec\!\!\!\!\!\sim\!\!\!\!\!\succ\!\!-\!\!\bullet = \text{——}\!\!\bigcirc\!\!\text{——} \;. \tag{1.3.17}$$

In this way we can construct a perturbative solution to our problem. One also sees that we are somehow constructing Feynman diagrams from Chapter 1.2. These are the basic ideas behind the equivalence of field-theoretic models and stochastic processes that are going be formulated in the more general theorem in the following section.

1.3.2 De Dominicis-Janssen action functional

The algorithm of calculating expectation values described in the last section is quite cumbersome. A more effective way of performing perturbation theory is to use field-theoretic methods. Here we will describe the derivation of the action functional formalism for classical stochastic processes described by the Langevin equation[13] (1.3.9) [6, 11, 16, 22].

From now on, the integration over all variables that are not written explicitly will be always assumed (if not specified explicitly), i.e.

$$A\varphi \equiv \int \mathrm{d}^d x \mathrm{d}t \; A(\boldsymbol{x}, t)\varphi(\boldsymbol{x}, t) \;, \tag{1.3.18}$$

where d is the dimension of the space and A, φ are some fields. Consider the stochastic process described by the Langevin equation (1.3.9) with (1.3.10) and the two-point random force correlator that is δ correlated in space and time $D(\varphi; \boldsymbol{x}', t'; \boldsymbol{x}, t) = \tilde{D}(\varphi; \boldsymbol{x}, t)\delta(\boldsymbol{x} - \boldsymbol{x}')\delta(t - t')$. Suppose that the probability distribution for the random force can be found from (1.3.9) as

$$\mathcal{W}[\eta] \propto \exp\left\{-\eta D^{-1}\eta/4\right\} \;, \tag{1.3.19}$$

where the integration over all variables and summation over all indexes is implied[14]. Since D may generally be an operator involving gradients, D^{-1} should be understood as

---

[13]The construction of the field theory for the stochastic problem can be also done using the Fokker-Planck equation [32].

[14]Generally we could have stochastic process described by the set of fields φ_i. Corresponding probability distribution will be then proportional to $\exp\{-\eta_i (D^{-1})_{ij}\eta_j\}$ were η_i is the random force that acts on the field φ_i.

a Green's function. Suppose that $\overline{\varphi}$ is a solution of (1.3.9) with an initial condition φ_0 at $t \to -\infty$ and a given force η. The generating functional of the correlation functions of the stochastic problem is the functional

$$\mathcal{Z}[A] = \int \mathcal{D}\eta \, \mathcal{W}[\eta] \exp\{A\overline{\varphi}\} \ , \tag{1.3.20}$$

where A represents an external source of perturbations and the normalization $\mathcal{Z}[0] = 1$ is implied. The right hand side can be rewritten using the following formula

$$\exp\{A\overline{\varphi}\} = \int \mathcal{D}\varphi \, \delta(\varphi - \overline{\varphi}) \exp\{A\varphi\} \ , \tag{1.3.21}$$

with a δ function $\delta(\varphi - \overline{\varphi}) \equiv \Pi_{\boldsymbol{x},t}(\varphi(\boldsymbol{x},t) - \overline{\varphi}(\boldsymbol{x},t))$. We know that φ will be our solution $\overline{\varphi}$ only if the Langevin equation is satisfied, i.e. $\varphi = \overline{\varphi} \Leftrightarrow Q(\varphi,\eta) = -\partial_t\varphi + U(\varphi) + \eta = 0$. Therefore, the following coordinate transformation can be performed

$$\delta(\varphi - \overline{\varphi}) = \det M \, \delta(Q(\varphi,\eta)), \quad M = \frac{\delta Q}{\delta\varphi} \ . \tag{1.3.22}$$

Performing the Fourier transformation of the delta function and then substituting $i\varphi' \to \varphi'$ we obtain

$$\exp\{A\overline{\varphi}\} = \int \mathcal{D}\varphi'\mathcal{D}\varphi \, \det M(\varphi) \exp\{\varphi'Q(\varphi,\eta) + A\varphi\} \ , \tag{1.3.23}$$

where one has to keep in mind that φ' generally represents a complex field. Now one can easily integrate out a random force η from (1.3.20) and obtain

$$\mathcal{Z}[A] = \int D\varphi'\mathcal{D}\varphi \, \exp\{-\mathcal{S}[\varphi',\varphi] + A\varphi\} \ , \tag{1.3.24}$$

$$\mathcal{S}[\varphi',\varphi] = -\frac{1}{2}\varphi'D\varphi' + \varphi'(\partial_t\varphi - U(\varphi)) \ , \tag{1.3.25}$$

where $\det M(\varphi)$ has been skipped, since it yields only an unimportant constant[16, 22]. Action functional (1.3.25) is also known as *De Dominicis-Janssen action functional*[11] and the field φ' is sometimes referred as *Martin-Siggia-Rose response field*. It is usually convenient to also introduce the source A' of the field φ' so that the correlation function can be found as

$$G^{(n,n')}(\{\boldsymbol{x}_i,t_i\}) = \frac{1}{\mathcal{Z}[0,0]} \frac{\delta^N \mathcal{Z}[A,A']}{\delta A(\boldsymbol{x}_1,t_1)\cdots\delta A(\boldsymbol{x}_n,t_n)\delta A'(\boldsymbol{x}_{1'},t_{1'})\cdots\delta A'(\boldsymbol{x}_{n'},t_{n'})}\Bigg|_{A,A'=0} . \tag{1.3.26}$$

The variational derivative with respect to sources A and A' reproduces both correlation functions of a type (1.2.1) and the response functions (1.3.5). The role of η is therefore played by the value of A' in the final expressions. Similarly we can obtain the vertex functions $\Gamma^{(n,n')}$ from the effective action Γ as in the case of static models (see section 1.2.2).

Perturbation theory of models such as (1.3.24) goes in the standard way as in the case of static systems described in the section 1.2. Propagators are found from the quadratic part of the action functional, while the vertex factors are obtained from the interaction part. However, models such as (1.3.24) usually contain a multi-component field action

functional and the quadratic part therefore has a form of scalar product of a matrix and two multi-field component "vectors" . For example, in the case of model A [22], the action functional reads

$$\mathcal{S}[\phi, \phi'] = -\frac{1}{2}\phi' D \phi' + \phi'(\partial_t - \overline{D}(-\partial^2 + \tau))\phi + \frac{g}{3!}\phi'\phi , \qquad (1.3.27)$$

where the integration over all variables is implied, $D(\boldsymbol{x}, t, \boldsymbol{x}', t') = \tilde{D}\delta(\boldsymbol{x} - \boldsymbol{x}')\delta(t - t')$ is the random force correlator and $\tilde{D}$ is some constant. The quadratic part can be rewritten as

$$\mathcal{S}_0[\phi', \phi] = \frac{1}{2} \begin{pmatrix} \phi' \\ \phi \end{pmatrix}^\dagger \begin{pmatrix} (-\tilde{D}) & \partial_t - \overline{D}(-\partial^2 + \tau) \\ \{\partial_t - \overline{D}(-\partial^2 + \tau)\}^\dagger & 0 \end{pmatrix} \begin{pmatrix} \phi' \\ \phi \end{pmatrix} . \qquad (1.3.28)$$

Inverting the above matrix, propagators are found to be [22]

$$G_0^{\phi\phi'}(\boldsymbol{k}, \omega) = \frac{1}{-i\omega + \overline{D}(k^2 + \tau)}, \quad G_0^{\phi\phi}(\boldsymbol{k}, \omega) = \frac{\tilde{D}}{\omega^2 + \overline{D}^2(k^2 + \tau)^2} , \qquad (1.3.29)$$

or in the $(\boldsymbol{k}, t)$ space

$$G_0^{\phi\phi'}(\boldsymbol{k}, t) = \theta(t)\exp\{-\overline{D}(k^2 + \tau)t\} , \qquad (1.3.30)$$

$$G_0^{\phi\phi}(\boldsymbol{k}, t) = \frac{\tilde{D}}{k^2 + \tau}\exp\{-\overline{D}(k^2 + \tau)|t|\} , \qquad (1.3.31)$$

where $\theta(t)$ is the Heaviside step function. One should notice that propagators $G_0^{\phi\phi'}$ and $G_0^{\phi'\phi} = (G_0^{\phi\phi'})^\dagger$ are *retarded* and *advanced* Green's functions.

The calculation of Feynman diagrams in the case of dynamical systems is more complex. In contrast to static processes, where in the momentum space the loop integration goes only over the loop momentum, in dynamical systems the integration has to be taken also over the loop frequency. Usually, these integrals do no not contain divergences, and residue theorem can easily be applied. This also leads to some simplifications in the calculation of the Feynman diagrams [22]. Consider vertex function with zero external fields ϕ'. Loop corrections will contain calculation of closed loops of retarded Green's functions $G_0^{\phi\phi'}$ and they will therefore vanish. In other words, for the calculation of vertex functions, it is sufficient to consider only functions with at least one field ϕ'.

1.3.3   Dynamical Renormalization group

In the field-theoretic formulation of dynamical systems such as (1.3.24) one struggles with the infinities arising from the loop calculations as well. On the other hand, methods of renormalization and renormalization group introduced for static systems in 1.2 can be applied with a straightforward generalization [16, 22].

First, one has to correctly renormalize the correlation and vertex functions, which in momentum space reads

$$G_R^{(n',n)}(\{\boldsymbol{k}_i\}, \{\omega_i\}; g_R(\mu), \tau_R(\mu), \mu) = Z_\varphi^{-n'}(g_R(\mu))Z_{\varphi'}^{-n}(g_R(\mu))G_0^{(n',n)}(\{\boldsymbol{k}_i\}, \{\omega_i\}; g_0, \tau_0) , \qquad (1.3.32)$$

$$\Gamma_R^{(n',n)}(\{\boldsymbol{k}_i\}, \{\omega_i\}; g_R(\mu), \tau_R(\mu), \mu) = Z_\varphi^{n'}(g_R(\mu))Z_{\varphi'}^{n}(g_R(\mu))\Gamma_0^{(n',n)}(\{\boldsymbol{k}_i\}, \{\omega_i\}; g_0, \tau_0) , \qquad (1.3.33)$$

where $\{\boldsymbol{k}_i\}$ and $\{\omega_i\}$ are the whole sets of momenta and frequencies, g is a set of massless parameters, τ the whole set of massive parameters and μ is the renormalized mass scale introduced in (1.2.56). After the renormalizaton, one can then find anomalous behaviour in the large scale and long time scaling properties of the systems similarly as described above.

In contrast to static systems, any dynamical quantity F is described by two numbers – the frequency dimension d_F^ω and the momentum dimension d_F^k such that $[F] \sim [L]^{-d_F^k}[T]^{-d_F^\omega}$. From the Fourier transformation (A.1.1) we can identify relations

$$d_k^k = -d_x^k = 1, \quad d_\omega^k = d_t^k = 0 \ , \tag{1.3.34}$$

$$d_\omega^\omega = -d_t^\omega = 1, \quad d_k^\omega = d_x^\omega = 0 \ . \tag{1.3.35}$$

Using generalized homogeneity (1.2.65), independent equations for renormalized (n', n) point correlation functions are derived, one for space and one for time scale dimension

$$\left(\mathcal{D}_\mu + \mathcal{D}_{\boldsymbol{k}} + d_e^k \mathcal{D}_e - d_\varphi^k n - d_{\varphi'}^k n'\right) G_R^{(n',n)}(\{\boldsymbol{k}_i\}, \omega, e_R(\mu)) = 0 \ , \tag{1.3.36}$$

$$\left(\mathcal{D}_\omega + d_e^\omega \mathcal{D}_e - d_\varphi^\omega n - d_{\varphi'}^\omega n'\right) G_R^{(n',n)}(\{\boldsymbol{k}_i\}, \omega, e_R(\mu)) = 0 \ , \tag{1.3.37}$$

where again $\mathcal{D}_e = e\partial_e$ with e being the set of all parameters of the theory (masses and coupling constants). The idea now is to introduce the *total canonical dimension* d_F (or the total scaling dimension) for the quantity F that will take the same role as the classical canonical dimension in static systems. In order to do that we sum equations (1.3.36) with (1.3.37) multiplied by a *frequency dimension* d_ω and obtain

$$\left(\mathcal{D}_\mu + \mathcal{D}_{\boldsymbol{k}} + d_\omega \mathcal{D}_\omega + d_e \mathcal{D}_e - d_\varphi n - d_{\varphi'} n'\right) G_R^{(n',n)}(\{\boldsymbol{k}_i\}, \omega, e_R(\mu)) = 0 \ , \tag{1.3.38}$$

where the total canonical dimension is

$$d_F = d_F^k + d_\omega d_F^\omega \ . \tag{1.3.39}$$

One has to keep in mind that this is not a real dimension in any way. It only tells us how the parameters of the theory are going to be scaled within our choice of d_ω[15]. The reason for the multiplication with d_ω is the following. The linear operator L in dynamical systems (1.3.9) usually has the form of $\partial_t + \text{const} \cdot \partial^{d_\omega}$. The proper choice of d_ω can actually make the proportionality constant dimensionless, which will simplify the renormalization procedure. We shall take this dimension to be[16] $d_\omega = -d_\nu^k/d_\nu^\omega$, where ν is some parameter of the theory that will become dimensionless (usually viscosity or a diffusion constant). In the language of RG it means that ν is marginal. The RG equation then tells us

$$\left(\mathcal{D}_\mu + \beta_g \partial_{g_R} - \gamma_\nu \partial_{\nu_R} - \gamma_\tau \partial_{\tau_R}\right) G_R^{(n',n)}(\{\boldsymbol{k}_i\}, \omega, g_R(\mu), \nu_R(\mu), \tau_R(\mu)) = 0 \ , \tag{1.3.40}$$

where g_R represents the whole set of renormalized dimensionless (in both momentum and frequency space) parameters, ν_R is massless only due to the proper choice of d_ω and τ_R can be the whole set of parameters with nonzero total dimension. If one tries now to use the last equation in order to eliminate $\mathcal{D}_\mu$ from (1.3.38)(while looking at the large scale and long time behaviour described by the IR fixed point $\beta_{g_R}(g_R^*) = 0$), one will obtain

---

[15]In the sense of Wilsonian RG that would mean that we scale variables as $\boldsymbol{k} \to \boldsymbol{k}' = b\boldsymbol{k}$, $\omega \to \omega' = b^{d_\omega}\omega$.

[16]It most of the models the choice is $d_\omega = 2$ (for example model A,C and reaction diffusion systems), but in some other cases $d_\omega = 4$ (for example model B,J). See [22] for more details.

the scaling equation that will still contain $\gamma_{\nu_R}^* \mathcal{D}_{\nu_R}$. This term can be eliminated using the frequency space homogeneity equation (1.3.37), and the result will be the *total effective homogeneity differential equation*

$$\left(\mathcal{D}_{\boldsymbol{k}} + \Delta_\omega \mathcal{D}_\omega + \Delta_\tau \mathcal{D}_{\tau_R} - \Delta_\varphi n - \Delta_{\varphi'} n'\right) G_R^{(n',n)}(\{\boldsymbol{k}_i\}, \omega, g_R(\mu), \nu_R(\mu), \tau_R(\mu)) = 0 \ , \tag{1.3.41}$$

where

$$\Delta_i = d_i^k + \Delta_\omega d_i^\omega + \gamma_i^* \quad i \in \{\tau_R, \varphi, \varphi'\}, \quad \Delta_\omega = -\frac{d_\nu^k + \gamma_\nu^*}{d_\nu^\omega} \ . \tag{1.3.42}$$

As we can see again from (1.3.41), the arbitrarily mass scale μ modifies the total canonical dimension of parameters of the model, and we obtain the *effective dimensions* Δ_F.

In dynamical systems the renormalization of vertex functions is considered according to the total canonical dimension. The total canonical dimension d_Γ of 1-irreducible functions Γ (equivalent to the total canonical dimension (1.2.61) in static systems) with n_Φ number of fields $\Phi = \varphi, \varphi'$ is given by following relations

$$d_\Gamma^p = d - \sum_\Phi n_\Phi d_\Phi^p, \quad d_\Gamma^\omega = 1 - \sum_\Phi n_\Phi d_\Phi^\omega \ , \tag{1.3.43}$$

$$d_\Gamma = d + d_\omega - \sum_\Phi n_\Phi d_\Phi, \quad d_\Phi = d_\Phi^p + d_\omega d_\Phi^\omega \ . \tag{1.3.44}$$

While calculating contributions, one has to consider possible modifications (for example real UV exponent (1.2.63)) and various symmetries e.g. isotropy, Galilean invariance.

1.4 Reaction-diffusion processes

Reaction-diffusion processes describe various problems in nature such as chemical reactions, predator-prey problems etc. The usual approach is made in terms of kinetic rate equations [26] for the concentration field $n(\boldsymbol{x}, t)$. One can also perform a simple approximation and assume that the density is spatially homogeneous $n = n(t)$. For example, in this approximation the kinetic rate equation of the annihilation reaction $A + A \to \emptyset$ is [26]

$$\partial_t n(t) = -K n^2(t) \ , \tag{1.4.1}$$

with the solution

$$n(t) = \frac{n_0}{1 + n_0 K t} \xrightarrow{t \to \infty} n(t) \propto t^\gamma \ , \tag{1.4.2}$$

where K is the reaction rate for the $A + A \to \emptyset$ reaction and $n_0 = n(0)$. It is clear from (1.4.2) that the long time behaviour is described by the exponent $\gamma = 1$, which seems to be universal and does not depend on the microscopic properties of the molecule A. Since we are neglecting density fluctuations, these results are referred to as a mean-field approximation. Similarly to the in theory of critical phenomena, they are valid above a certain critical dimension d_c, which depends on the structure of the reaction (in this case it can be shown that $d_c = 2$ [23]). Below d_c, another approach has to be taken. In what follows, we will give a schematic description of a field-theoretic formulation that can be used for calculating corrections to this mean-field approximation. A more detailed description can be found in [23, 33].

1.4.1   Doi's second-quantized representation

Let us consider the d-dimensional hypercubic lattice with lattice spacing l. The lattice sites are labeled by $i = 1, 2, \cdots$. Particles A can diffuse on this lattice by hopping to the nearest lattice sites with the probability D. Let us also consider the simple reaction process - particles can annihilate with the probability λ. The full description of such a stochastic problem is given in terms of probabilities $P(t, \{n\})$, where $\{n\} = \{n_1, n_2, \dots\}$ and n_i represent the number of particles on the site i, given by a set of the Master equations [26]

$$\frac{\mathrm{d}P(t; \{n\})}{\mathrm{d}t} = \sum_m R_{m \to n} P(t; \{m\}) - \sum_m R_{n \to m} P(t; \{n\}) , \qquad (1.4.3)$$

where $P(t, \{n\})$ is the probability of the system being in the system configuration $\{n\}$ at time t, $R_{m \to n}$ is the transition probability from the state m to the state n, and the sum goes over all lattice configurations n and m, respectively. Following the work of Doi [13], this problem can be rewritten in terms of creation and annihilation operators well-know from quantum mechanics (also known as second quantization). This allows us to find perturbative solutions to correlations and response functions. If we don't consider any restriction on the site occupations we can introduce bosonic operators for each lattice site i with the following commutation relations

$$[a_i, a_j^\dagger] = \delta_{ij}, \quad [a_i, a_j] = [a_i^\dagger, a_j^\dagger] = 0 , \qquad (1.4.4)$$

where the ground state $|0\rangle$ is defined as

$$a_i |0\rangle = 0 \quad \text{for all sites } i. \qquad (1.4.5)$$

The state $|\{n\}\rangle$ that represents the lattice configuration $\{n\} = \{n_1, n_2, \cdots\}$ is then defined as

$$|\{n\}\rangle = a_1^{\dagger n_1} a_2^{\dagger n_2} \dots |0\rangle . \qquad (1.4.6)$$

It can be shown that the following relations hold (note the different normalization that arises here and in the second quantization method in quantum field theory)

$$a_i^\dagger |\{n\}\rangle = |\{n_1, n_2, \dots, n_i + 1, \dots\}\rangle , \qquad (1.4.7)$$
$$a_i |\{n\}\rangle = n_i |\{n_1, n_2, \dots, n_i - 1, \dots\}\rangle , \qquad (1.4.8)$$
$$a_i^\dagger a_i |\{n\}\rangle = n_i |\{n\}\rangle , \qquad (1.4.9)$$

where in the last row one can define the particle number operator

$$n_i = a_i^\dagger a_i . \qquad (1.4.10)$$

We can associate a state in the Fock-Space with a set of probabilities at time t (also known as the Doi formalism)

$$|\Phi(t)\rangle \equiv \sum_{\{n\}} P(t; \{n\}) |\{n\}\rangle , \qquad (1.4.11)$$

where the summation goes over all possible lattice configurations. This allows us to rewrite the Master equation into a Schrödinger-like form[17] for the state vector $|\Phi(t)\rangle$

$$\frac{\mathrm{d}}{\mathrm{d}t}|\Phi(t)\rangle = -\mathcal{H}|\Phi(t)\rangle \ , \tag{1.4.12}$$

with some "Hamiltonian" $\mathcal{H}$, which will be calculated later, and its exact form depends on the system under consideration. The formal solution to last equation can be written as

$$|\Phi(t)\rangle = \mathrm{e}^{-\mathcal{H}t}|\Phi(0)\rangle \ , \tag{1.4.13}$$

with an initial state $|\Phi(0)\rangle$ that needs to be specified. In the case of chemical reactions, the initial probability distribution $P(0,\{n\})$ is usually known, and therefore the initial state can be calculated from (1.4.11). From a technical point of view, in the case of mono-molecular reactions it is most convenient to chose the Poisson distribution

$$P(0;\{n\}) = \prod_i \left(\frac{\overline{n}^{n_i}}{n_i!} e^{-\overline{n}} \right) \ , \tag{1.4.14}$$

where $\overline{n}$ stands for the mean particle number (initial density of the particles). This corresponds to the initial state

$$|\Phi(0)\rangle = \sum_{\{n_1\}} \mathrm{e}^{-\overline{n}} \frac{\overline{n}^{n_1}}{n_1!} a_1^{\dagger n_1} \sum_{\{n_2\}} \mathrm{e}^{-\overline{n}} \frac{\overline{n}^{n_2}}{n_2!} a_2^{\dagger n_2} \dots |0\rangle \ . \tag{1.4.15}$$

In fact, single species reaction processes are unlike bi-molecular reactions independent of the initial conditions [34].

1.4.2 Single species annihilation reaction-diffusion process

We can separate the full "Hamiltonian" into two parts: diffusion and reaction. These parts can be handled separately as follows.

Diffusion. We first derive the diffusion part $\mathcal{H}_D$ of the full "Hamiltonian" $\mathcal{H}$ which corresponds to the random walk of the A particles. For simplicity we start only with n_1 and n_2 particles on sites 1 and 2 respectively. Particles are allowed to perform one-way hopping process $1 \to 2$ with the probability D. The master equation (1.4.3) of this process is

$$\frac{\mathrm{d}P(t;n_1,n_2)}{\mathrm{d}t} = D\Big[(n_1+1)P(t;n_1+1,n_2-1) - n_1 P(t;n_1,n_2)\Big] \ , \tag{1.4.16}$$

where the combinatorial factors n_1+1 and n_1 arise from the fact that particles jump independently of each other. Multiplying the last equation by the state (1.4.6) and performing the sum over all possible occupations yields

$$\frac{\mathrm{d}}{\mathrm{d}t} \sum_{\{n_1,n_2\}} P(t;n_1,n_2)|n_1,n_2\rangle =$$
$$= D \sum_{\{n_1,n_2\}} \Big[a_2^\dagger a_1 P(t;n_1+1,n_2-1)|n_1+1,n_2-1\rangle - a_1^\dagger a_1 P(t;n_1,n_2)|n_1,n_2\rangle \Big] \ .$$

---

[17]Or imaginary time Schrödinger equation.

This can be rewritten using the definition of state (1.4.11) as

$$\frac{\mathrm{d}|\Phi\rangle}{\mathrm{d}t} = D(a_2^\dagger - a_1^\dagger)a_1|\Phi\rangle \ . \tag{1.4.17}$$

If we now assume that particles can hop also from site 2 to site 1 we arrive at

$$\frac{\mathrm{d}|\Phi\rangle}{\mathrm{d}t} = -D(a_2^\dagger - a_1^\dagger)\,(a_2 - a_1)\,|\Phi\rangle \implies \mathcal{H}_D^{(1\leftrightarrow2)} = D(a_2^\dagger - a_1^\dagger)\,(a_2 - a_1)\ , \tag{1.4.18}$$

where we identify $1 \leftrightarrow 2$ hopping Hamiltonian $\mathcal{H}_D^{(1\leftrightarrow2)}$. This procedure can be easily generalized to include all the lattice sites via the Master equation

$$\frac{\mathrm{d}P(t;\{n\})}{\mathrm{d}t} = D\sum_{\langle i,j\rangle}\Big[(n_i + 1)P(t;\dots,n_i+1,n_j-1,\dots) - n_i P(t;\dots,n_i,n_j,\dots)\Big]\ , \tag{1.4.19}$$

where $\langle i,j\rangle$ represents sum over nearest neighbours. The resulting Schrödinger-like equation and diffusion Hamiltonian are

$$\frac{\mathrm{d}|\Phi\rangle}{\mathrm{d}t} = -D\sum_{\langle i,j\rangle}(a_i^\dagger - a_j^\dagger)\,(a_i - a_j)\,|\Phi\rangle \implies \boxed{\mathcal{H}_D = D\sum_{\langle i,j\rangle}(a_i^\dagger - a_j^\dagger)\,(a_i - a_j)}\ . \tag{1.4.20}$$

Reactions. Let us now consider the single species annihilation reaction $A + A \xrightarrow{\lambda} \emptyset$ on a single site. The corresponding Master equation of this process is

$$\frac{\mathrm{d}P(n)}{\mathrm{d}t} = \lambda\big[(n+2)(n+1)P(n+2) - n(n-1)P(n)\big]\ , \tag{1.4.21}$$

where $(n+i)$ are again combinatorial factors that arise from the fact that any particles can react together. Similar to above algebra, (1.4.21) can be rewritten into the Doi formalism

$$\frac{\mathrm{d}|\Phi\rangle}{\mathrm{d}t} = \lambda(a^2 - a^{\dagger2}a^2)|\Phi\rangle \ . \tag{1.4.22}$$

This can be generalized to the whole lattice by summing over all lattice sites and after that we identify corresponding reaction Hamiltonian to be

$$\boxed{\mathcal{H}_R^{(A+A\to\emptyset)} = \lambda\sum_i(a_i^{\dagger2} - 1)a_i^2}\ . \tag{1.4.23}$$

In conclusion we see that the process contributes to $\mathcal{H}_R$ with two terms of the form

$$(\text{rate})\Big[\textcolor{blue}{(\text{reactants})} - \textcolor{red}{(\text{reactions})}\Big]\ , \tag{1.4.24}$$

$\textcolor{blue}{(\text{reactants})}$ creation and annihilation operators for each reactants (normal ordered)
$\textcolor{red}{(\text{reactions})}$ annihilation operators for each reactions, creation operator for each product (normal ordered)
  Some examples are [23]

$$\begin{aligned}
A + A \xrightarrow{\lambda} \emptyset :&\quad \lambda\big[a^{\dagger2}a^2 - a^2\big]\ , &\quad \text{Hop } 1 \xrightarrow{D} 2 :&\quad D\big[a_1^\dagger a_1 - a_2^\dagger a_1\big]\ , \\
A \xrightarrow{\rho} A + A :&\quad \rho\big[a^\dagger a - a^{\dagger2}a\big]\ , &\quad A + B \xrightarrow{\sigma} C :&\quad \sigma\big[a^\dagger b^\dagger ab - c^\dagger ab\big]\ .
\end{aligned} \tag{1.4.25}$$

1.4.3 Observables and coherent state path integral formalism

The whole Hamiltonian of the single particle reaction-diffusion system is

$$\mathcal{H} = \mathcal{H}_D + \mathcal{H}_R = D \sum_{\langle i,j \rangle} \left(a_i^\dagger - a_j^\dagger \right) \left(a_i - a_j \right) + \lambda \sum_i \left(a_i^{\dagger 2} - 1 \right) a_i^2 . \tag{1.4.26}$$

Non-hermiticity of such a Hamiltonian means that the reaction rates in (1.4.3) do not satisfy the detailed balance condition and thus the equilibrium state cannot be characterized by the Gibbs distribution. In addition, physical observables $\mathcal{O}$ in the Doi formalism cannot be given as a bilinear product $\langle \Phi | \mathcal{O} | \Phi \rangle$ since according to (1.4.11) this would mean that they would be bilinear in the probability $P(t; \{n\})$. It is physically reasonable to assume that $\mathcal{O}$ can be expressed as a function of the occupation numbers $\mathcal{O} = \mathcal{O}(\{n\})$. The ensemble average of $\mathcal{O}$ is given by

$$\mathcal{O} = \sum_{\{n\}} P(t; \{n\}) \mathcal{O}(\{n\}) . \tag{1.4.27}$$

In order to eliminate the problem of having the product that is bilinear in the probability we try to find the *projection state*[18] $\langle \mathcal{P} |$ such that the following identity is valid

$$\langle \mathcal{O}(t) \rangle = \sum_{\{n\}} P(t; \{n\}) \langle \mathcal{P} | \mathcal{O}(\{a^\dagger a\}) a_1^{\dagger n_1} a_2^{\dagger n_2} \dots | 0 \rangle = \langle \mathcal{P} | \mathcal{O} | \Phi(t) \rangle , \tag{1.4.28}$$

where the operator $\hat{\mathcal{O}}(\{a^\dagger a\})$ can be obtained from $\mathcal{O}(\{n\})$ with the substitution $n_i \to a_i^\dagger a_i$ at every site i. Comparing (1.4.28) and (1.4.27) one can find that the projection state $\langle \mathcal{P} |$ has to satisfy the following conditions

$$\langle \mathcal{P} | a_1^{\dagger n_1} a_2^{\dagger n_2} \dots | 0 \rangle = 1 \implies \langle \mathcal{P} | a_i^\dagger = \langle \mathcal{P} | \quad \forall i, \quad \langle \mathcal{P} | 0 \rangle = 1 . \tag{1.4.29}$$

This state is then found to be

$$\langle \mathcal{P} | = \langle 0 | e^{\sum_i a_i} . \tag{1.4.30}$$

From the conservation of probability we can find another important property

$$1 = \langle \mathcal{P} | e^{-\mathcal{H}(\{a^\dagger, a\})t} | \Phi(0) \rangle \tag{1.4.31}$$

$$= \langle \mathcal{P} | (1 - \mathcal{H}(\{a^\dagger, a\})t + \dots) | \Phi(0) \rangle , \tag{1.4.32}$$

which requires that $\langle \mathcal{P} | \mathcal{H} = 0$ or equivalently using (1.4.29) is

$$\mathcal{H}(\{a^\dagger = 1, a\}) = 0 , \tag{1.4.33}$$

These conditions need to be satisfied for any quasi-Hamiltonian derived using Doi's formalism. Naturally, this is true for our Hamiltonian (1.4.26) and it is an expression for the conservation of probability.

Starting from this point, one can derive the coherent state path integral formulation using standard procedures used in condensed matter field theory [2]. There are certain differences that we will mention, but we will skip the actual derivation here. For a detailed

---

[18]Not to be confused with the projection operator.

derivation see [23]. Following the standard procedures, the expectation value for (1.4.28) is found to be

$$\langle \mathcal{O}(t) \rangle = \int \mathcal{D}\psi' \mathcal{D}\psi \; \mathcal{O}[\psi', \psi] \exp\{-\mathcal{S}[\psi' + 1, \psi]\} \; , \tag{1.4.34}$$

with

$$\mathcal{S}[\psi' + 1, \psi] = \int \mathrm{d}^d x \mathrm{d}t \; \left\{ \psi'(\boldsymbol{x}, t)\partial_t \psi(\boldsymbol{x}, t) - \mathcal{H}[\psi' + 1, \psi] \right\} + n \int \mathrm{d}^d x \; \psi'(\boldsymbol{x}, 0) \; , \tag{1.4.35}$$

which is known as the *Doi-Peliti action functional* [14]. In (1.4.34) and (1.4.35), fields $\psi(\boldsymbol{x}, t)$ and $\psi'(\boldsymbol{x}, t)$ correspond to the coherent state eigenvalues of the bosonic creation and annihilation operators $a_i, a_i^\dagger$ at the position i and the time instance t after performing the continuum limit. One has to keep in mind that these fields are generally complex and even though the field $\psi'(\boldsymbol{x}, t)$ represents a complex conjugated field to the field $\psi(\boldsymbol{x}, t)$, it is quite common in condensed matter physics to tread these fields independently [2].

There are two main differences between (1.4.35) and the usual coherent state path integral formalism. First is the *Doi shift* $\psi' \rightarrow \psi' + 1$ that can be seen in the action functional $\mathcal{S}$ and it is performed due to the long time behaviour of the primed field $\psi'(\boldsymbol{x}, t \rightarrow \infty) = 1$ [23]. This shift is also simplifying the structure of the action functional. The second difference is the appearance of the last term that represents the initial conditions. However, the long time behaviour of the mono-molecular reaction diffusion systems is independent from them, as mentioned above.

The action functional Hamiltonian $\mathcal{H}$ can usually be separated into two parts

$$\mathcal{H}[\psi' + 1, \psi] = \int \mathrm{d}^d x \mathrm{d}t \; \psi'(\boldsymbol{x}, t) D\partial^2 \psi(\boldsymbol{x}, t) + (\text{reactions}) \; , \tag{1.4.36}$$

where D is the diffusion constant and reactions are usually at least of third order in fields[19] ψ, ψ'. This means that from (1.4.35) we can identify the quadratic and the interaction part of the action functional and use perturbative renormalization group for investigating large scale and long time behaviour. From the quadratic part

$$\mathcal{S}_0[\psi' + 1, \psi] = \int \mathrm{d}^d x \mathrm{d}t \; \psi'(\boldsymbol{x}, t) \left(\partial_t - D\partial^2 \right) \psi(\boldsymbol{x}, t) \; , \tag{1.4.37}$$

we can identify the *diffusion propagator* $G_0^{\psi\psi'}(\boldsymbol{x}, t) = \langle \psi(\boldsymbol{x}, t)\psi'(0, 0) \rangle$, which in the Fourier representation has the form

$$G_0^{\psi\psi'}(\boldsymbol{k}, \omega) = \frac{1}{-i\omega + Dk^2} \; , \tag{1.4.38}$$

or in the $\boldsymbol{k}, t$ representation

$$G_0^{\psi\psi'}(\boldsymbol{k}, t) = \theta(t) \exp\{-Dk^2 t\} \; . \tag{1.4.39}$$

The similar situation may occur using the path integral formulation for stochastic processes (1.3.24).

---

[19]Exceptions are, for example, mass terms that will arise later when we will be describing percolation processes.

Chapter 2

Directed percolation

Imagine a simple epidemic process, where an infection is spreading among a number of species (humans, animals, bacteria etc.). If the density of this species is small, the infection will stop after some time. On the other hand, if the density is high enough, then the number of infected will grow exponentially. It is therefore natural to expect that there is a certain critical point where an epidemic breaks out. As mentioned in Chapter 1, in statistical physics various models show universal behaviour around a certain critical point. The epidemic break-out is an example of a dynamical second-order phase transition, called *directed percolation* (later DP). In fact, DP represents a prototype of a second order active-to-absorbing phase transition, i.e. transition from fluctuating phase to the phase from which the system cannot escape. These processes can be seen in various parts of the nature from physics, chemistry, biology to sociology. In this chapter we give a description of its basic properties.

First we introduce DP process generally and describe its general aspects. Assuming a certain microscopic description, we show that there is a continuous phase transition around the critical point. All critical exponents relevant to our problem are then derived in the following way. First we introduce static ($t \to \infty$) critical exponents and show, that their number is reduced due to the time-reversal symmetry. Static scale invariance then allows us to relate these exponents to physically measurable quantities. The physical interpretation of correlation lengths and critical exponents is given. Dynamical critical exponents are then introduced using dynamical scaling and their relation to static critical exponents is established. It turns out that there are only three independent critical exponents describing the DP phase transition.

In the following section we generalize the whole concept introducing the DP conjecture that determines which processes belong to the DP universality class. It turns out that the DP process is not solvable analytically in any spatial dimensions [35]. This also motivates us to use field-theoretic methods in order to study its large-scale behaviour. The field-theoretic formulation is derived using Doi-Peliti formalism described in Section 1.4. The Langevin formulation is found using the equivalence between field-theoretic models and stochastic processes and the mean-field critical exponents are derived. In the end we discuss how to calculate corrections to the mean-field approximation using RG methods and briefly mention experimental realisations of DP.

Time-reversal symmetry plays an important role, it reduces the number of independent critical exponents. However, this symmetry can be violated by introducing a random environment. The concept of time reversal symmetry breaking and its consequences will be discussed in Chapter 4.

2.1   What is directed percolation?

In general, the term percolation (derived from Latin *percolare* = to filter) means physical process of a liquid passing through porous substance, which can be composed of sand, paper or cloth. This problem turns out to be more general, allowing us to investigate properties of various problems in nature.

As a simplest example, imagine a lattice, where pores of the medium are represented by lattice sites. Neighbouring pores are connected via channels (bonds), that can be either open or blocked[1]. Percolating medium (liquid) can start from one point and the *percolating agent* can pass only through unblocked bonds. There are two fundamentally different versions of percolation. In the *isotropic percolation*, agent passes through open channels in any direction. In the *directed percolation*, the agent has a preferred direction of moving which can be caused by the gravitation field, wind force etc. In Fig. 2.1 one can see different paths constructed in two mentioned cases. In this thesis, we restrict ourselves only to directed percolation.

We can mimic the microscopic structure of the system by introducing *percolation probability p* that tells us how probable it is for the agent to pass through bonds. An interesting question might be how does this percolating probability control the behaviour of the system.

As stated above, in DP there is a preferred direction in which the agent is spreading. Temporal sequence of the individual steps allows us to interpret this specific direction as time. For example we may identify the vertical direction as time direction and measure the evolution of number of particles with respect to time $N(t)$. Schematic description is shown in Fig. 2.2. One can see that the percolating agent is passing through unbroken bonds and activating lattice sites.

If we take the percolating agent as an A particle we may interpret percolation process as a *reaction diffusion process*. For example particles A are *diffusing* on the lattice $A+\emptyset \rightarrow A+\emptyset$ if there is only one unbroken bond to percolate through. If there are two unbroken bonds, particles undergo *offspring production* reaction $A \rightarrow A + A$. Since there can be only one particle on the single site, we must consider *coalescence* process, if two particles

---

[1]A different example is a site DP, where the lattice sites are randomly blocked [35].
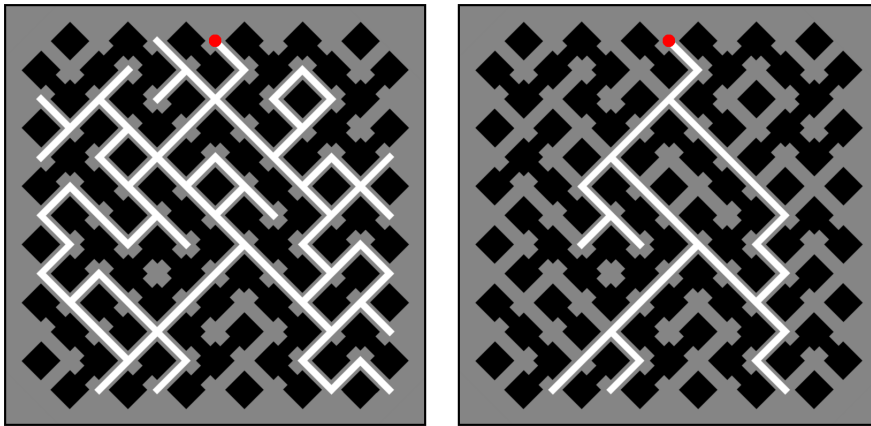
Figure 2.1:   An example of direct and isotropic percolation. In the left Figure, the agent is spreading isotropically while in right Figure the agent is spreading towards one specific direction (down).
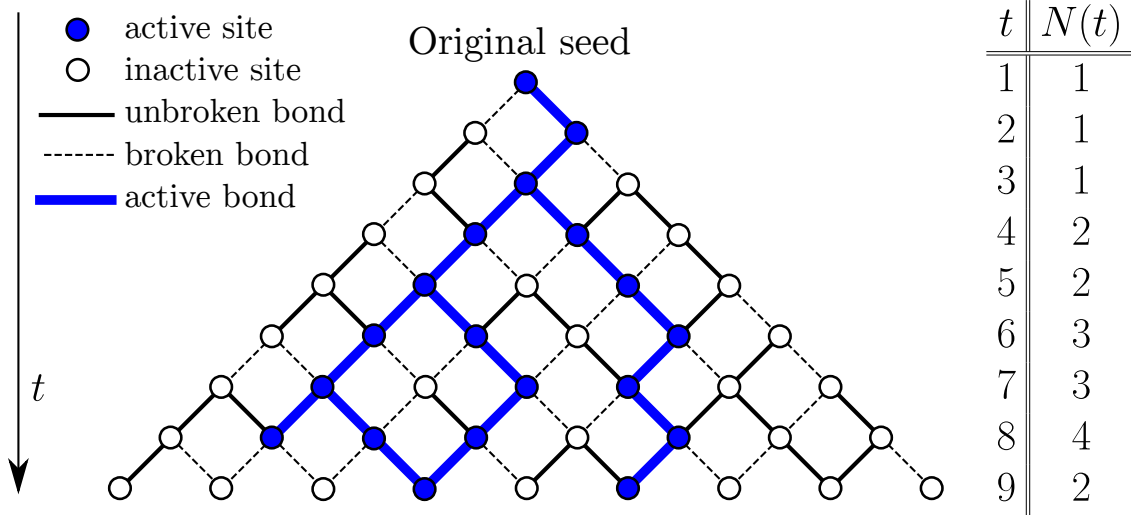
Figure 2.2: Reaction scheme for DP. Percolating agent starts at the top site and goes percolates down (time direction) through unbroken bonds. On the right hand side the evolution of $N(t)$ is depicted.

meet at a single site. Finally, if there is no unbroken bond, particles perform *death* process $A \to \emptyset$. Schematic description is depicted in Fig. 2.3.

It is very instructive to perform a simple numerical simulation and vary the percolation probability p_c. The results can be seen in Fig. 2.4. If the percolation probability is small (smaller than p_c) percolation stops after a short amount of time. If the p is large enough (larger than p_c) the number of particles grow indefinitely. This indicates that there might be a certain *critical percolation probability* p_c between these two *active* and *absorbing* states. It is also interesting to calculate the mean particle value $\langle N(t) \rangle$ as it is shown in Fig. 2.5. Using log-log scale, linear regime can be found at the critical probability $p_c = 0.6447$. This regime exhibits the power-law behaviour

$$\langle N(t) \rangle \propto t^{\Theta} \; , \tag{2.1.1}$$

where the critical exponent attains approximate value $\Theta \approx 0.302$.

2.2 Critical exponents

As has been stated in the section 2.1, DP process can be interpreted as a stochastic reaction-diffusion process with reactions shown in Fig. 2.3. If the probability of the offspring production is sufficiently large, system grows towards infinity - it remains in the *active state*. On the other hand, if the offspring production is sufficiently small, system approaches a state with no particles. Such state, from which system cannot escape, is
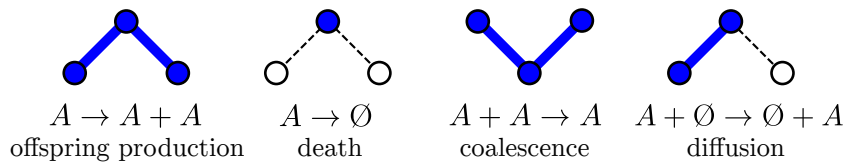
Figure 2.3: Reaction scheme for DP process
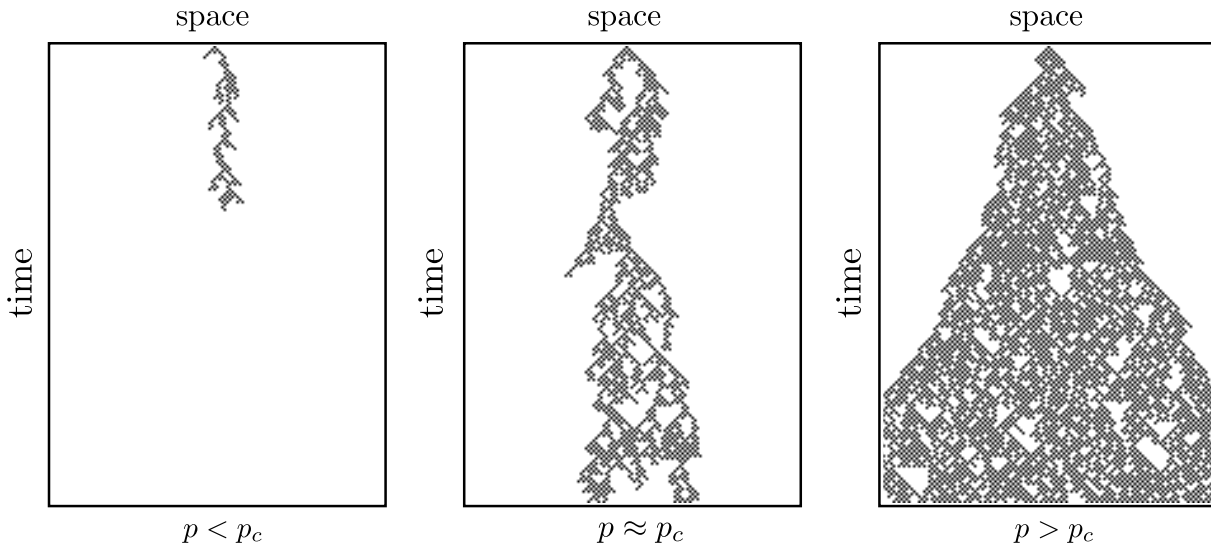
Figure 2.4: DP process in $1 + 1$ dimension for three different percolation probabilities.
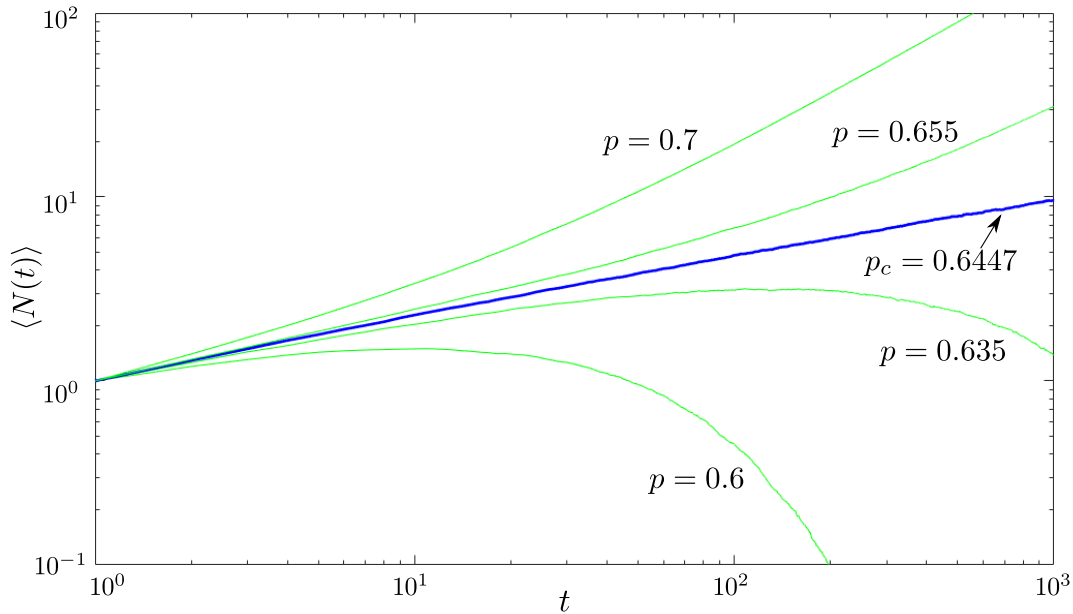
Figure 2.5:   Average number of particles $\langle N(t) \rangle$ with respect to time t for different probabilities plotted in the log-log scale. As we can see, for a certain probability $p_c = 0.6447$ we have linear dependence in log-log scale.

called *absorbing state*. This state cannot be in detailed balance with any active state and therefore the system is said to be out of thermal equilibrium. DP is therefore claimed to exhibit *non-equilibrium phase transition* from the fluctuating phase to the absorbing state. This transition is also referred to as *active-to-absorbing* phase transition[35].

As it has been mentioned in the Chapter 1, static as well as dynamic systems that undergo continuous phase transition can be assigned to certain universality classes which are uniquely characterized by critical exponents. In following sections we show, that in the case of DP there are at least 3 independent critical exponents $\beta, \nu_{||}$ and $\nu_{\perp}$ and we briefly describe DP scaling properties.

2.2.1 Rapidity symmetry

Let us first assume that our model is in active state. In analogy to critical phenomena we consider quantity $\tau \propto p - p_c > 0$ that plays the role of the deviation from the criticality, i.e. the "mass" term. In this case, the system relaxes into a fluctuating steady state with nonzero numbers of active sites. Space-time trajectory of such state can be interpreted as a infinite cluster of active particles which can be described with two different quantities [35]:

- The probability that a given site belongs to the infinite cluster generated at $t_0 = -\infty$ from a fully occupied lattice. This probability is equal to the density ρ of active sites in the stationary state at time t.

- The probability that an isolated seed of activity (a single particle on an empty lattice) at time t_0 will create an infinite cluster when $t \to \infty$. Such quantity is related to the percolation probability P_{perc}

Both of these quantities may be chosen as order parameters of our theory, where the first one is describing the past and the second one the future. In the long time limit $t \to \infty$ we expect them to behave as:

$$\rho \sim \tau^\beta , \quad P_{perc} \sim \tau^{\beta'} , \tag{2.2.1}$$

with two generally *different* critical exponents β and β'. In the case of bond DP, these two exponents merge due to the time reversal symmetry, called *rapidity symmetry* [36].

Let us consider an empty lattice. If we activate a single site at time $t_0 = 0$, we can ask for the probability of finding at least one active site at time t - the *survival probability* $P_{\mathrm{sur}}(t)$. Because there is a finite probability that the cluster will survive in active phase for $t \to \infty$, in the long time limit this probability should tend to a constant called *ultimate survival probability*. Although, this is nothing else than just the percolation probability

$$P_{\mathrm{perc}}(\tau) = \lim_{t \to \infty} P_{\mathrm{sur}}(t; \tau) . \tag{2.2.2}$$

As we can observe from Fig. 2.6, the bond DP process running backward in time can be interpreted as a process running forward in time but the difference is in the exchange of initialisation and measurement. It can be shown [36], that in the case of DP process the probability of finding the direct connection between a single site at $t_0 = 0$ and some site on the horizontal line at time t is equal to the probability of finding a direct connection between a fully occupied line at $t_0 = 0$ and a particular site at time t

$$P_{\mathrm{sur}}(t) = \rho(t) , \tag{2.2.3}$$

which implies that the corresponding critical exponents $\beta = \beta'$ are identical. However, this relation which is the direct result of the rapidity symmetry is not valid for all DP processes. In fact, it is valid only for bond DP processes and for other realisations of DP (like for example site DP) this symmetry is not generally exact [35].

2.2.2 Correlation length and correlation functions

Dynamic systems are usually described by two critical exponents. In the case of DP we can identify the space correlation length $\xi_\perp$ and the time correlation length $\xi_{||}$. In the vicinity of the critical point, they should follow power-law behaviour [35]

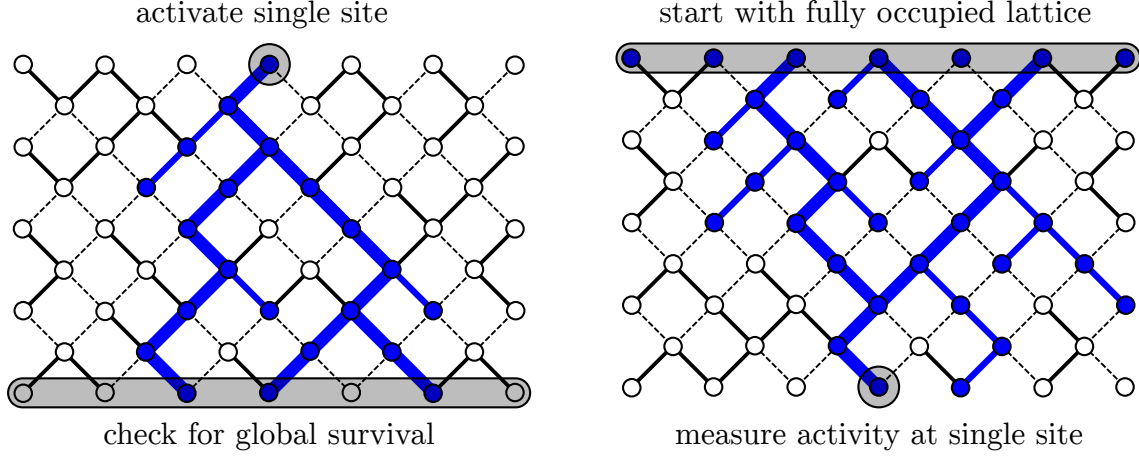$$\xi_\perp \sim |\tau|^{-\nu_\perp} , \quad \xi_{||} \sim |\tau|^{-\nu_{||}} , \tag{2.2.4}$$

Figure 2.6: Rapidity symmetry reversal. As we can see, the evolution of our system is symmetric with respect to the the time reversal symmetry (thick blue line is the same, just inversed).

where $\nu_{||}$ and $\nu_{\perp}$ stand for two different critical exponents that govern their behaviour. In the scaling regime, they are found to be related as follows

$$\xi_{||} \sim \xi_{\perp}^{z} \ , \tag{2.2.5}$$

where $z = \nu_{||}/\nu_{\perp}$ is the dynamical critical exponent [16]. This exponent describes how fast the local perturbation spreads. Three general cases can be distinguished:

- $z = 1$ - deterministic (ballistic) spreading
- $1 < z < 2$ - superdiffusive spreading
- $2 < z$ - subdiffusive spreading

In the case of many-particle models that are described by the short range interactions, the value of this exponent usually varies in the range $1 < z \le 2$. It is also an universal quantity, which means that it also has to be determined by the universality class and the dimension of the system. The physical interpretation of $\xi_{||}$ and $\xi_{\perp}$ can be seen in Fig. 2.7.

2.2.3 Scale invariance

The phenomenological scaling theory for DP phase transition is based on the assumption, that there are only two divergent length scales $\xi_{||}$ and $\xi_{\perp}$. This means, that all critical exponents can be expressed in terms of four independent exponents $\beta, \beta', \nu_{||}, \nu_{\perp}$ (where β and β' coincide if the rapidity symmetry holds) introduced in the previous section.

The crucial assumption is that if we rescale the control parameter, which in our case is the deviation from the criticality, as [35]

$$\tau \to \lambda\tau \ , \tag{2.2.6}$$

all other order parameters and correlation lengths are to be rescaled as follows

$$\rho \to \lambda^{\beta}\rho \ , \quad P_{\mathrm{perc}} \to \lambda^{\beta'} P_{\mathrm{perc}} \ , \quad \xi_{\perp} \to \lambda^{\nu_{\perp}}\xi_{\perp} \ , \quad \xi_{||} \to \lambda^{\nu_{||}}\xi_{||} \ . \tag{2.2.7}$$
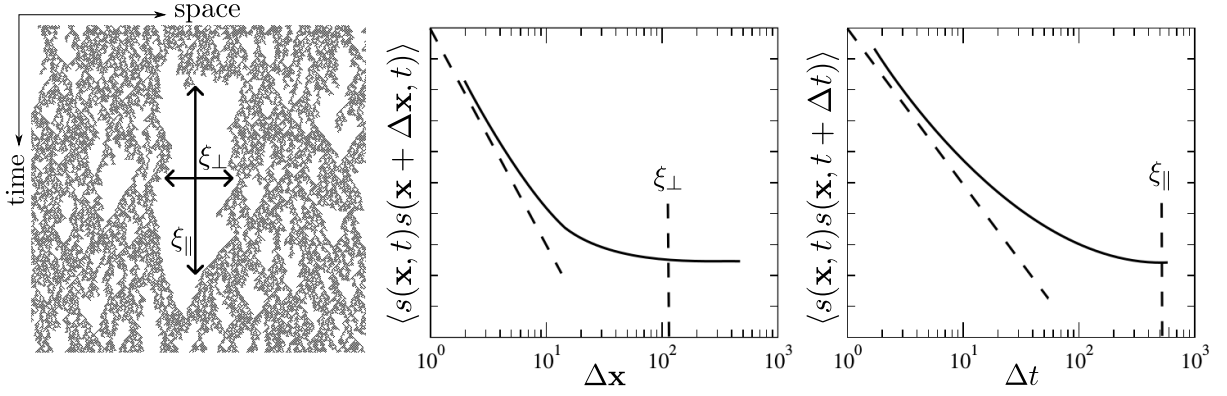
Figure 2.7: A schematic physical interpretation of the correlation lengths $\xi_\perp$ and $\xi_{||}$. Size of the void areas (left) are determined by correlation lengths as well as the slope of the decay (dashed lines on the right) of the two point correlation functions are equal to $-2\beta/\nu_\perp$ and $-2\beta/\nu_{||}$. Results from a simulation can be found for example in [35].

In the same way, scale invariance implies that all measurable quantities and parameters rescale with λ^κ, where κ is the *scaling power*. Since correlation lengths $\xi_{||}$ and $\xi_\perp$ have the dimension of time and length, all spatial and temporal intervals rescale in the same way

$$\Delta t \to \lambda^{-\nu_{||}}\Delta t \ , \quad x \to \lambda^{-\nu_\perp}x \ . \tag{2.2.8}$$

This procedure helps us to find specific universal properties from the function under consideration.

Let us for example take the two point correlation function

$$C(\boldsymbol{x}_1, t_1; \boldsymbol{x}_2, t_2) = \langle s(\boldsymbol{x}_1, t_1)s(\boldsymbol{x}_2, t_2)\rangle \ , \tag{2.2.9}$$

in the active state $\tau > 0$. Due to the spatial and temporal translational invariance and isotropy, we can rewrite (2.2.9) in the following way

$$C(x, \Delta t; \tau) = \langle s(\boldsymbol{x}_1, t_1)s(\boldsymbol{x}_2, t_2)\rangle \ , \tag{2.2.10}$$

where $\Delta t = t_2 - t_1$ and $x = |\boldsymbol{x}_2 - \boldsymbol{x}_1|$. Sufficiently close to the critical point $\tau \approx 0$, we can write the following relation for the correlation function[2]

$$C(\lambda^{-\nu_\perp}x, \lambda^{-\nu_{||}}\Delta t; \lambda\tau) \simeq \lambda^\kappa C(x, \Delta t; \tau) \ , \tag{2.2.11}$$

which holds for any positive λ. We are now free to choose λ in a suitable way, that will simplify the last relation. By choosing $\lambda = \tau^{-1}$, one of the arguments becomes a constant, i.e.,

$$C(x, \Delta t; \tau) \simeq \tau^\kappa C(\tau^{\nu_\perp}x, \tau^{\nu_{||}}\Delta t; 1) = \tau^\kappa c(x/\xi_\perp, \Delta t/\xi_{||}) \ , \tag{2.2.12}$$

where $c(\cdots)$ is a scaling function that does not depend on τ. The value of the scaling exponent κ can be determined by looking at the large scale behaviour in the stationary active state. For the limit $x \to \infty$ any two points become uncorrelated and therefore

---

[2]Symbol $\simeq$ denotes the asymptotic equality, i.e. in this case $f(\tau) \simeq g(\tau) \iff \lim_{\tau \to 0}\frac{f(\tau)}{g(\tau)} = 1$.

$C(\Delta t, \infty; \tau > 0) = \rho^2$. Since we know that the density scales as τ^β we find $\kappa = 2\beta$. Eq. (2.2.12) can be then written as

$$C(x, \Delta t; \tau) \simeq \lambda^{-2\beta} C(\lambda^{-\nu_\perp} x, \lambda^{-\nu_{||}} \Delta t, \lambda \tau) . \tag{2.2.13}$$

Let us now consider the equal time correlation function

$$C(x, 0; \tau) \simeq \lambda^{-2\beta} c(\lambda^{-\nu_\perp} x, 0; \lambda \tau) . \tag{2.2.14}$$

If we now put $\lambda^{-\nu_\perp} x = 1$, we obtain in the vicinity of the critical point $(\tau \to 0)$

$$C(0, x; 0) = x^{-2\beta/\nu_\perp} c(0, 1, 0) \propto x^{-2\beta/\nu_\perp} . \tag{2.2.15}$$

We can show in the same way that the autocorrelation function $(x = 0)$ is proportional to $(\Delta t)^{-\beta/\nu_{||}}$. These results can also be seen in Fig. 2.7.

2.2.4   Dynamic scaling, pair-connectedness function

Now we turn our interest to exponents that describe evolution in time [35]. Time dependent order parameters exhibit *dynamical scaling* and to find the corresponding scaling behaviour, we start with rescaling the time as

$$t \to \lambda^{-\nu_{||}} t . \tag{2.2.16}$$

A simple example might be a decay of a particle density $\rho(t; \tau)$ in an infinite system, which starts at a fully active initial configuration. Scale invariance yields

$$\rho(t; \tau) \simeq \lambda^{-\beta} \rho(\lambda^{-\nu_{||}} t; \lambda \tau) . \tag{2.2.17}$$

Following the same procedure as with the equal time correlation function (2.2.14) we find that at the critical point $\tau = 0$ the density behaves as

$$\rho(t; \tau) \simeq t^{-\delta} \rho(1; t^{\nu_{||}} \tau) \implies \quad \rho(t; 0) \propto t^{-\delta} , \tag{2.2.18}$$

where $\delta = \beta/\nu_{||}$. Note that arround the critical point $\tau \approx 0$, the last scaling relation can be verified by plotting $t^\delta \rho(t; \tau)$ as a function of $t^{\nu_{||}} \tau$.

If we have the nontrivial initial configuration, the best way to describe our system is via the *pair-connectedness function*(PCF) $G(\boldsymbol{x}_1, t_1; \boldsymbol{x}_2, t_2; \tau)$. In the case of DP processes, this function is defined as the probability of finding a direct path of active sites from site $(\boldsymbol{x}_1, t_1)$ to the site $(\boldsymbol{x}_2, t_2)$. A more general definition might be that it describes the probability that a generated cluster at $(\boldsymbol{x}_1, t_1)$ on an empty lattice will activate a site at $(\boldsymbol{x}_2, t_2)$. Due to the translational invariance, it can depend only on the differences in the space and time $x = |\boldsymbol{x}_2 - \boldsymbol{x}_1|$ and $t = |t_2 - t_1|$.

It should be stressed that the definition of the PCF is different from the ordinary two-point correlation function in the way that PCF probes the existence of a causal path between two points. This means that in order to construct the steady state asymptotic behaviour, we have to take into account two probabilities:

- The probability that the seed at $(\boldsymbol{x}_1, t_1)$ will generate an infinite cluster, i.e., the survival probability
- The probability that in the limit $t_2 \to \infty$ the randomly chosen site belongs to the infinite cluster, i.e., the steady state density ρ_s

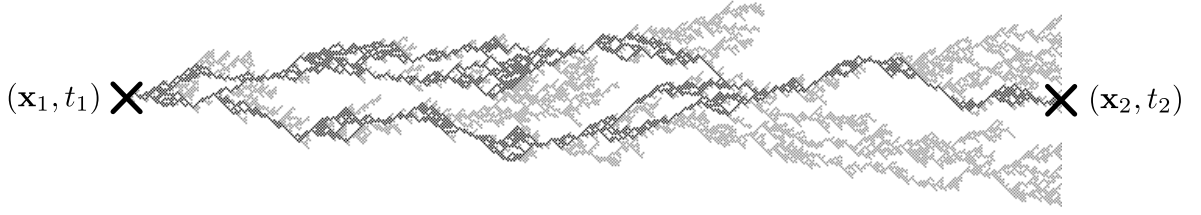Figure 2.8: Graphical visualization of the backbone

Hence we conclude that the long time behaviour is described as

$$\lim_{t\to\infty} G(t,r;\tau) = P_{\text{perc}}(\tau)\rho_s(\tau) \sim \tau^{\beta+\beta'} \ . \tag{2.2.19}$$

Knowing the above limit, we can assume that the PCF has to be rescaled

$$G \to \lambda^{\beta+\beta'}G \ , \tag{2.2.20}$$

so the corresponding scaling form is

$$G(t,r;\tau) \simeq \lambda^{-\beta-\beta'}\tilde{G}(\lambda^{-\nu_{||}}t, \lambda^{-\nu_\perp}; \lambda\tau) \ . \tag{2.2.21}$$

Because of the rapidity symmetry (section 2.2.1) these two exponents coincide.

The PCF is very useful for analysis of clusters generated from a single seed on an empty lattice. It can be determined numerically by activating a seed at the point $(\boldsymbol{x}_1, t_1)$ and measuring the response at the point $(\boldsymbol{x}_2, t_2)$ averaged over many times. As one can see from Fig. 2.8, not all lattice sites contribute to the response at $(\boldsymbol{x}_2, t_2)$. The dark path, that is connecting points $(\boldsymbol{x}_1, t_1)$ and $(\boldsymbol{x}_2, t_2)$ is called the *backbone* of the PCF. Roughly speaking, the backbone is a set of bonds and lattice sites that are connecting points $(\boldsymbol{x}_1, t_1)$ and $(\boldsymbol{x}_2, t_2)$ by cutting out all dangling ends. PCF is a useful tool for studying the DP absorbing phase transition and calculating corresponding critical exponents. While in the absorbing phase $\tau < 0$ generated clusters remains finite, in the active phase $\tau > 0$ a nonzero probability for generating an infinite cluster arises. There are three basic quantities to characterize cluster growth in both phases:

- the survival probability $P(t)$
- the number of active sites $N(t)$
- the mean square spreading $R^2(t)$ from the origin (or the squared radius of gyration)

where $P(t)$ and $N(t)$ are averaged over all clusters and were the last is averaged one only over surviving clusters. These quantities can be at the criticality described by the following power laws

$$P(t) \sim t^{-\delta'}, \quad N(t) \sim t^{\Theta}, \quad R^2(t) \sim t^{\tilde{z}} \ , \tag{2.2.22}$$

where δ is the *survival probability exponent*, Θ is the *slip exponent* and $\tilde{z}$ is the *spreading exponent* (different from the dynamical exponent z defined in (2.2.5)). Around the critical

point, (2.2.22) should follow scaling laws[3]:

$$P(t;\tau) \simeq \lambda^{-\delta'\nu_{||}} P(\lambda^{-\nu_{||}}t; \lambda\tau) , \qquad (2.2.23)$$

$$N(t;\tau) \simeq \lambda^{\Theta\nu_{||}} N(\lambda^{-\nu_{||}}t; \lambda\tau) , \qquad (2.2.24)$$

$$R(t;\tau) \simeq \lambda^{\nu_\perp} R(\lambda^{-\nu_{||}}t; \lambda\tau) . \qquad (2.2.25)$$

In the active phase, long-time behaviour of the percolation probability is by definition equal to the ultimate survival probability (2.2.2) and so we conclude

$$\delta' = \beta'/\nu_{||} . \qquad (2.2.26)$$

Let us now focus on the exponents Θ and $\tilde{z}$. They can be both calculated from the PCF. The average number of particles is given by the relation:

$$N(t;\tau) \propto \int \mathrm{d}^d x \, G(\boldsymbol{x}, t; \tau) \qquad (2.2.27)$$

$$\simeq \lambda^{-\beta-\beta'} \int \mathrm{d}^d x \, G(\lambda^{-\nu_\perp}\boldsymbol{x}, \lambda^{-\nu_{||}}t; \lambda\tau) \qquad (2.2.28)$$

$$\simeq \lambda^{d\nu_\perp-\beta-\beta'} N(\lambda^{-\nu_{||}}t; \lambda\tau) , \qquad (2.2.29)$$

where in the last expression we have rescaled the space variable with $\boldsymbol{x} \to \lambda^{\nu_\perp}\boldsymbol{x}$. Comparing this with (2.2.24) we will obtain d-dependent relations called *generalized hyper-scaling relation* [37]

$$\Theta = \frac{d}{z} - \delta - \delta' , \qquad (2.2.30)$$

where $\delta = \beta/\nu_{||}$ and $\delta' = \beta'/\nu_{||}$. As was already pointed out, due to the rapidity symmetry β and β' merge into the one exponent and therefore $\delta = \delta'$.

Critical exponent $\tilde{z}$ for the radius of gyration is found in the same way using the definition

$$R^2(t;\tau) = \langle |\boldsymbol{x}|^2 \rangle = \frac{\int \mathrm{d}^d x \, \boldsymbol{x}^2 \, G(\boldsymbol{x}, t; \tau)}{\int \mathrm{d}^d x \, G(\boldsymbol{x}, t; \tau)} \qquad (2.2.31)$$

$$\simeq \lambda^{2\nu_\perp} R(\lambda^{-\nu_{||}}t; \lambda\tau) , \qquad (2.2.32)$$

from which using relation (2.2.22) we conclude that

$$\tilde{z} = \frac{2\nu_\perp}{\nu_{||}} = \frac{2}{z} . \qquad (2.2.33)$$

From equations (2.2.26), (2.2.30) and (2.2.33) we immediately see that there are 4 independent critical exponents. However, if the rapidity symmetry holds critical exponents β and β' coincide. This gives us a very important conclusion, which is that by measuring dynamical critical exponents (2.2.22) we can obtain all other exponents by simply using relations described above.

---

[3]These relations follow from the fact, that after the rescaling $\lambda^{-\nu_{||}}t = 1$ one must obtain (2.2.22).

2.3 Directed percolation universality class

Description given above might describe a wide range of different physical processes that differ from each other in their microscopic properties. In order to determine the range of models belonging to the DP universality class, Janssen and Grassberger formulated the DP *conjecture*[35]. According to this conjecture, a physical model belongs to the DP university class if it satisfies the following conditions:

- the model displays a continuous active-to-absorbing state phase transition,
- the transition is characterized by a non-negative one-component order parameter,
- the dynamic rules are short-ranged,
- the system has no special attributes such as unconventional symmetries, conservation laws, or quenched randomness.

If the model satisfies the above conditions, critical exponents describing active-to-absorbing state phase transition must be identical to the DP critical exponents. In fact, several generalizations have been made and it seems that the range of models that belong to the DP universality class is even wider. Some of them even violate the above conditions such as models with several absorbing states or multicomponent order parameters [35].

   In contrast to the equilibrium universality classes such as Ising model, which has been solved up to 2 dimensions, the DP process has not been solved even in $1 + 1$ dimensions[4]. This also motivates us to use field-theoretic approach to this problem that will be the object of the following sections.

2.3.1 Field-theoretic formulation of DP

In this section, we derive field-theoretic formulation of DP using the concept described in section 1.4 [38, 23]. This will allows use the powerful methods of RG described in the Chapter 1.

   Master equations for percolation reactions (see Fig. 2.3) at a single site read[5]:

$$A \xrightarrow{\sigma} \emptyset: \quad \frac{\mathrm{d}P(\{n\})}{\mathrm{d}t} = \sigma \left[(n+1)P(n) - nP(n) \right] , \tag{2.3.1}$$

$$A \xrightarrow{\rho} A + A: \quad \frac{\mathrm{d}P(\{n\})}{\mathrm{d}t} = \rho \left[(n-1)P(n-1) - nP(n) \right] , \tag{2.3.2}$$

$$A + A \xrightarrow{\kappa} A: \quad \frac{\mathrm{d}P(\{n\})}{\mathrm{d}t} = \kappa \left[(n+1)nP(n+1) - n(n-1)P(n) \right] . \tag{2.3.3}$$

Using the same procedure as in section 1.4.2, above equations may be recast into Schrödinger-like equations with corresponding "Hamiltonians"

$$A \xrightarrow{\sigma} \emptyset: \quad \frac{\mathrm{d}|\Phi\rangle}{\mathrm{d}t} = \sigma(1 - a^\dagger)a|\Phi\rangle \quad \implies \quad \mathcal{H}_R^{(A \to \emptyset)} = \sigma(a^\dagger - 1)a , \tag{2.3.4}$$

$$A \xrightarrow{\rho} A + A: \quad \frac{\mathrm{d}|\Phi\rangle}{\mathrm{d}t} = \rho(a^\dagger - 1)a^\dagger a|\Phi\rangle \quad \implies \mathcal{H}_R^{(A \to A+A)} = \rho(1 - a^\dagger)a^\dagger a , \tag{2.3.5}$$

$$A + A \xrightarrow{\kappa} A: \quad \frac{\mathrm{d}|\Phi\rangle}{\mathrm{d}t} = \kappa(1 - a^\dagger)a^\dagger a^2|\Phi\rangle \implies \mathcal{H}_R^{(A+A \to A)} = \kappa(a^\dagger - 1)a^\dagger a^2 . \tag{2.3.6}$$

---

[4]This is, however, a mystery since the 2D isotropic percolation model can be mapped onto the q-Potts model for the limit $q \to 1$, where the critical exponents are known exactly [35].

[5]It has been shown that the limiting constraint $n_i \leq 1$ for every lattice site can be using bosonic formalism implemented only through reaction $A + A \to A$ in order to avoid more cumbersome representation in terms of spin operators [39].

Q	ψ'	ψ	D	τ	g	κ
d_Q^k	$d/2$	$d/2$	-2	2	$(2-d)/2$	$-d$
d_Q^ω	0	0	1	0	1	1
d_Q^ω	$d/2$	$d/2$	0	0	$(4-d)/2$	$2-d$

Table 2.1: Momentum, frequency and total scaling dimensions of the model (2.3.8).

To obtain the whole reaction Hamiltonian, we have to sum over all lattice sites

$$\mathcal{H}_R = \sum_i \left[\sigma(a_i^\dagger - 1)a + \rho(1 - a_i^\dagger)a_i^\dagger a_i + \kappa(a_i^\dagger - 1)a_i^\dagger a_i^2 \right] . \tag{2.3.7}$$

The Doi-Peliti action functional (1.4.35) for the bond DP then reads

$$\mathcal{S}^{\mathrm{DP}}[\psi' + 1, \psi] = \psi'[\partial_t + D(-\partial^2 + \tau)]\psi - g(\psi' - \psi)\psi\psi' + \kappa\psi^2\psi'^2 , \tag{2.3.8}$$

where the integration over all variables is implied, $\tau = (\sigma - \rho)/D$, $g = \sqrt{\sigma\kappa}/2$, and we have rescaled fields according to

$$\psi' \to \gamma\psi' , \quad \psi \to \gamma^{-1}\psi , \quad \gamma^2 = \kappa/\sigma . \tag{2.3.9}$$

The initial term $\psi'(\boldsymbol{x}, 0)$ has also been neglected, since for the long-time and large scale-behaviour it is irrelevant[6].

Equation (2.3.8) shows two different coupling constants g and κ. However, using dimensional analysis, one can show that κ does not affect the universal behaviour. Providing that the action functional (2.3.8) is dimensionless, scaling dimensions are derived and they are shown on the Tab. 2.1. The RG approach to dynamical systems introduced in the section 1.3.3 allows us to introduce the total canonical scaling dimension (1.3.42), which will make one parameter of the system dimensionless. Therefore we choose $d_\omega = 2$ and the corresponding dimensionless parameter is the diffusion constant D. By doing this, we see that the total canonical dimension for coupling constants g and κ are $(4-d)/2$ and $2 - d$. Therefore, we conclude that the upper critical dimension for the bond DP process is $d_c = 4$ (g becomes dimensionless) and that the coupling constant κ is in the sense of RG an irrelevant parameter, since around d_c it has a negative scaling dimension. Hence, the last term in (2.3.8) is irrelevant from the RG point of view. It does not affect large-scale behaviour and in the further considerations it will be neglected.

We thus arrive at the *effective* field theory action for the bond DP

$$\mathcal{S}^{\mathrm{DP}}[\psi', \psi] = \psi'[\partial_t + D(-\partial^2 + \tau)]\psi - g(\psi' - \psi)\psi\psi' , \tag{2.3.10}$$

where we have denoted $\psi' \equiv \psi' + 1$ on the left hand side to make the notation simpler. This is actually a well known action functional for so-called *Reggeon field-theory* from particle physics which describes high-energy hadron scattering [40].

The action functional (2.3.10) is also invariant under the *duality transformation*

$$\psi(\boldsymbol{x}, t) \leftrightarrow -\psi'(\boldsymbol{x}, -t) . \tag{2.3.11}$$

This symmetry can be considered as a field-theoretic equivalent to the rapidity-symmetry of DP discussed in the Chapter 2.2.1 [35].

---

[6]Or alternatively we can put $\psi(\boldsymbol{x}, 0) = \delta(\boldsymbol{x})$ which yields an irrelevant constant to the action functional.

2.3.2 Mean-field theory

In this part, we will describe stochastic formulation and find the mean-field approximation of DP. Even though Doi-Peliti action functional (1.4.35) is derived differently than the formalism introduced by De Dominicis and Janssen (1.3.24), we can still use the latter to find the Langevin equation of (2.3.10). This is found to be

$$\partial_t \psi(\boldsymbol{x}, t) = D(\partial^2 - \tau)\psi(\boldsymbol{x}, t) - g\psi^2(\boldsymbol{x}, t) + \eta(\boldsymbol{x}, t) \ , \tag{2.3.12}$$

where the noise properties are given by first two moments

$$\langle \eta(\boldsymbol{x}, t) \rangle = 0, \quad \langle \eta(\boldsymbol{x}, t)\eta(\boldsymbol{x}', t') \rangle = g\psi(\boldsymbol{x}, t)\delta(\boldsymbol{x} - \boldsymbol{x}')\delta(t - t') \ . \tag{2.3.13}$$

One can notice the appearance of the field $\psi(\boldsymbol{x}, t)$ in the correlator (2.3.13). This multiplicative noise is connected to the fact, that the fluctuations of $\psi(\boldsymbol{x}, t)$ should vanish in the absorbing state $\psi(\boldsymbol{x}, t) = 0$. Note also that the duality symmetry (2.3.11) cannot be seen in the Langevian formulation of bond DP (2.3.12).

The mean-field approximation can be derived as follows. First, spatial and temporal correlation lengths in (2.3.12) satisfy the same relation as in section 1.3

$$\xi_\perp \sim \tau^{-1}, \quad \xi_\| \sim \xi_\perp^2 \ . \tag{2.3.14}$$

Second, neglecting the random force and the spatial fluctuations Eq. (2.3.12) simplifies to

$$\partial_t \Psi(t) = -D\tau\Psi(t) - g\Psi^2(t) \ , \tag{2.3.15}$$

where Ψ is the spatially independent DP field. One also has to remember, that for $\tau < 0$ we get the active state. Asymptotic behaviour is found to be

$$\Psi(t) \sim t^{-1} \ (\tau = 0), \qquad \Psi(t = \infty) \sim \begin{cases} 0, & (\tau > 0) \\ (-\tau), & (\tau < 0) \end{cases} \ . \tag{2.3.16}$$

In the mean-field approximation, critical exponents describing static properties are

$$\beta_{\mathrm{MF}} = 1, \quad \nu_{\perp,\mathrm{MF}} = 1/2, \quad z_{\mathrm{MF}} = 2 \ , \tag{2.3.17}$$

and the dynamic properties are described by exponents (using (2.2.30) and (2.2.33))

$$\Theta_{\mathrm{MF}} = 0, \quad \tilde{z}_{\mathrm{MF}} = 1, \quad \delta_{\mathrm{MF}} = \delta'_{\mathrm{MF}} = 1 \ , \tag{2.3.18}$$

where we have substituted $d = 4$. As we can see from (2.3.18) mean-field approximation of DP is similar to a single particle diffusion ($N = \mathrm{const.}$, $R(t) \propto t^{1/2}$). However, the situation is different from the single particle diffusion, since the function $N(t)$ describes mean particle number and not particle number itself. In addition, the particle density decay and the survival probability obey identical power law due to the rapidity symmetry.

Let us note, that the same results can be found utilizing the saddle point approximation, i.e.

$$\frac{\delta \mathcal{S}^{\mathrm{DP}}[\psi', \psi]}{\delta \psi'} = \frac{\delta \mathcal{S}^{\mathrm{DP}}[\psi', \psi]}{\delta \psi} = 0 \ . \tag{2.3.19}$$

Using these constraints, one obtains equations for ψ and ψ', where in the one $\psi' = 0$ is always fulfilled and the second one yields (2.3.12) without the random force.

It is also worth mentioning that there is a simple alternative way of deriving Langevin equation for general systems undergoing active-to-absorbing phase transition [23]. Consider a general Langevin equation of the form

$$\partial_t \psi(\boldsymbol{x}, t) = D(\partial^2 - R[\psi(\boldsymbol{x}, t)])\psi(\boldsymbol{x}, t) + \eta(\boldsymbol{x}, t) \; , \tag{2.3.20}$$

$$\langle \eta(\boldsymbol{x}, y)\eta(\boldsymbol{x}', t')\rangle = \psi(\boldsymbol{x}, t)N[\psi(\boldsymbol{x}, t)]\delta(\boldsymbol{x} - \boldsymbol{x}')\delta(t - t') \; , \tag{2.3.21}$$

where $R[\psi]$ and $N[\psi]$ are some reaction and noise correlation functionals and field ψ has been factored out from both of them, since in absorbing state the process must remain inactive. After expanding $R[\psi] = \tau + g\psi + \ldots$ and $N[\psi] = g + \ldots$ with respect to the density ψ and neglecting higher order terms, one arrives at Eq. (2.3.12). There are two reasons why higher order terms can be actually neglected in such way. The first one is that in the phase transition, the field ψ is generally small. The second one is, that since we are interested only in the universal behaviour, higher order terms will be irrelevant in the sense of RG.

2.3.3 The renormalization group approach

mean-field exponents derived in the previous section are correct only above critical dimensions $d_c = 4$. Below d_c, fluctuations of the field $\psi(\boldsymbol{x}, t)$ cannot be neglected, and a more sophisticated approach has to be made. Here, we will briefly discuss the RG approach to the DP process. A more detailed calculation can be found in [23, 38].

As mentioned in section 2.3.1, in the case of DP we construct the total canonical dimension with $d_\omega = 2$ which implies zero total scaling dimension of the diffusion constant D. In the large scale and long time limit $(\boldsymbol{k}, \omega) \to 0$ the effective scaling dimension of any quantity F (1.3.42) is then

$$\Delta_F = d_F^k + \Delta_\omega d_F^\omega + \gamma_F^*, \quad \Delta_\omega = 2 - \gamma_D^* \; , \tag{2.3.22}$$

from which one can show that

$$\Delta_\psi = \frac{d}{2} + \gamma_\psi^*, \quad \Delta_{\psi'} = \frac{d}{2} + \gamma_{\psi'}^* \; . \tag{2.3.23}$$

The anomalous dimensions γ_F^* are calculated as a series expansion of the coupling constant g^* using methods described in the Chapter 1. Corresponding critical exponents for the dynamical observables introduced in the section 2.2.4 are then derived as follows. Number of particles and mean square radius are found in the standard way

$$N(t) = \int \mathrm{d}^d x \; \langle \psi'(\boldsymbol{0}, 0)\psi(\boldsymbol{x}, t)\rangle \propto t^\Theta \; , \tag{2.3.24}$$

$$R^2(t) = N^{-1} \int \mathrm{d}^d x \; \boldsymbol{x}^2 \langle \psi'(\boldsymbol{0}, 0)\psi(\boldsymbol{x}, t)\rangle \propto t^{\tilde{z}}, \tag{2.3.25}$$

while the active density and the survival probability are found using the following formulas [41]:

$$\rho(t) = \langle \psi(\boldsymbol{0}, t)\rangle \propto t^{-\delta} \; , \tag{2.3.26}$$

$$P(t) = -\lim_{k \to \infty} \langle \psi'(\boldsymbol{0}, -t)e^{-k \int \mathrm{d}^d x \; \psi(\boldsymbol{x}, 0)}\rangle \propto t^{-\delta'} \; . \tag{2.3.27}$$

The following formulas are found for above dynamical exponents:

$$\Theta = -\frac{\gamma_{\psi'}^* + \gamma_{\psi}^*}{\Delta_\omega}, \quad \tilde{z} = \frac{2}{\Delta_\omega}, \quad \delta = \frac{d/2 + \gamma_{\psi}^*}{\Delta_\omega}, \quad \delta' = \frac{d/2 + \gamma_{\psi'}^*}{\Delta_\omega}, \tag{2.3.28}$$

where the critical exponents δ and δ' coincide if the rapidity-symmetry (2.3.11) holds (since the anomalous dimensions γ_ψ^* and $\gamma_{\psi'}^*$ will be the same). Relations (2.3.28) hold only below the critical dimension $d_c = 4$. Above, the anomalous dimensions vanish and the exponents are equal to their mean-field values (2.3.18) (for $d = 4$).

2.3.4 Experimental realization of DP

The rareness of the experimental realization of bond DP is surprising, especially since various possible experimental applications have been proposed (see section 3.4 in [35]). This problem is still an open question and performing different experimental settings is a challenging problem for the future.

One may think that the simplest experimental realization of bond DP might be the percolating water in a porous medium subjected to an external gravitational force. However, this application, which seems to represent the most natural realization of bond DP (and even gave it its name), is almost impossible to realise experimentally. This is due to the fact, that the theoretical model (2.3.10) describes a non-conserved spreading agent while the percolating liquid model clearly assumes conserved volume of water. Non-conservation of the DP field is intuitive from the reaction schemes (2.3) and can be seen directly from the Langevin equation (2.3.12), which (without the random force) does not have a form of a continuity equation [7].

The most recent measurements show that one possible experimental realization of the DP process is the laminar-to-turbulent flow phase transition in the Couette flow [42] (corresponding to 1+1 D percolation, i.e. percolation that is directed in time) or in the confined 2D channel flow [43] (2+1 D percolation) . Experimental measurements of the critical exponents are in quite good agreement with theoretical predictions [35]. For other possible experimental realizations we recommend the reader to [44, 45].

In this thesis however, we are interested in studying the influence of the random environment on the DP phase transition. Therefore one *should not* consider the DP process as a laminar-to-turbulent phase transition, but rather a percolating agent describing forest fires or epidemic processes. In the next chapter, we will therefore give a description of how to model a random environment of the DP process as a fully developed turbulence.

---

[7]For more details about the field-theoretic modes for conserved fields see Chapter 3.2 in [16] or Chapter 5.8 in [22].

Chapter 3

Turbulent mixing

Various physical, chemical and biological processes in nature occur in the presence of a dynamical environment. In many cases these fluctuations cannot be neglected and therefore constructing a suitable model for their description is worthwhile. The aim of this thesis is to study the influence of the random environment on the bond DP phase transition. Here we will describe a phenomenon that has attracted the attention of physicists for more than four hundred years – the *fully developed turbulence*.

Starting from conservation laws, we introduce the basics of fluid dynamics. Even if the general description of the fluids is given by a complicated set of coupled partial differential equations (called the *Navier-Stokes equations*) under certain conditions there are only two independent parameters describing the statistics of a flow - Reynolds and Mach number. These parameters determine the possible symmetries of the system under consideration. Usually, by increasing the magnitude of the Reynolds number, symmetries of the system are violated one by one. However in the limit of a high Reynolds number all possible symmetries are recovered and we approach a self-similar state of fully developed turbulence.

In Section 3.2 the properties of fully developed turbulence are introduced in terms of incompressible fluids. It is shown that this state undergoes an energy cascade of the kinetic energy from the largest to the smallest scales where the energy is dissipated into heat. In order to maintain the fully developed turbulence steady state an additional source of kinetic energy must be added into our dynamical equations. This is usually done by introducing a random Gaussian force. These ideas are then generalized in Section 3.3 for the case of compressible fluids. Energy dissipation and the structure of the energy spectra are discussed in both cases. In what follows we construct the field-theoretic models for both incompressible and compressible turbulence and discuss the properties of the energy spectra. In the end of this Chapter we briefly discuss turbulent diffusion processes.

It should be noted that even the case of incompressible fully developed turbulence is an unsolved problem. The methods of the renormalization group that we are going to use have mostly been used in the last decades in order to investigate properties of incompressible turbulence and turbulent diffusion. Few attempts to include compressibility have been undertaken, where one of the derived models we employ for our purposes. The physical relevance of this model is however still unclear and the purpose of this thesis is also to test this model for investigating large-scale and long-time properties of turbulent reaction-diffusion systems and compare them with results obtained by previous authors.

3.1   Basics of fluid dynamics

The basic equations that govern hydrodynamic flow are the mass and momentum conservation equations [46, 47]

$$\partial_t \rho + \partial_i (v_i \rho) = 0 \ , \tag{3.1.1}$$

$$\partial_t (\rho v_i) + \partial_j \Pi_{ij} = 0 \ , \tag{3.1.2}$$

where ρ, v_i are density and velocity of the fluid and Π_{ij} is *the momentum flux tensor*. The general form of the latter for an inviscid (friction-less) fluid reads

$$\Pi_{ij} = p \delta_{ij} + \rho v_i v_j \ , \tag{3.1.3}$$

where p is the pressure of the fluid. This momentum flux represents the reversible transfer of the momentum that is simply due to the movement of the fluid and the fluid pressure. Eq. (3.1.1) and (3.1.2) are also know as *continuity equations* and they describe transport of the density ρ and the momentum density ρv_i where the total mass and total momentum are conserved.

One can notice from (3.1.1) and (3.1.2) that in the three dimensional case there are four equations, but five independent variables ρ, v_i and p. In order to obtain a solvable set of equations, we have to impose an additional constraint on our system. General closure is given by the energy conservation equation and equation of state. If the the influence of the heat flow in our system is negligible we can express the fluid pressure as a function of density only. In this case, the solvable set of equations is given without the energy conservation equation and the corresponding fluid is then called a *barotropic fluid*[1]. There are several ways how to impose such a constraint [46], but in this thesis we will focus our attention on the *isothermal fluids*

$$(p - \overline{p}) = c^2 (\rho - \overline{\rho}) \ , \tag{3.1.4}$$

where $\overline{p}, \overline{\rho}$ are the mean pressure and density and c is the adiabatic speed of the sound. By employing this condition we also assume, that the temperature variations of the fluid are negligible.

3.1.1   Dissipation

In order to obtain general equations of motion describing a viscous fluid we have to include additional terms into the momentum conservation law (3.1.2). This can be done by modifying the momentum flux tensor with the additional term σ'_{ij}, which stands for an irreversible transfer of momentum in the fluid. As we will see later, this term allows dissipation of energy at the smallest scales. Equation (3.1.3) can then be modified as

$$\Pi_{ij} = p \delta_{ij} + \rho v_i v_j - \sigma'_{ij} = -\sigma_{ij} + \rho v_i v_j \ , \tag{3.1.5}$$

where $\sigma_{ij} = -p \delta_{ij} + \sigma'_{ij}$ is called the *stress tensor* and σ'_{ij} the *viscous stress tensor*. The tensor σ_{ij} represents the part of the flux that is not due to the direct transfer of momentum with the mass of the moving fluid. The main ideas for constructing σ'_{ij} are the following [47]. Since the friction occurs only when the nearest particles have different velocities,

---

[1]Which is a good approximation for the water flow. However, even air is not barotropic in general, under certain circumstances this approximation can be useful.

this tensor inevitably contains partial derivatives. In addition, σ'_{ij} must vanish in the case of a uniform rotation and therefore σ'_{ij} must be symmetric. If one assumes small velocity gradients, the general form can be written down

$$\sigma'_{ij} = A \left(\partial_j v_i + \partial_i v_j \right) + B \delta_{ij} \partial_k v_k \ , \tag{3.1.6}$$

where expressions A and B are proportionality constants also know as *Lamé coefficients*. Since only the trace of the stress tensor is responsible for the volume deformations [48] it is convenient to write this expression as a combination as a traceless and isotropic tensors

$$\sigma'_{ij} = \eta \left(\partial_j v_i + \partial_i v_j - \frac{2}{3} \delta_{ij} \partial_k v_k \right) + \zeta \delta_{ij} \partial_k v_k \ , \tag{3.1.7}$$

where we have introduced two independent numbers η and ζ being the *shear* and *bulk viscosity*. The first term in (3.1.7) in the bracket represents a gradual shearing deformation, with no change in volume, while the second one is connected to pure volume deformations. Generally, both viscosities depend on p and T, but in most cases this dependence can be neglected. From equations (3.1.1) and (3.1.2), we can then obtain a general expression for the partial differential equation describing non-relativistic fluid dynamics

$$\rho(\partial_t v_i + v_j \partial_j v_i) = \eta \left(\partial^2 v_i + \frac{1}{3} \partial_i \partial_j v_j \right) + \zeta \partial_i \partial_j v_j - \partial_i p \ , \tag{3.1.8}$$

known as *Navier-Stokes equation* (later only NS equation). Physically this equation represents the second Newton's law per unit volume.

3.1.2 Reynolds and Mach number

Even though equations (3.1.1) and (3.1.8) with the isothermal closure (3.1.4) represent a set of complicated coupled second order partial differential equations, under certain conditions there are only two independent constants describing the statistics of the flow. Let us assume that the bulk viscosity is small and therefore it can be neglected. This is a good assumption for diluted mono-atomic gases and it is also known as the *Stokes hypothesis*[49]. Expressing the variables in terms of dimensionless quantities

$$v'_i = v_i/V, \quad \rho' = \rho/P, \quad x'_i = x_i/L, \quad t' = tV/L \ , \tag{3.1.9}$$

where V, P, L are some typical values of variables, we obtain

$$\partial'_t \rho' + \partial'_i(\rho' v'_i) = 0 \tag{3.1.10}$$

$$\rho' \partial'_t v'_i + \underbrace{\rho' v'_i \partial'_i v'_j}_{\text{inertia}} = \frac{1}{\text{Re}} \underbrace{\left(\partial^{2\prime} v'_i + \frac{1}{3} \partial'_i \partial'_j v'_j \right)}_{\text{dissipation}} - \frac{1}{\text{Ma}^2} \partial'_i \rho' \ , \tag{3.1.11}$$

where

$$\text{Re} = \frac{LV}{\nu} = \frac{\text{inertial forces}}{\text{viscous forces}} \text{ or } \frac{\text{intertia}}{\text{dissipation}}, \quad \text{Ma} = \frac{U}{c} \ , \tag{3.1.12}$$

and $\nu = \eta/P$ is called the *kinematic viscosity*. The first dimensionless number in (3.1.12) is known as the *Reynolds number* (Re) and describes the degree of nonlinearity of the flow, i.e. the ratio of the inertial forces and viscous forces:

- small Re - inertial forces are small and can be neglected in some cases. Flows of this type are usually stable (laminar).

- large Re - viscous forces can be neglected. These flow are usually unstable and they easily becomes chaotic.

The latter in (3.1.12) is called the *Mach number* and it describes the ratio of the typical velocity (or the root mean squared velocity) of the flow and the speed of sound. Fluid flow can be divided into several groups by using the Ma number

- Ma ≈ 0 - *Incompressible range*

- $0 < $ Ma < 0.8 - *Subsonic range*

- $0.8 < $ Ma < 1.2 - *Transonic range*

- $1.2 < $ Ma < 5 - *Supersonic range*

- $5 < $ Ma - *Hypersonic range*

High Ma numbers are typical for high compressible fluids, which can create additional mathematical problems [2].

3.2   Incompressible 3D turbulence

In this section we will give a description of a simplified model of turbulence that arises in incompressible flow. The incompressibility condition $\partial_i v_i = 0$ allows us to simplify the general form of the NS equations(3.1.8) to

$$\nabla_t v_i = \nu \partial^2 v_i - \partial_i p + f_i \ , \tag{3.2.1}$$

where $\nabla_t = \partial_t + v_i \partial_i$ is the *covariant (material) derivative*, f_i is some external force and we rescaled the viscosity and the pressure with the density, since the assumption $\rho = $ const. is reasonable for incompressible flows[3]. Neglecting variations of density implies that the speed of sound is infinite and therefore Ma $= 0$. The only number that describes the statistics of the incompressible flow is then the Re number. In what follows, we will also consider three dimensional turbulence only. Two dimensional turbulence exhibits different properties [50].

3.2.1   Fully developed turbulence

Under certain conditions the fluid flow can posses several types of symmetries. Changing parameters of the model may create instabilities which can modify or destroy symmetries completely [50].

---

[2]For example around Ma ≈ 1 shock waves are present in the fluid which makes the velocity field discontinuous and therefore a problem of defining derivatives arises. For more details see [47].

[3]Note that from the continuity equation (3.1.1) the incompressibility condition $\partial_i v_i = 0$ generally does not necessarily imply that $\rho = $ const., but that the volume element is constant along the stream line $\nabla_t \rho = 0$. In other words, different volume elements can have different densities.

A typical example of this situation can be seen in Fig. 3.1 where a cylindrically symmetric object is placed into a laminar flow of water. Here, the flow of water goes from the left to the right (along the x direction) and different shades of gray colour represent different streamlines. The first figure describes the situation for Re ≈ 1. In this case the flow possesses the following symmetries:

- left-right symmetry (x-reversal)
- up-down symmetry (y-reversal)
- time-translation (t-invariance)
- space-translations along the axis of the cylinder (z-invariance)

By increasing the Re number breaking of symmetries occurs. For Re ≈ 10 the left-right symmetry is violated and two symmetric vortices behind the cylinder appear. At Around Re ≈ 140 the creation of periodic vortices called *Kármán street* behind the cylinder occurs. In this case the continuous t-invariance is broken in favour of the discrete t-invariance. Further increase of the Re number leads to the violation of all symmetries and the system becomes *chaotic*. However, at very high Re number, i.e. about Re $\sim 10^4$, symmetries are recovered at least in the statistical sense. This state, which is characterized by chaotic changes in pressure and the flow velocity is called the *fully developed turbulence* (FDT). Another such an example is a flow of a liquid through a grid or turbulence in the atmosphere. In FDT, we assume that a flow can be separated into a laminar and a turbulent part. Since the laminar part may be eliminated by performing suitable Galilean transformation, in what follows we will thus refer to the purely turbulent part as simply the velocity field v_i.

For the statistical description of FDT we will need to define the velocity-velocity correlation function

Figure 3.1: Schematic visualisation of a flow of water around a cylinder. From top to the bottom: i) Laminar flow - Re ≈ 1, ii) left-right symmetry broken - Re ≈ 10, iii) Kármán streets - Re ≈ 140, iv) Chaotic flow - Re $\approx 10^3$, v) Fully developed turbulence - Re $> 10^4$.

$$G_{ij}^{vv}(\boldsymbol{x}) = \langle v_i(\boldsymbol{r})v_j(\boldsymbol{r}+\boldsymbol{x}) \rangle \,, \tag{3.2.2}$$

where $\boldsymbol{r}$ is the reference position and the average $\langle \dots \rangle$ is taken over all the possible configurations of the velocity field. We assume fully developed homogeneous turbulence, which
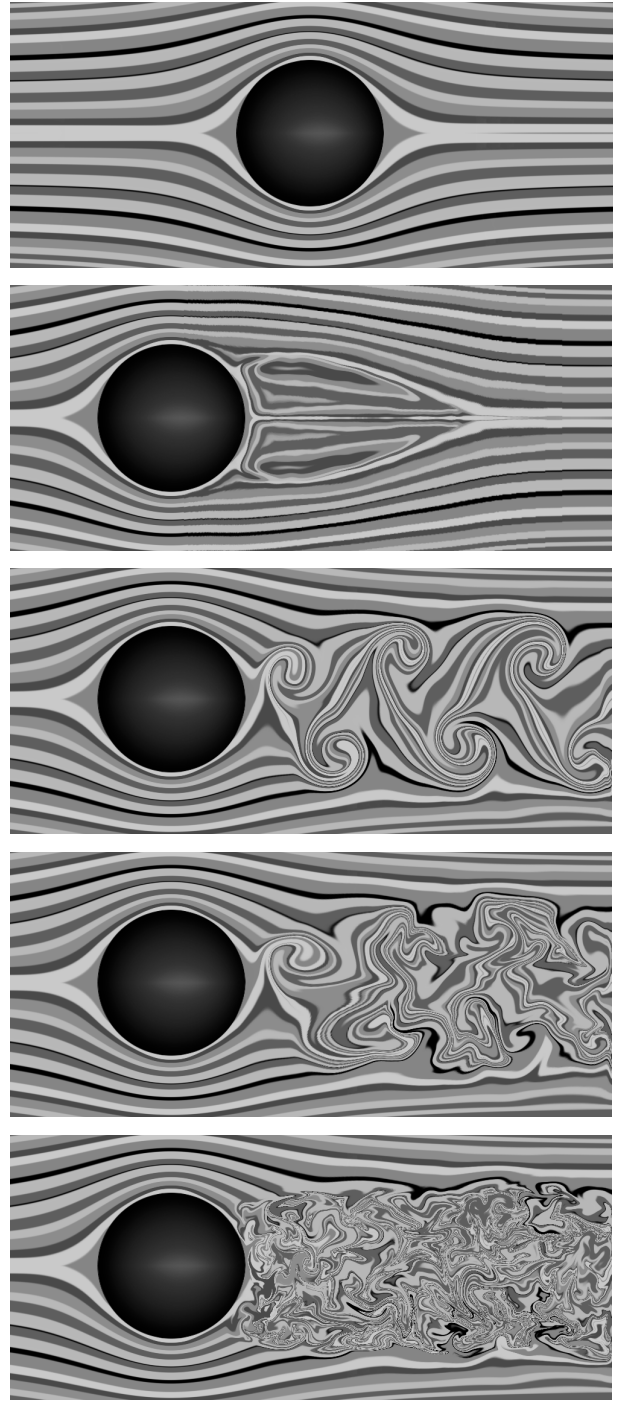
implies that the flow is space and time translational invariant and hence the correlation function (3.2.2) is independent of the reference position $\boldsymbol{r}$ and time t. In addition, we assume that the flow is isotropic, so the correlation function (3.2.2) will also be independent of the direction of $\boldsymbol{x}$ and depend only on its magnitude. The total kinetic energy E and the kinetic energy spectrum $E(k)$ of the 3D turbulent flow are then defined as

$$E \equiv \int \mathrm{d}^3k \; G_{ii}^{vv}(\boldsymbol{k}) = \int \mathrm{d}k \; E(\boldsymbol{k}) \implies E(\boldsymbol{k}) = S_2 k^2 G_{ii}^{vv}(\boldsymbol{k}) \;, \qquad (3.2.3)$$

where S_2 is the surface of the two dimensional unit sphere, $G_{ii}^{vv}(\boldsymbol{k})$ is the Fourier transformation of (3.2.2) and summation over repeated indices is implied. $E(\boldsymbol{k})\mathrm{d}k$ can be interpreted as a contribution from turbulent "eddies" of scales $(k, k + \mathrm{d}k)$ to the total kinetic energy E. Measurements show [50] that the energy spectrum for the fully developed turbulence has the universal character. In the case of incompressible turbulence the spectrum can be seen in Fig. 3.2. One can clearly see certain range of scales, called *inertial range*, where the energy spectrum obeys a power law

$$E(\boldsymbol{k}) \propto k^{-5/3} \;. \qquad (3.2.4)$$

This is also known as the *Kolmogorov 5/3 law*. The size of the inertial range is determined by two length scales: Λ, which is called the *integral scale* and m, which is called the *dissipation scale*. A more detailed explanation of these length scales will be given later.

3.2.2   Kinetic energy dissipation

In the fluid flow, viscous forces are responsible for dissipation of the kinetic energy, which is transferred into heat. In the case of incompressible turbulence, where the dynamics are described by the incompressible NS equation (3.2.1) one can show that the mean kinetic energy E changes with respect to time as [46]

$$\partial_t E \equiv \partial_t \langle v^2/2 \rangle = -2\nu \langle \omega^2 \rangle + \langle f_i v_i \rangle \;, \qquad (3.2.5)$$

where $\omega_i = \varepsilon_{ijk}\partial_j v_k$ is called the *vorticity* and here the average is taken over the whole space (or a periodic domain). It is clear from the Eq. (3.2.5) that in the case of the force free model $f_i = 0$ the energy is conserved only for the inviscid ($\nu = 0$) or the irrotational ($\omega = 0$) flow. In the case of rotational viscous flow however, energy is dissipated due to the first term on the right hand side of (3.2.5) and in order to maintain the steady state
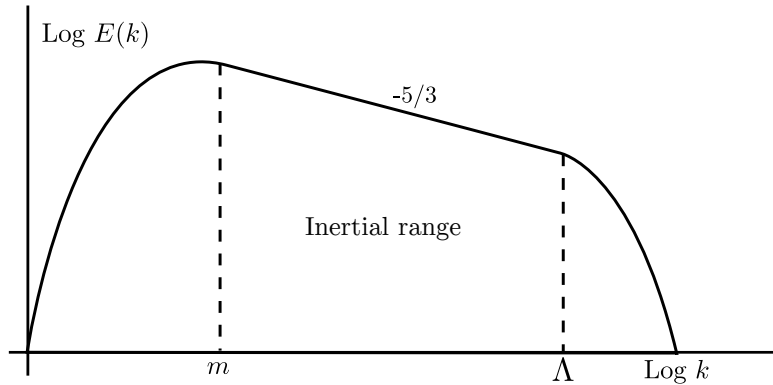

Figure 3.2: Schematic visualisation of the energy spectrum of incompressible turbulence.

$\partial_t E = 0$ one has to add a nonzero energy source via the external (random) force. The steady state solution is then

$$\varepsilon \equiv \langle f_i v_i \rangle = \nu \langle \omega^2 \rangle \ , \tag{3.2.6}$$

where we introduced the external force energy flux ε. For the practical calculations and numerical simulations, the external force f_i is usually taken to be the random Gaussian variable with zero mean and correlator

$$\langle f_i(\boldsymbol{k}, t) \rangle = 0, \quad \langle f_i(\boldsymbol{k}', t') f_j(\boldsymbol{k}, t) \rangle = \delta(t - t') \delta(\boldsymbol{k} - \boldsymbol{k}') P_{ij}(\boldsymbol{k}) D^f(\boldsymbol{k}) \ , \tag{3.2.7}$$

with the spectrum $D^f(\boldsymbol{k})$ usually chosen in a way, that the energy pumping comes from the largest scales $k \to 0$. Transversal projection operator $P_{ij}(\boldsymbol{k}) = \delta_{ij} - k_i k_j / k^2$ is introduced since the longitudinal modes of the random force would generate sound waves (which we neglected in the case of and incompressible fluid).

One can notice from the NS equations(3.2.1) that the viscous term is proportional to the second spatial derivative. It is clear from the Fourier representation that this term becomes relevant at the smallest spatial scales, i.e., $k \to \infty$. The energy pumping from the force f_i to the system however, is usually assumed to come from the largest spatial scales, i.e., $k \to 0$. This tells us that there has to be a redistribution of the energy in the inertial range that is not obvious from the conservation of energy.

Note that Eq. (3.2.5)(sometimes referred to as *energy balance equation*) does not contain any contributions from the nonlinear term in the Navier-Stokes equation. In fact, *nonlinearities do not affect the global energy budget, but they are responsible for the redistribution of energy among various scales.* In order to see that, one has to investigate properties of the incompressible NS equation on different length scales. This can be done by splitting the spectrum of the velocity field as

$$v_i(\boldsymbol{x}) = v_{iK}^<(\boldsymbol{x}) + v_{iK}^>(\boldsymbol{x}) \ , \tag{3.2.8}$$

where

$$v_{iK}^<(\boldsymbol{x}) = \int_{k \leq K} \mathrm{d}^d k \ v_i(\boldsymbol{k}) e^{i\boldsymbol{kx}}, \quad v_{iK}^>(\boldsymbol{x}) = \int_{k > K} \mathrm{d}^d k \ v_i(\boldsymbol{k}) e^{i\boldsymbol{kx}} \ , \tag{3.2.9}$$

are the *low-pass filtered* and the *high-pass filtered* velocity field functions. $v_{iK}^<$ represents the the Fourier spectrum of the function v_i that comes from turbulent eddies of the scales k smaller than K and the $v_{iK}^>$ the opposite. Using (3.2.8) one can derive from the NS equation the *scale-by-scale energy budged equation* [50] :

$$\partial_t E_K = -\Pi_K - \nu \langle |\omega_K^<|^2 / 2 \rangle + \overrightarrow{\langle f_{iK}^< v_{iK}^< \rangle} \ , \tag{3.2.10}$$

where

$$E_K = \langle |v_{iK}^<|^2 / 2 \rangle, \quad \Pi_K = \overrightarrow{\langle v_{iK}^<(v_{jK}^< \partial_j) v_{iK}^< \rangle} + \overrightarrow{\langle v_{iK}^<(v_{jK}^> \partial_j) v_{iK}^> \rangle} \ , \tag{3.2.11}$$

are *cumulative energy* and *cumulative energy flux* and arrows are denoting the direction of the flux in each term. Eq. (3.2.10) can be interpreted as follows: the rate of change of the energy E_K at scales down to $l = K^{-1}$ is equal to the energy injected at such scales by the force $\overrightarrow{\langle f_{iK}^< v_{iK}^< \rangle}$ minus the energy dissipated at such scales $\nu \langle |\omega_K^<|^2 / 2 \rangle$ minus the flux of energy Π_K to smaller scales (to $> K$) due to nonlinear interaction. Since the dissipation of the energy is equal to the energy flux from the largest scales in the stationary case (3.2.6) and the energy flux goes only in one direction, the energy flux remains constant in the whole inertial range.

3.2.3   KO41 theory

In 1941 Kolmogorov and Obukhov introduced their famous theory of turbulence (later only KO41)[51]. Here we will briefly describe the phenomenological interpretation that is a direct outcome of his theory and conclude with the similarity hypothesis [50].

The central assumption of KO41 theory is the *self-similarity* of the velocity field in the inertial range. Richardson came up with a very intuitive idea of self-similar energy cascade inside the inertial interval [52]. The energy from an external source flows into the system form large scale structures (eddies) of size $L = m^{-1}$, where m is the integral scale. Non-linearities presented in (3.2.1) are then redistributing the energy over the inertial range by continuously splitting turbulent eddies down to smaller scales. At the smallest lengths $l_d = \Lambda^{-1}$, where Λ is the dissipation scale, the viscosity begins to play an important role and the energy is dissipated to the internal energy. This process is called an *energy cascade* and it is qualitatively depicted in Fig. 3.3.
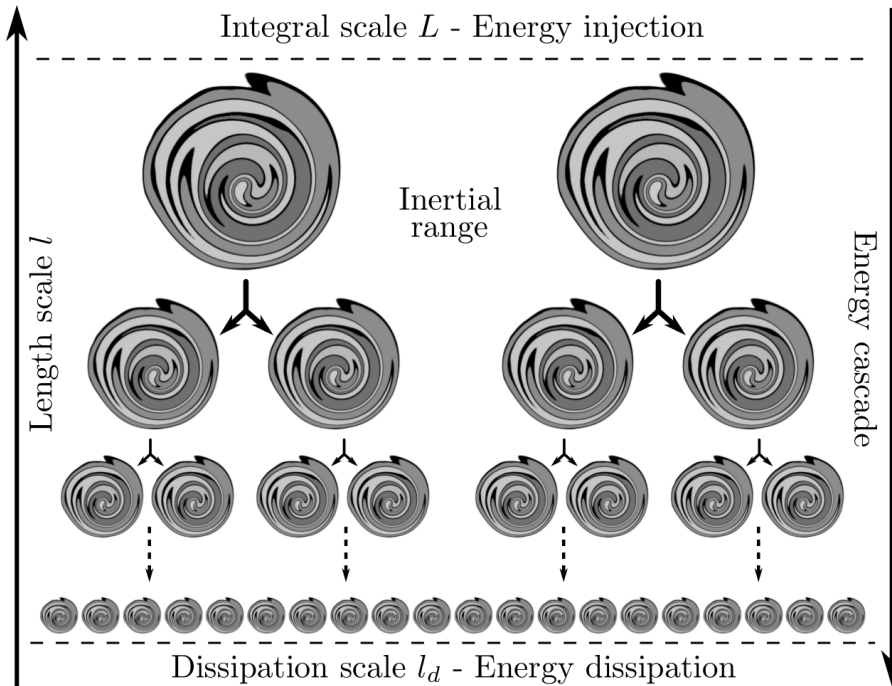
Figure 3.3: Richardson cascade

The energy spectrum can be qualitatively guessed using simple assumptions and dimensional analysis in the following way. Let us consider v_l to be a typical value of the velocity associated with scales $\sim l$ inside of the inertial range (or the velocity differences between two points at the distance l). The *eddy turnover time* τ_l, i.e. the typical time for a structure (e.g. turbulent eddy) of size $\sim l$ to undergo a significant distortion due to relative motion of its components is defined as

$$\tau_l = \frac{l}{v_l} \; . \tag{3.2.12}$$

From the dimensional analysis, one assumes that the energy flux on the scale l has the form

$$\Pi_l \sim \frac{v_l^2}{\tau_l} \sim \frac{v_l^3}{l} \; . \tag{3.2.13}$$

Since in the inertial range, there is neither energy input nor energy dissipation, one may assume a constant energy flux independent of the length scale

$$\varepsilon \sim \Pi_l \ . \tag{3.2.14}$$

Using (3.2.3) the energy spectrum for the 3D turbulence is then found to be

$$E(\boldsymbol{k}) = C_K \varepsilon^{2/3} k^{-5/3} \ , \tag{3.2.15}$$

where C_K is the *Kolmogorov constant* and its experimental value around 1.5 [53]. Until now, there is no satisfactory theory for the power law (3.2.15). One should also note that the value $-5/3$ is not precise. There are some small corrections that cannot be obtained for isotropic and homogeneous FDT using the dimensional analysis [50].

Phenomenologically we can also obtain another important scale of the fully developed turbulent system [50]. From the dimensional analysis, the typical time τ_l^{ν} for the viscous forces to dissipate the energy of the eddy of size l is

$$[\nu] = L^2 T^{-1} \implies \tau_l^{\nu} \sim \frac{l^2}{\nu} \ . \tag{3.2.16}$$

One may notice that the dissipation time increases quadratically with the size of the eddy. It then follows that the dissipation scale l_d at which the viscous forces become relevant is

$$[\varepsilon] = L^2 T^{-3} \implies l_d \sim \left(\frac{\nu^3}{\varepsilon}\right)^{1/4} \ . \tag{3.2.17}$$

The quantity (3.2.17) is also known as *Kolmogorov (dissipation) length scale* and it basically represents the size of the smallest eddies in the fluid. Using the ratio of the integral scale L and the Kolmogorov length scale, one can find

$$\frac{L}{l_d} \sim \left(\frac{L^3 v_L^3}{\nu^3}\right)^{1/4} \sim \mathrm{Re}^{3/4} \ . \tag{3.2.18}$$

This relation gives us the size of the inertial range for a specific Re number that should exhibit universal Kolmogorov scaling.

From the phenomenological ideas above, one can conclude that the fully developed turbulence is characterized by a large Re number and therefore large inertial range $m \ll k \ll \Lambda$ and a frequency range $\omega_{\min} \ll \omega \ll \omega_{\max}$. The maximal time scale can be taken as an inverse of the dissipation time (3.2.16), i.e. $\omega_{\max} = (\tau_{l_d}^{\nu})^{-1} = \nu_0 \Lambda^2$ and the minimal time scale can be calculated from the integral scale eddy turnover time (3.2.12), i.e. $\omega_{\min} = (\tau_{l_d}^{\nu})^{-1} = \varepsilon^{1/3} m^{2/3}$. The Kolmogorov-Obukhov theory is then based on two hypotheses [12]

- *Hypothesis 1*: Within the range $k \gg m$, $\omega \gg \omega_{\min}$ simultaneous distribution functions of spatial Fourier components of the random velocity field $v(\boldsymbol{k}, t)$ depend on the energy pumping ε but are independent of "details of its construction". In particular it does not depend on the energy pumping scale m and converges to a finite limit as $m/k \to 0$[4].

---

[4]This hypothesis was originally formulated in a different way for the dynamic correlator, but it later appears to be incorrect so a modification was necessary. For the original formulation see [54].

- *Hypothesis 2*: In the range $k \ll \Lambda$, $\omega \ll \omega_{\max}$, the above distribution does not depend on the viscosity coefficient ν.

Using these hypotheses and dimensional analysis, one can derive the following representation for the static (equal-time) pair correlator

$$\langle v_i(\boldsymbol{k}', t) v_j(\boldsymbol{k}, t) \rangle = (2\pi)^d \delta(\boldsymbol{k}' + \boldsymbol{k}) P_{ij}(\boldsymbol{k}) D_{st}(k), \quad D_{st}(k) = \varepsilon^{2/3} k^{-11/3} f(m/k) , \quad (3.2.19)$$

with a dimensionless function $f(m/k)$ and transversal projection operator $P_{ij}(\boldsymbol{k}) = \delta_{ij} - k_i k_j / k^2$ is introduced since the momentum space representation of the incompressibility condition $k_i v_i = 0$ implies that the velocity field v_i is transversal. According to Hypothesis 1 the function $f(m/k)$ has a finite limit $m/k \to 0$. After taking the limit $m/k \to 0$ and using the relations for the energy spectrum (3.2.3) one can find that the function $f(0)$ is related to the Kolmogorov constant introduced in (3.2.15).

3.3   Compressible 3D turbulence

The description given in the last section is valid only for turbulence with negligible Mach number. However a purely incompressible flow does not exist and in order to obtain a more realistic description, one has to imply corrections due to compressibility. A lot of work on the compressible turbulence has been done in the last years also due to advanced computer simulations. In this section we will briefly describe some recent results. A good general overview of this topic can be found in [55, 56]. In this thesis however, we will restrict ourselves to isothermal compressible turbulence.

3.3.1   Kinetic energy dissipation

The situation for compressible turbulence is much more difficult than it is for the incompressible case. Here, the incompressibility condition $\partial_i v_i = 0$ is not valid anymore and we have to consider the full set of hydrodynamic equations

$$\nabla_t \rho = -\rho \partial_i v_i , \tag{3.3.1}$$

$$\rho \nabla_t v_i = \eta \left(\partial^2 v_i + \frac{1}{3} \partial_i \partial_j v_j \right) + \zeta \partial_i \partial_j v_j - \partial_i p + f_i , \tag{3.3.2}$$

$$(p - \overline{p}) = c^2 (\rho - \overline{\rho}) . \tag{3.3.3}$$

Dissipation of kinetic energy (3.2.5) now requires certain modifications. Using compressible NS equations(3.3.2) one can show that the mean kinetic energy change is equal to [46]

$$\partial_t E_c \equiv \partial_t \langle \rho v^2 / 2 \rangle = -\eta \langle \omega^2 \rangle - \left(\frac{4}{3}\eta + \zeta \right) \langle (\partial_i v_i)^2 \rangle - \langle v_i \partial_i p \rangle + \langle f_i v_i \rangle . \tag{3.3.4}$$

Comparing with (3.2.5) one can see the appearance of additional terms in (3.3.4) due to compressibility. The stationary state can also be assumed here if the external force is balancing the dissipation forces.

  In contrast to (3.2.7), the random force is now taken to be

$$\langle f_i(\boldsymbol{k}, t) \rangle = 0, \quad \langle f_i(\boldsymbol{k}', t') f_j(\boldsymbol{k}, t) \rangle = \delta(t - t') \delta(\boldsymbol{k} - \boldsymbol{k}')(P_{ij}(\boldsymbol{k}) + \alpha Q_{ij}(\boldsymbol{k})) D(\boldsymbol{k}) , \quad (3.3.5)$$

where we have introduced the longitudinal projection operator $Q_{ij}(\boldsymbol{k}) = k_i k_j / k^2$ responsible for the generation of sound waves and the parameter α describing the structure of the random force (ratio of the transversal and longitudinal modes). One should note however, that the limit $\alpha \to 0$ does not correspond to an incompressible limit. This can be seen from the following argument. Consider the full stochastic NS equations(3.1.8) with an external (random) force f_i in the more compact form

$$\partial_t(\rho v_i) + \partial_j(\rho v_j v_i) = \partial_j(\sigma'_{ij} - p\delta_{ij}) + f_i \; , \tag{3.3.6}$$

where σ'_{ij} is the viscous stress tensor (3.1.7). By taking the divergence of (3.3.6) and inserting it into the time derivative of the continuity equation (3.1.1) we obtain

$$\partial^2_{tt}\rho - c^2\partial^2\rho = \partial_i\partial_j(\rho v_j v_i - \sigma'_{ij}) + \partial_i f_i \; , \tag{3.3.7}$$

where we have used the isothermal condition (3.1.4). Without the random force term this inhomogeneous wave equation is know as the *Lighthill equation* of aeroacoustics and it describes the behaviour of sound waves in the medium [57]. It is easy to see that even if the random force is purely transversal ($\partial_i f_i = 0$), sound waves may be generated by nonlinear terms of the right hand side, i.e. transversal modes of the velocity field. The velocity field can therefore have both transversal and longitudinal modes, for any values of α.

In the highly compressible fluid another important length scale appears. Consider a flow with high Ma number, within the super-sonic range. As stated in section 3.2.2 viscosity becomes relevant at small scales. Dissipation of energy is therefore faster at smaller scales which will cause the large-scale super-sonic turbulence to become sub-sonic at smaller scales. The scale at which this transition occurs is called the *sonic scale* k_s [56].

The question of the energy flux in the case of compressible turbulence is also much more difficult than it is in the case of incompressible turbulence. The reason for that is that there are additional terms arising in the scale-by-scale energy budget equation (3.2.10) due to invalidity of the incompressibility condition $\partial_i v_i = 0$. These calculations are technically very difficult so we will not go into details of the problem, but we mention some results that were previously accomplished.

It has been shown [58] that compressible nonlinearities of the equation (3.2.10) creates an additional energy flux in the system with an oscillating direction in the scale. Therefore one can introduce an *effective energy flux* $\varepsilon_{\mathrm{eff}}$ that fluctuates in time in the following way. When the system is in the process dilatation (positive divergence) additional terms are negative and the effective energy $\varepsilon_{\mathrm{eff}}$ is smaller than ε. On the other hand in the phase of compression, $\varepsilon_{\mathrm{eff}}$ becomes larger than ε. Even though the effective energy flux $\varepsilon_{\mathrm{eff}}$ is different from classical energy flux ε, its value is still positive and the direction goes from the larger to smaller scales. A schematic picture of this situation can be seen in the Fig. 3.4. This problem can be eliminated by introducing the *mean effective flux* $\overline{\varepsilon}_{\mathrm{eff}}$ that will play the same role in deriving the structure of the energy spectra as in the case of incompressible turbulence.

3.3.2 Energy spectra

Since the velocity field in the compressible turbulence has two components - transversal and longitudinal - two energy spectra are expected as well [56]. The spectrum can be
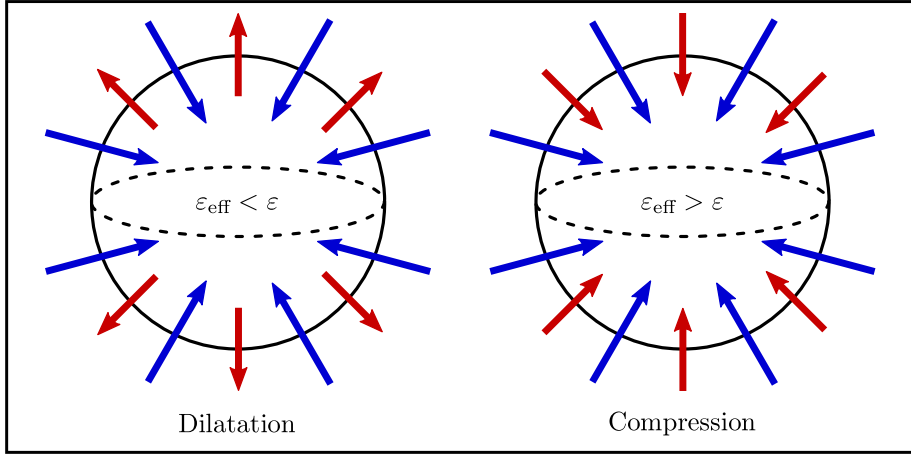
Figure 3.4: Effective flux of the energy for the compressible turbulence. The blue arrows represent the classical energy flux ε in the case of incompressible turbulence. If the compressibility is employed, additional energy related to the dilation of the fluid arises. In the case of dilatation, the additional flux behaves as an inverse energy cascade process, while in the process of compression, it flows in the classical direction (from larger to smaller scales). The resulting effective flux ε_{eff} shows an oscillating behaviour.

separated as

$$E_c(\boldsymbol{k}) = E_\perp(\boldsymbol{k}) + E_\|(\boldsymbol{k}) \;, \tag{3.3.8}$$

where $E_\perp$ and $E_\|$ are the transversal and longitudinal energy spectrum and the final form of (3.3.8) depends on the magnitude of the Ma number and the structure of the random force (3.3.5).

In [59] a direct numerical simulation of isothermal 3D turbulence for Ma $= 6$ with the forcing parameter $\alpha = 2/3$ has been done and the total energy spectrum with exponent ≈ -1.95 instead of Kolmogorov $-5/3$ has been found. It has also been proposed, that the Kolmogorov spectrum can be obtain if one uses the density-weighted velocity field as

$$w_i = \rho^{1/3} v_i \;. \tag{3.3.9}$$

In [60] authors where numerically studying the influence of different structures of the random force on the energy spectra for 3D isothermal turbulence at Ma ≈ 5.5. The total energy spectrum was found to be ≈ -1.86 for purely transversal forcing ($\alpha \to 0$) and ≈ -1.94 for the longitudinal forcing ($\alpha \to \infty$). A spectrum close to Kolmogorov $-5/3$ was found using the density weighted velocity field (3.3.9) only for purely transversal forcing, while the longitudinal forcing showed ≈ -2.1. As stated in [55] the problem of the latter might be connected with a wrong interpretation of the inertial range. It was also pointed out, that the observed -2.1 spectrum might belong to the super-sonic scale, while the proper redefinition of the inertial range will yield a -1.64 exponent, i.e. a power spectrum close to the Kolmogorov $-5/3$ law.

Similar results were found in [58] where it was shown by using dimensional analysis that the energy spectrum obeys

$$E_c^w(\boldsymbol{k}) \sim \bar{\varepsilon}_{\text{eff}}^{2/3} k^{-5/3} \;, \tag{3.3.10}$$

where E_c^w stands for the density weighted velocity field (3.3.9) energy spectrum and $\bar{\varepsilon}_{\text{eff}}$ being the mean effective energy flux mentioned in the previous section. In compressible

turbulence however, the assumption that the energy flux is independent of the energy scale might not be correct. If one assumes that the effective energy flux is also scale dependent one can expect deviations from the Kolmogorov $-5/3$ law at the largest scales $k \to 0$. According to [58] this spectrum can be up to $-19/9 \approx -2.1$. This transition may occur at the sonic scale.

For the case of small Mach number, the phenomenological Kolmogorov-Obukhov theory can be generalized in the following way. A static correlator (3.2.19) can be written for the case of the finite speed of sound c as

$$D_{stat}(\boldsymbol{k}) = \varepsilon^{2/3} k^{-11/3} F\left(\varepsilon^{2/3} k^{-2/3} c^{-2}\right) \ , \tag{3.3.11}$$

where we have already taken the limit $m/k \to 0$. The function F can be expanded in terms of small $1/c$ and the corresponding energy spectrum will be

$$D_{stat}(\boldsymbol{k}) \propto \varepsilon^{2/3} k^{-11/3} (1 + \text{const } \text{Ma}^2 (Lk)^{-2/3}) \ , \tag{3.3.12}$$

where the relations $\varepsilon \sim v_{\text{rms}}^3 L^{-1}$ and $\text{Ma} = v_{\text{rms}}/c$, with v_{rms} being the root-mean-squared velocity of the flow, have been used. This phenomenological relation has been verified for the purely transversal random force $\alpha = 0$ using RG methods in [61]. Eq. (3.3.12) is also independent of the viscosity ν which proves that the KO41 theory (3.2.19) can be extended to the case of a small Ma number.

However, the numerical simulations show, that the energy spectrum of the weakly compressible turbulence should have negligible deviations from the KO41 $-5/3$ spectrum [62]. This might be due to the fact, that the proportionality constant in (3.3.12) is not determined by the RG methods.

3.4 Field-theoretic formulation of turbulence

The field-theoretic RG approach to fully developed turbulence and related problems is very complex. First attempts of using RG in turbulence were done in [10, 11] where Wilson's recursion RG approach, i.e. a method based on the approach described in section 1.3.1 was employed. In this thesis we are going to use the equivalence of field-theoretic models and stochastic differential equations (section 1.3.2) and directly use the methods of field-theoretic RG. A more detailed description of this approach can be found in [12].

Since we will be interested only in the turbulent behaviour of a fluid, in the following we will assume that the velocity v_i in (3.1.8) represents only the turbulent part of the flow and that the laminar flow was subtracted. The theoretical formulation of the turbulent flow problem can be done in two ways:

- Statistically - by defining the velocity field v_i as a Gaussian random variable
- Dynamically - by defining the velocity field v_i as a solution to a stochastic dynamical (usually NS) equations

The first model is a drastic simplification of the problem that has often been used for studying anomalous scaling in turbulent reaction-advection-diffusion processes [63]. The latter one is more complicated but also represents the more realistic case. In this thesis we are interested only in the dynamically modelled turbulence. However, since we also want to compare our results with previous works, we start by introducing the statistical description of turbulence.

The simplest statistical description of turbulence that is suitable for the use of field-theoretic RG methods is the *Kraichnan* or *Rapid-Change model* [64]. In this case, the two point velocity field correlator takes the following form

$$\langle v_i(\boldsymbol{x}',t')v_j(\boldsymbol{x},t)\rangle = \frac{\delta(t-t')D}{(2\pi)^d}\int \mathrm{d}^d k \ k^{-d-\xi}(P_{ij}(\boldsymbol{k})+\alpha Q_{ij}(\boldsymbol{k}))\exp\{i\boldsymbol{k}(\boldsymbol{x}-\boldsymbol{x}')\}\ ,$$

$$(3.4.1)$$

where D, d are the amplitude and the dimension of the space, ξ is the RG expansion parameter, equivalent to ε from the theory of critical phenomena (see sec. 1.2.3) and $P_{ij}(\boldsymbol{k})$ and $Q_{ij}(\boldsymbol{k})$ are the transversal and longitudinal projection operators defined in (3.3.5). The parameter α is an independent parameter describing the ratio of the longitudinal and transversal modes (e.g. sound waves and turbulent flow) of the velocity field v. The value $\alpha = 0$ represents the incompressible case where the velocity field becomes transversal. It should be noted however that in models such as (3.4.1) the physical value of the parameter α should be small since large values imply a high degree of compressibility and additional problems such as shock waves arise. The physical value of the parameter ξ is 4/3, which after performing RG approach yields the Kolmogorov $-5/3$ energy spectrum [63].

The model (3.4.1) was later also modified for the case of infinite correlation time using equation for the "synthetic" velocity field that is not Galilean invariant [65]. This model is also useful for studying diffusion in random environments that are "frozen in time" (static random environment). However the model (3.4.1) is still only an approximation and the real dynamics are believed to be found using dynamical equations for turbulent flow as will be explained in the following sections.

3.4.1 Incompressible Navier-Stokes equation

The field-theoretic formulation of fully developed turbulence using incompressible NS equation is the following [12]. The De Dominicis-Janssen action functional (1.3.24) for (3.2.1) is found to be

$$\mathcal{S}^{\mathrm{NS}}[\boldsymbol{v}',\boldsymbol{v}] = -v_i' D_{ij}^f v_j'/2 + v_i'\big\{\nabla_t - \nu_0\partial^2\big\}v_i\ ,\qquad(3.4.2)$$

where v_i' is the Martin-Siggia-Rose response field, $D_{ij}^f(\boldsymbol{x}',t',\boldsymbol{x},t) = \langle f_i(\boldsymbol{x}',t')f_j(\boldsymbol{x},t)\rangle$ is the two point random force correlator, ν_0 is the non-renormalized kinematic viscosity and the summation and integration over all indices and variables is implied. The random force is taken to be Gaussian with the following properties.

$$\langle f_i(\boldsymbol{x},t)\rangle = 0,\quad \langle f_i(\boldsymbol{x}',t')f_j(\boldsymbol{x},t)\rangle = \frac{\delta(t-t')}{(2\pi)^d}\int \mathrm{d}^d k \ P_{ij}(\boldsymbol{k})D^f(\boldsymbol{k})\exp\{i\boldsymbol{k}(\boldsymbol{x}-\boldsymbol{x}')\}\ ,$$

$$(3.4.3)$$

where $D^f(\boldsymbol{k})$ is the spectrum of the random force to be determined and $P_{ij}(\boldsymbol{k})$ is the transversal projection operator, since in the incompressible case we do not allow generation of sound waves. Note that the pressure term in (3.4.2) has been eliminated using the transversality of the v_i' field.

There is no unique rule for choosing the random force correlator for the stochastic NS equation. In RG theory of turbulence both physical and technical arguments have to be given in order to construct the correlator. Physical arguments are such that the realistic pumping for this problem must come from the large scale structures $k \sim m = L^{-1} \to 0$,

i.e. from the IR region. On the other hand, in order to use standard field-theoretic RG technique it is necessary to have a power law asymptote at large k. The latter is satisfied if we choose the correlator to be [11, 66]

$$D^f(\boldsymbol{k}) = D k^{4-d}(k^2 + m^2)^{-y/2} \,, \tag{3.4.4}$$

where D is the amplitude (coupling constant), d is the dimension of space and $y > 0$ is an independent parameter of the model that plays the same role as the expansion parameter $\varepsilon = 4 - d$ does in the RG approach to the theory of critical behaviour[5]. In this case however, it is completely unrelated to the dimension of space and it determines the spectrum of the random force. In the range $0 < y < 4$ the integral (3.4.3) diverges for $k \to \infty$ and an upper momentum cut-off Λ is necessary. This can be chosen to be $\Lambda = l_d^{-1}$ where l_d is the dissipation length (3.2.17). The energy pumping is then $W \sim \Lambda^{4-y}$ which means that it comes from the smallest scales and it is therefore said to be *ultraviolet*. The realistic pumping occurs only for $y > 4$ where the integral (3.4.3) is dominated by the smallest scales and $W \sim m^{4-y}$ - *infrared pumping*. The parameter m here plays a role of the IR ($k \to 0$) cut-off and we can choose it to be the inverse of the integral scale $m = L^{-1}$.

In most RG studies of fully developed turbulence and related phenomena a simpler random force correlator is considered [22]

$$D^f(\boldsymbol{k}) = D k^{4-d-y} \,, \tag{3.4.5}$$

which corresponds to the "massless" ($m \to 0$) version of (3.4.4). This choice is suitable if we are only interested in the IR scaling properties such a scaling dimensions of the system. In this case it can be shown [12] that the random force correlator (3.4.3) with the spectrum (3.4.5) (or (3.4.4)) is related to the energy pumping flux ε via the following relation:

$$\varepsilon = \frac{d-1}{2(2\pi)^d} \int^\Lambda \mathrm{d}^d k \; D^f(\boldsymbol{k}) \,. \tag{3.4.6}$$

By calculating the corresponding integral in the UV domain $y \to 4^-$ one obtains the following relation for the bare random force correlator and the energy flux

$$D = \frac{2(4-y)}{S_d} \varepsilon \Lambda^{y-4} \,. \tag{3.4.7}$$

Inserting this back into (3.4.5) for the limit $y \to 4^-$ one finds [6]

$$D^f(\boldsymbol{k}) = \frac{2\varepsilon}{S_d k^d} \lim_{y \to 4^-} (4-y) \left(\frac{k}{\Lambda}\right)^{4-y} = 2\varepsilon\delta(k) \,. \tag{3.4.8}$$

It follows from above that the random force correlator (3.4.5) in the boundary limit $y \to 4^-$ between the UV and IR energy pumping (in the massless case $m \to 0$) represents the most realistic case of the energy pumping that comes from the largest scales $\boldsymbol{k} \to 0$. It can be shown [22] that in this boundary limit, the energy spectrum of 3D incompressible turbulence satisfies the Kolmogorov $-5/3$ law (3.2).

---

[5]In the language of regularization, the correlator (3.4.4) represents the case of the *analytic regularization*.

[6]Where we used the modified power-law representation for the δ function [22]

$$\delta(k) = \lim_{\Delta \to 0^+} \int \mathrm{d}^d x \; (\Lambda x)^{-\Delta} \exp\{i\boldsymbol{k} \cdot \boldsymbol{x}\} = S_d^{-1} k^{-d} \lim_{\Delta \to 0^+} \Delta (k/\Lambda)^\Delta \,.$$

3.4.2   Compressible Navier-Stokes equation

The compressible form of NS equation represents one of the most general description of
non-relativistic fluids. Compressibility in the simplified Kraichnan model of turbulence
(3.4.1) was modelled by considering longitudinal modes of the velocity-velocity correlator
(e.g. longitudinal projection operator Q_{ij}) with a corresponding "compressibility" param-
eter α. In the case of NS the situation is more difficult. The general RG approach to
weakly compressible fluids was studied in detail in works [21, 61, 67][7].

Following mainly the work of [21] we will now describe this model. Let us first start
with the general form of the NS equations(3.1.8) and divide it by ρ

$$\nabla_t v_i = \nu[\delta_{ij}\partial^2 - \partial_i\partial_j]v_j + u\nu\partial_i\partial_j v_j - \rho^{-1}\partial_i p + f_i \ , \qquad (3.4.9)$$
$$\nabla_t \rho = -\rho(\partial_i v_i) \ , \qquad (3.4.10)$$

where we replaced ρ in the viscous term with its mean value, $\nu = \mu/\overline{\rho}$ is the kinematic
viscosity and u is related to the bulk viscosity ξ in the following way

$$\nu(u-1) = \nu/3 + \zeta/\overline{\rho} \ . \qquad (3.4.11)$$

The purpose for separating the transversal and longitudinal parts of the Laplace operator
in (3.4.9) is to simplify the derivation of propagators in the field-theoretic formulation.
The approximation of replacing ρ with its mean value in the viscous terms was implicitly
justified by the analysis of [67] and it is needed to obtain a renormalizable field-theoretic
model. In order to obtain a full set of equations we imply the isothermal closure (3.1.4).
Defining the new density related field as

$$\phi = c^2 \ln \rho/\overline{\rho} \ , \qquad (3.4.12)$$

we derive the De Dominicis-Janssen action functional (1.3.24) for the compressible stochas-
tic NS equation

$$\begin{aligned}\mathcal{S}^{\text{cNS}}[\boldsymbol{v}', \boldsymbol{v}, \phi', \phi] = &-\frac{1}{2}v_i' D_{ij}^f v_j' + v_i' \left\{\nabla_t v_i - \nu[\delta_{ik}\partial^2 - \partial_i\partial_k]v_k - u\nu\partial_i\partial_k v_k + \partial_i\phi\right\} + \\ &+ \phi' \left\{\nabla_t \phi + c^2\partial_i v_i\right\} \ ,\end{aligned} \qquad (3.4.13)$$

where D_{ij}^f is again the two point random force correlator now defined as

$$\langle f_i(x)f_j(x')\rangle = \frac{\delta(t-t')}{(2\pi)^d} \int_{k \geq m} \mathrm{d}^d k D^f(\boldsymbol{k}) \left(P_{ij}(\boldsymbol{k}) + \alpha Q_{ij}(\boldsymbol{k})\right) \exp\{i\boldsymbol{k}(\boldsymbol{x} - \boldsymbol{x}')\} \ . \quad (3.4.14)$$

Here, $k \geq m$ is the IR cut-off and $D(\boldsymbol{k})^f$ is the spectrum of the random force (3.4.5).

Properties of the model (3.4.13) were investigated in [61] in 3 dimensions using RG
methods where the spectrum of the random force was chosen in the same simplified form
as in the case of incompressible turbulence (3.4.5) (up to the longitudinal projection
operator). In the first order of perturbation theory, authors have shown that in the large
scale "energy pumping" limit $y \to 4$ the static velocity-velocity correlator (3.3.11) has the
following form

$$D_{\text{stat}}(\boldsymbol{k}) \propto \varepsilon^{2/3}k^{-11/3} \left(P_{ij}(\boldsymbol{k}) + \alpha(1 + a\text{MaRe}^{1/4}(kL)^{-2/3})Q_{ij}(\boldsymbol{k})\right) \ , \qquad (3.4.15)$$

---

[7]RG approach to compressible turbulence was first done in [68] but as stated in [21] authors did
not pay attention to the multiplicative renormalization of their model and therefore their approach was
mathematically inconsistent.

with a being some proportionality constant that cannot be determined by the means of RG. One can see corrections to the Kolmogorov $-5/3$ law due to the Ma number and the corrections increase with higher value of α. It seems that the $-5/3$ law is obtained in the limit $\alpha \to 0$. However, as stated in section 3.3.1 the limit $\alpha \to 0$ does not correspond to an incompressible limit.

3.4.3   Turbulent diffusion

There are two main models describing advection-diffusion processes in compressible flow [47]

- Advection of the *tracer* field $\theta(\boldsymbol{x}, t)$

$$\partial_t \theta + (v_i \partial_i)\theta = D\partial^2 \theta + f \ , \tag{3.4.16}$$

  where D is the diffusion constant and $f = f(\boldsymbol{x}, t)$ is an external (random) force. This equation describes a quantity that is conserved in the absence of the diffusivity and the random force along the Lagrangian trajectories $\nabla_t \theta = 0$. (e.g. entropy, temperature).
- Advection of the *passive scalar* density field $\rho(\boldsymbol{x}, t)$

$$\partial_t \rho + \partial_i(v_i \rho) = D\partial^2 \rho + f \ , \tag{3.4.17}$$

  where we used the same notation as above. Eq. (3.4.17) without the right hand side has a form of the continuity equation and therefore the total "mass" $\int \rho(\boldsymbol{x}, t)\mathrm{d}^d x$ is conserved (e.g. density of the pollutant).

Note that equations (3.4.16) and (3.4.17) coincide for the incompressible case. However, in the compressible case we have to distinguish them. In order to study the turbulent advection generally we can replace the temporal derivative by the *generalized Galilean-invariant covariant derivative*

$$\partial_t \theta \to \partial_t \theta + (1 - a)v_i\partial_i\theta + a\partial_i(v_i\theta) = \nabla_t \theta + a(\partial_i v_i)\theta \ , \tag{3.4.18}$$

where we introduce a new dimensionless parameter a that corresponds to advection of the tracer field (3.4.16) for $a = 0$ and to advection of the scalar field (3.4.17) for $a = 1$.

   The field-theoretic formulation for the models above can be done by finding the De Dominicis-Janssen action functional (1.3.24). The substitution (3.4.18) can also be used for coupling the velocity field to fields describing reaction-diffusion processes described in section 1.4 and we will also use it in order to study turbulent advection of the percolation process in the next chapter. By means of the RG methods we can then find scaling dimensions for corresponding fields and parameters. In some special cases however (and not only incompressible cases), one can simply work with models (3.4.16) or (3.4.17) and obtain the same results for both models (see for example [69]).

Chapter 4

Directed percolation process advected by compressible turbulent fluid

There are few experimental realisations of the DP phase transition. One of the reasons might be that additional external factors play an important role in this type of phase transition. Several modifications of the DP model have been done in the past years [15, 16, 17, 23]. In this chapter we will study the influence of the random environment on the DP phase transition.

A schematic visualisation of this process is displayed in Fig. 4.1. The black path that starts from the single seed on the left-hand side and spreads to the right-hand side represents the path of the percolating agent. The background represents the fully developed turbulence. It can be imagined as a disease spreading among species that are randomly moving around (e.g. animals, bacteria). Another example of this process might
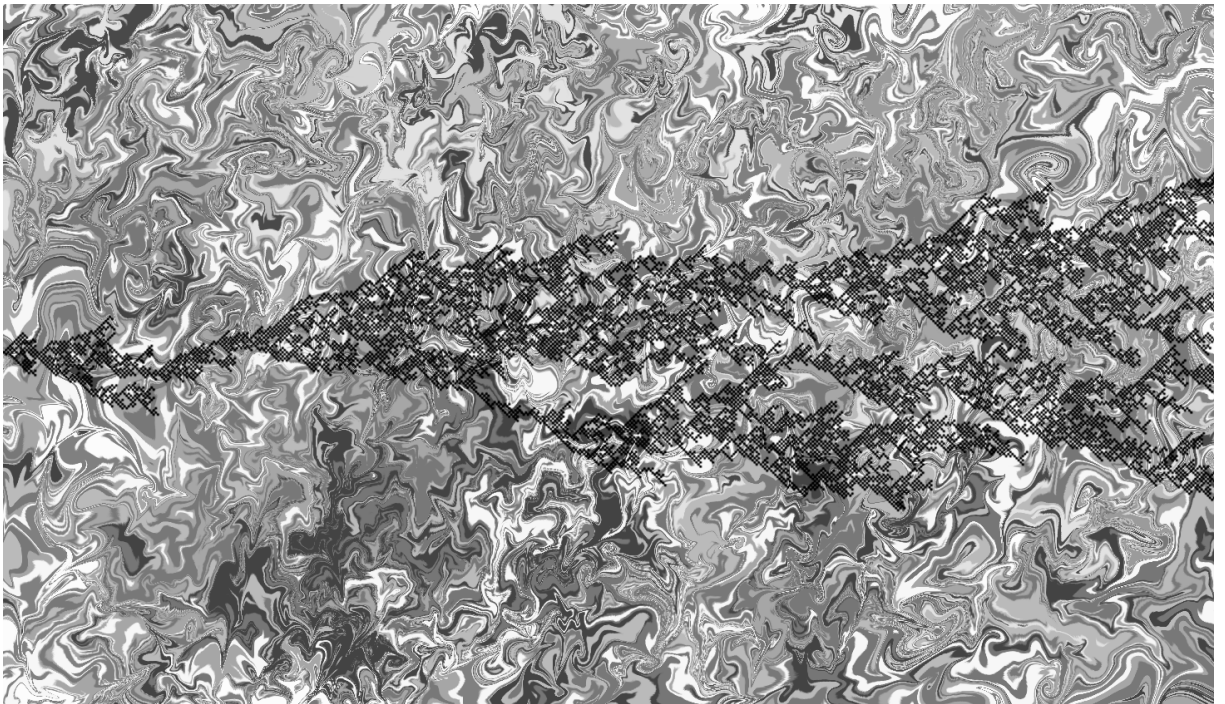
Figure 4.1: Schematic picture of the DP process influenced by the turbulent mixing.

be a forest fire advected by the turbulent air. In this case, the laminar component of the air forces the fire to move towards one direction, and we will study only the influence of the turbulent component to the DP phase transition. This example is, however, not completely precise since it assumes stationary species on which the percolation transition occurs. One should also keep in mind that Fig. 4.1 is only a schematic picture and not a proper visualisation of this process, since there are currently no experimental realisations or simulations of this process.

The problem of the DP process advected by turbulent flow has been already studied by several authors [18, 19, 20]. In [19], the field-theoretic model of the random environment was based on the incompressible NS equation. It has been shown, that in the physical region, the percolation should be irrelevant and the system belongs to the universality class of the turbulent diffusion. A similar result have been obtained in [18], where the random environment was modelled by the compressible Kraichnan model (3.4.1). By considering a certain degree of compressibility, the DP process becomes relevant. This also motivates us to study this process using the compressible form of the NS equation. It should be noted that all calculations previous in works have been done only in the one-loop approximation.

In the beginning of this chapter we define the field-theoretic formulation for both – DP and compressible NS turbulence and describe the structure of the perturbation theory. Multiplicative renormalization based on the analysis of UV divergences is then discussed. Here we assume several aspects of perturbation theory that determine the form of the counterterms necessary to eliminate all UV divergences. An important fact is that the rapidity symmetry is violated which has not been discussed by the previous authors when they introduced incompressible NS turbulence [19]. The model is then renormalized. In contrast to the incompressible case, our model shows an additional divergence around dimension $d = 4$. Since the upper critical dimension of the DP process is $d_c = 4$, in order to be mathematically consistent, we must also consider additional divergences arising in the compressible NS model. Both models are then renormalized. The counterterms are calculated in a double-expansion form of y and ε, where y describes the formulation of the turbulent velocity random force and $\varepsilon = 4 - d$ is the deviation from the upper critical dimension.

Since in this thesis we assume only the passive advection of the DP process, i.e. the DP field does not influence the compressible NS velocity field, the analysis of the fixed points and their stability can be discussed separately. The long-time and large-scale properties of the turbulent mixing are discussed. This analysis has been calculated independently and published recently in [70]. In what follows, we analyse the asymptotic behaviour of the DP process advected by compressible turbulent fluid.

It should be noted however that our model properly describes only the situation with $d = 3$, while the case $d = 2$ is not accessible. This is due to the additional divergences arising in the process of the renormalization of the compressible NS model around $d = 2$ [71]. It is also unclear how to approach the two dimensional case of the DP process with this model, since it would require an expansion of the DP process around $d = 2$.

4.1 Definition of the model, perturbation theory

In order to study compressible turbulent advection of the DP process, we have to study the field-theoretic model given by the sum

$$\mathcal{S}[\boldsymbol{v}'_0, \boldsymbol{v}_0, \phi'_0, \phi_0, \psi'_0, \psi_0] = \mathcal{S}^{\text{cNS}}[\boldsymbol{v}'_0, \boldsymbol{v}_0, \phi'_0, \phi_0] + \mathcal{S}^{\text{DP}}[\psi'_0, \psi_0] + \mathcal{S}^{\text{Adv}}[\psi'_0, \psi_0, \boldsymbol{v}_0] , \quad (4.1.1)$$

where $\mathcal{S}^{\text{cNS}}, \mathcal{S}^{\text{Per}}$ are the action functionals for the compressible NS model and DP process and $\mathcal{S}^{\text{Adv}}$ is the turbulent advection action functional. From now on, the summation over all doubled indices and integration over all variables is implied, if not specified explicitly. In addition, non-renormalized quantities are labelled with subscript 0, while renormalized ones without subscript.

Following section 3.4.2, the field-theoretic formulation for the compressible NS equations is

$$\mathcal{S}^{\text{cNS}}[\Phi_0] = -\frac{1}{2}v'_{i0}D^f_{ij}v'_{j0} + v'_{i0}\left\{\nabla_t v_{i0} - \nu_0[\delta_{ij}\partial^2 - \partial_i\partial_k]v_{k0} - u_0\nu_0\partial_i\partial_j v_{j0} + \partial_i\phi_0\right\} +$$
$$+ \phi'_0\left\{\nabla_t\phi_0 - \tilde{v}_0\nu_0\partial^2\phi_0 + c_0^2\partial_i v_{i0}\right\} , \quad (4.1.2)$$

where $\Phi_0 = \{\boldsymbol{v}'_0, \boldsymbol{v}_0, \phi'_0, \phi_0\}$, all fields and parameters have the usual meaning and the random force correlator in the momentum-frequency space is now

$$D^f_{ij}(\boldsymbol{k}, \omega) = g_{10}\nu_0^3 k^{4-d-y}\left(P_{ij}(\boldsymbol{k}) + \alpha_0 Q_{ij}(\boldsymbol{k})\right) + g_{20}\nu_0^3\delta_{ij} . \quad (4.1.3)$$

In (4.1.2) and (4.1.3), the terms $\tilde{v}_0\nu_0\partial^2\phi$ and $g_{20}\nu_0^3\delta_{ij}$ with coupling constants $\tilde{v}_0$, g_{20} have been added in order to ensure the multiplicative renormalizability as will be explained later. The physical value of these parameters is 0 and their appearance emerges during the renormalization procedure.

The field-theoretic formulation means that all correlation and response functions (1.3.5) are represented by the functional averages over the full set of fields with the functional weight $\exp\{-\mathcal{S}^{\text{cNS}}\}$ (1.3.26). Feynman diagramatic techniques can then be applied. The propagators are found as an inverse of the quadratic part of $\mathcal{S}^{\text{cNS}}$ (see the Appendix A)

$$G_0^{v_i v_j}(\boldsymbol{k}, \omega) \equiv \langle v_i v_j\rangle_0 = \frac{d^f_1}{|\epsilon_1|^2}P_{ij} + d^f_2\left|\frac{\epsilon_3}{R}\right|^2 Q_{ij} , \quad G_0^{\phi\phi}(\boldsymbol{k}, \omega) \equiv \langle\phi\phi\rangle_0 = \frac{c_0^4 k^2}{|R|^2}d^f_2 ,$$

$$G_0^{v'_i v_j}(\boldsymbol{k}, \omega) \equiv \langle v'_i v_j\rangle_0 = \frac{1}{\epsilon_1^*}P_{ij} + \frac{\epsilon_3^*}{R^*}Q_{ij} , \quad G_0^{\phi'\phi}(\boldsymbol{k}, \omega) \equiv \langle\phi'\phi\rangle_0 = \frac{\epsilon_2^*}{R^*} ,$$

$$G_0^{v'_i\phi}(\boldsymbol{k}, \omega) \equiv \langle v'_i\phi\rangle_0 = \frac{ic_0^2 k_i}{R^*} , \quad G_0^{v_i\phi}(\boldsymbol{k}, \omega) \equiv \langle v_i\phi\rangle_0 = \frac{ic_0^2\epsilon_3 k_i}{|R|^2}d^f_2 ,$$

$$G_0^{v_i\phi'}(\boldsymbol{k}, \omega) \equiv \langle v_i\phi'\rangle_0 = \frac{-ik_i}{R} ,$$

$$(4.1.4)$$

where the following abbreviations have been introduced

$$\begin{aligned}
\epsilon_1 &= -i\omega + \nu_0 k^2, & d^f_1 &= \nu_0^3(\alpha_0 g_{10}k^{4-d-y} + g_{20}), \\
\epsilon_2 &= -i\omega + \nu_0 u_0 k^2, & d^f_2 &= \nu_0^3(g_{10}k^{4-d-y} + g_{20}), \\
\epsilon_3 &= -i\omega + \nu_0\tilde{v}_0 k^2, & R &= \epsilon_1\epsilon_2 + c_0^2 k^2.
\end{aligned} \quad (4.1.5)$$

The physical interpretation of the above propagators is the following. The propagators constructed from any primed field φ' and any un-primed field φ represent a response function from φ' to φ. The propagator G_0^{vv} is connected to the kinetic energy spectrum, while
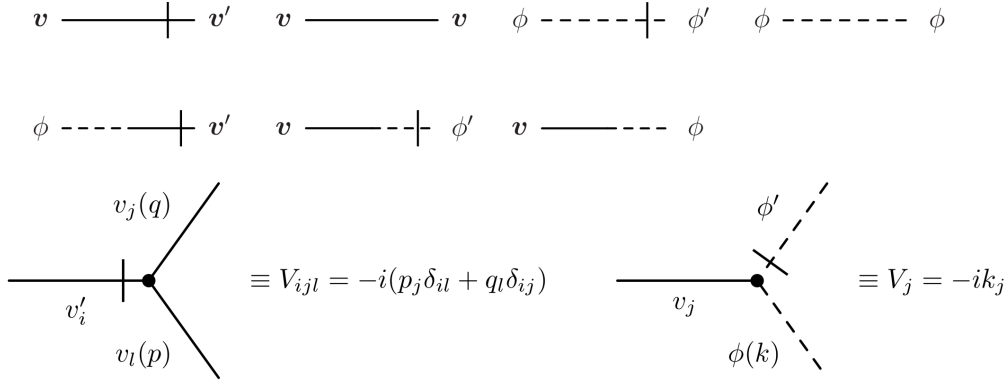
Figure 4.2: Feynman correspondence rules for the compressible NS model (4.1.2). Explicit formulas for propagators are given in (4.1.4).

propagator $G_0^{\phi\phi}$ is connected to the spectrum of the density variations in the free theory. In the incompressible limit $c_0 \to \infty$, propagators $G_0^{vv'}, G_0^{vv}$ become purely transversal while $G_0^{v\phi'}, G_0^{\phi\phi'}$ and $G_0^{v\phi}$ vanish. This means that the velocity field v_i decouples from the density field ϕ and it can be treated independently[1]. The field v_i becomes transversal, which satisfies the incompressibility condition $\partial_i v_i = 0$. One should also note, that the incompressible limit can be obtained by performing the limit $u \to \infty$ which gives the additional constraint $\partial_i v_i = 0$ to our system. In this case the propagators G_0^{vv} and $G_0^{v'v}$ become purely transversal and the velocity field decouples from the density field.

The vertex factors can be obtained from the Fourier transformation of the interaction part of the action (4.1.2) (see Appendix A.2)

$$-v_i' v_j \partial_j v_l \to V_{ijl}^{\text{cNS}} = -i(p_j \delta_{il} + q_l \delta_{ij}) \;, \tag{4.1.6}$$

$$-\phi' v_i \partial_i \phi \to V_i^{\text{cNS}} = -i k_i \;. \tag{4.1.7}$$

Feynman diagramatic techniques can then be defined as seen in Fig. 4.2.

The field-theoretic formulation of the DP process has been introduced in section 2.3.12

$$\mathcal{S}^{\text{DP}}[\psi_0', \psi_0] = \psi_0' \big\{ \partial_t + D_0(-\partial^2 + \tau_0) \big\} \psi_0 - \frac{D_0 \lambda_0}{2} \big\{ \psi_0' - \psi_0 \big\} \psi_0' \psi_0 \;, \tag{4.1.8}$$

where the coupling constant has been rescaled to a more convenient form $g_0 = \lambda_0 D_0$ and the rest of the parameters and fields have the usual meaning. The first bracket in (4.1.8) stands for the diffusion part, while the latter stands for the DP interaction part. In order to study advection by the turbulent compressible fluid flow, one assumes temporal dependence of the spatial variables $\boldsymbol{x} = \boldsymbol{x}(t)$. The time derivative is then replaced by the total time derivative and this leads to appearance of the advection action functional

$$\mathcal{S}^{\text{Adv}}[\psi_0', \psi_0, \boldsymbol{v}_0] = \psi_0' \big\{ v_{i0} \partial_i + a_0 (\partial_i v_{i0}) \big\} \psi_0 \;, \tag{4.1.9}$$

where we have introduced the additional term with a parameter a_0 in order to ensure the multiplicative renormalization (see below). The physical value of this parameter is 0 or 1 which corresponds to the advection of the tracer field or the scalar density field (see section 3.4.3). Note that the rapidity symmetry (2.3.11) for the full model (4.1.8) with

---

[1]The fact that the density field does not decouple from the velocity field ($G_0^{v'\phi}$ does not vanish) is unimportant to us, since the density field does not influence turbulent diffusion directly.
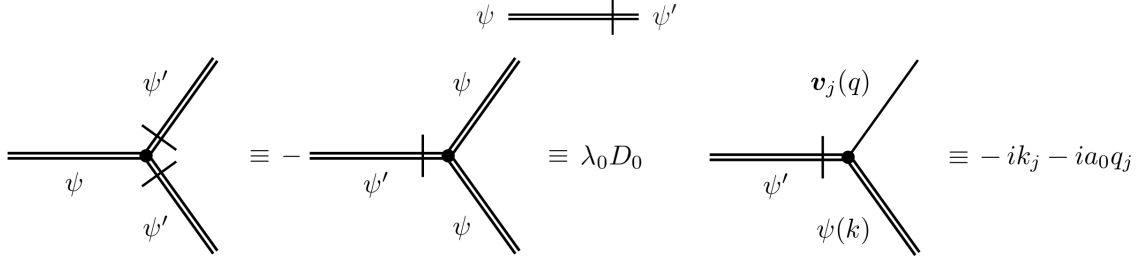
Figure 4.3: Feynman correspondence rules for the DP process advected by the velocity field.

(4.1.9) is violated, since the action functional for the velocity field (4.1.2) is in general not invariant with respect to time inversion. This implies that the number of independent critical exponents describing the DP phase transition (see section 2.2) increases from three to four.

Propagators and vertex factors are found in the standard way:

$$G_0^{\psi'\psi}(\boldsymbol{k}, \omega) \equiv \langle \psi'\psi \rangle_0 = \frac{1}{-i\omega + D_0(k^2 + \tau_0)} \, , \tag{4.1.10}$$

$$D_0\lambda_0\psi'^2\psi = -D_0\lambda_0\psi'\psi^2 \rightarrow \; V^{\text{Per}} = D_0\lambda_0 \, , \tag{4.1.11}$$

$$-\psi'\{v_i\partial_i + a_0(\partial_i v_i)\}\psi \rightarrow V_i^{\text{Per}} = -i(k_i + a_0 q_j) \, . \tag{4.1.12}$$

The graphical representation is depicted in Fig. 4.3. Note, that the DP field ψ is not affecting the compressible turbulence determined by (4.1.2) and therefore we can interpret it in terms of passive reaction-diffusion process.

4.2 UV divergences, the renormalization group

As mentioned in section 1.3.3 dynamical models involve two independent scales. In order to apply RG methods the introduction of the total canonical dimension (1.3.39) is necessary. The choice $d_\omega = 2$ makes the viscosity coefficient dimensionless and the total canonical dimension is then

$$d_F = d_F^k + 2d_F^\omega \, . \tag{4.2.1}$$

The canonical dimensions for the model (4.1.2) are summarized in Tab. 4.1. The total canonical dimension for any vertex function Γ (1.3.44) yields

$$d_\Gamma = d + 2 - \sum_\Phi d_\Phi N_\Phi, \quad d_\Phi = d_\Phi^k + 2d_\Phi^\omega \, , \tag{4.2.2}$$

Q	$\boldsymbol{v}'_0$	$\boldsymbol{v}_0$	ϕ'_0	ϕ_0	m, μ, Λ	ν_0, ν	c_0, c	g_{10}	g_{20}	$u_0, v_0, u, v, g_1, g_2, \alpha_0, \alpha$
d_Q^k	$d+1$	-1	$d+2$	-2	1	-2	-1	y	ε	0
d_Q^ω	-1	1	-2	2	0	1	1	0	0	0
d_Q	$d-1$	1	$d-2$	2	1	0	1	y	ε	0

Table 4.1: Canonical dimensions of the bare fields and bare parameters for the model of velocity fluctuations. Parameters m and Λ play the role of IR and UV cut-off and μ is the scale setting parameter.

where Φ is the set of all fields that the vertex function is constructed from, d_Φ is the corresponding total canonical dimension and N_Φ is the number of fields Φ entering the vertex function.

The choice $d_\omega = 2$ is related to the dispersion law for diffusion modes $\omega \sim k^2$ and it merely means, that we are interested in the correlated long time and large scale limit $\omega \sim k^2 \to 0$. Another choice, for example $d_\omega = 1$ would lead to the analysis of sound in a turbulent media. However, this choice leads to unrenormalizable model [69].

4.2.1   Renormalization of the velocity field

Renormalization of the model (4.1.2) was done in [21] in three dimensions. Since the upper critical dimension of the DP process is four, in order to perform consistent RG calculation, the model (4.1.2) must be also renormalized around $d = 4$. This can be done by eliminating all possible UV divergences arising in the vertex function (see section 1.2.3) around $d = 4$. The following calculations have been done independently and recently published in [70]. Superficial divergences that require elimination by counterterms are present in the vertex functions Γ with non-negative UV exponent (1.2.62),(1.3.44),

$$\delta_\Gamma = d_\Gamma|_{d=4} = 6 - 3N_{v'} - N_v - 2(N_{\phi'} + N_\phi) \ . \tag{4.2.3}$$

UV exponents for various vertex functions are given in Tab. 4.2. However, additional facts have to be taken into account:

- As explained in the section 1.3.2 all vertex functions with zero response fields $N_{v'} = 0$ or $N_{\phi'} = 0$ are equal to zero, therefore no such a counterterms appear.

- The field ϕ appears in the vertex $\phi'(v_i\partial_i)\phi$ together with its derivative and hence the real UV exponent is reduced as (1.2.63) to

$$\delta'_\Gamma = \delta_\Gamma - n_\phi \ , \tag{4.2.4}$$

  For example, the function $\Gamma^{\phi'\phi}$ has $\delta_\Gamma = 2$, but $\delta'_\Gamma = 1$ and ϕ must enter the counterterms with at least one ∂. The counterterm $\phi'\partial_t\phi$ is therefore forbidden and the only possible structure is $\phi'\partial^2\phi$. Similar situations apply for vertex functions containing v_i, since it enters the vertex as $v'_i(v_j\partial_j)v_i$.

- The Galilean invariance of the model (4.1.2)

$$v_i^w(\boldsymbol{x}, t) = v_i(\boldsymbol{x} + \boldsymbol{w}t, t) - w_i, \ \Phi^w(\boldsymbol{x}, t) = \Phi(\boldsymbol{x} + \boldsymbol{w}t, t), \ \Phi = \{\boldsymbol{v}', \phi, \phi'\} \ , \tag{4.2.5}$$

  where w_i is a constant vector, requires that the covariant derivative ∇_t must enter the counterterms as a whole. As a consequence, the counterterm for $\Gamma^{\phi'v\phi}$ with $\delta'_\Gamma = 0$ which can only have the form $\phi'(v_i\partial_i)\phi$ is forbidden, since $\phi'\partial_t\phi$ is also forbidden.

δ_Γ	4	3	2		1		0			
Γ	v^2	v^3	v^4	ϕ^2	v^5	v^2v'	v^6	$v^2\phi^2$	v'^2	ϕ^3
		$v\phi$	$v^2\phi$	$\phi\phi'$	$v^3\phi$	$v'\phi$	$v^4\phi$	$v^2\phi\phi'$	$vv'\phi$	$\phi^2\phi'$
		$v\phi'$	$v^2\phi'$	ϕ'^2	$v^3\phi'$	$v'\phi'$	$v^4\phi'$	$v^2\phi'^2$	$vv'\phi'$	$\phi\phi'^2$
			vv'				v^3v'			ϕ'^3

Table 4.2: The vertex functions with non-negative UV exponent.

- For $\Gamma^{v'v}$ we have $\delta_\Gamma = 2(\delta'_\Gamma = 1)$ and for $\Gamma^{v'vv}$ we have $\delta_\Gamma = 1(\delta'_\Gamma = 0)$. These divergences can be eliminated by the counterterms $v'_i\partial^2 v_i$ and $v'_i\nabla_t v_i$. The latter is forbidden by the same reason, as $\phi'\nabla_t\phi$. In fact, $v'_i\nabla_t v_i$ is invariant also with respect to the *generalized Galilean invariance* [11]

$$v^w_i(\boldsymbol{x},t) = v_i(\boldsymbol{x}+\boldsymbol{w}t,t) - w_i(t), \quad \Phi^w(\boldsymbol{x},t) = \Phi(\boldsymbol{x}+\boldsymbol{u},t) , \tag{4.2.6}$$

$$u_i(t) = \int_{-\infty}^{t} w_i(t')\mathrm{d}t', \qquad\qquad \Phi = \{\boldsymbol{v}',\phi,\phi'\} . \tag{4.2.7}$$

  It should be stressed, that the action functional (4.1.2) is not generally invariant with respect to the above transformation since $\mathcal{S}[\Phi^w] = \mathcal{S}[\Phi] + v'_i\partial_t w_i$. However, the relation between the action functional and the effective potential (1.2.29) is invariant and therefore counterterms are invariant.

- From the explicit form of the propagators in (4.1.4), $G^{v'\phi}_0$ and $G^{v\phi}_0$ are proportional to c^2_0 while $G^{\phi\phi}_0$ is proportional to c^4_0. Since these factors have positive total canonical dimension, they appear as an external factor to every diagram. The real index of UV divergence is reduced with the number of fields containing this factor. The vertex function with $N_{\phi'} > N_\phi$ contains $c_0^{2(N_{\phi'}-N_\phi)}$. The counterterm for $\Gamma^{\phi'v}$ with $\delta_\Gamma = 3$ then necessarily reduces to $c^2_0\phi'(\partial v)$ and the structure $\phi'\partial^2(\partial v)$ and similar are forbidden. In the same way, $\Gamma^{\phi'vv}$ with $\delta = 2$ reduces to $c^2_0\phi v^2$ while $\phi(\partial v)^2$ is forbidden. In fact, $c^2_0\phi v^2$ cannot appear because of Galilean invariance as well.

Taking into account all above considerations, we conclude that all UV divergences can be removed by the following counterterms:

$$\phi'\partial^2\phi, \quad c^2_0\phi'(\partial_i v_i), \quad (v'_i\partial_i)\phi, \quad v'_i\partial^2 v_i, \quad (v'_i\partial_i)(\partial_j v_j), \quad v'_i v'_i . \tag{4.2.8}$$

The last term in (4.2.8) is a new counterterm that does not appear in the renormalization around $d = 3$. A similar situation occurs for $d = 2$ in case of incompressible turbulence, where this term represents the thermal fluctuations [71]. Renormalization of the action functional is then ensured by the multiplicative renormalization of the parameters and fields

$$\begin{aligned} g_{10} &= g_1\mu^y Z_{g_1}, & g_{20} &= g_2\mu^\varepsilon Z_{g_2}, & u_0 &= uZ_u, & \tilde{v}_0 &= \tilde{v}Z_{\tilde{v}}, \\ \nu_0 &= \nu Z_\nu, & c_0 &= cZ_c, & m_0 &= Z_m m, & \alpha_0 &= Z_\alpha\alpha, \\ v_{i0} &= Z_{v_i}v_i, & v'_{i0} &= Z_{v'_i}v'_i, & \phi_0 &= Z_\phi\phi, & \phi'_0 &= Z_{\phi'}\phi'. \end{aligned} \tag{4.2.9}$$

where we have suppressed the subscript "R" for the renormalized variables for simplicity. The renormalized action functional of the model (4.1.2) reads

$$\begin{aligned} \mathcal{S}^{\mathrm{cNS}}_R[\boldsymbol{v}',\boldsymbol{v},\phi',\phi] = & -\frac{1}{2}v'_i D^f_{ij}v'_j + v'_i\left\{\nabla_t v_i - Z_1\nu[\delta_{ij}\partial^2 - \partial_i\partial_k]v_k - Z_2 u\nu\partial_i\partial_j v_j + Z_4\partial_i\phi\right\} + \\ & + \phi'\left\{\nabla_t\phi - Z_3 v\nu\partial^2\phi + Z_5 c^2\partial_i v_i\right\} , \end{aligned} \tag{4.2.10}$$

with the random force correlator

$$D^f_{ij}(\boldsymbol{k}) = g_1\mu^y\nu^3 k^{4-d-y}\left(P_{ij}(\boldsymbol{k}) + Z_\alpha\alpha Q_{ij}(\boldsymbol{k})\right) + Z_6 g_2\mu^\varepsilon\nu^3 , \tag{4.2.11}$$

and the relations for the renormalization constants are

$$\begin{aligned} Z_{g_1}Z^3_\nu &= 1, & Z_1 &= Z_\nu, & Z_3 &= Z_{\tilde{v}}Z_\nu, & Z_5 &= Z_{\phi'}Z^2_c, & Z_v Z_{v'} &= 1, \\ Z_{\phi'}Z_\phi &= 1, & Z_2 &= Z_u Z_\nu, & Z_4 &= Z_\phi, & Z_6 &= Z_{g_2}Z^3_\nu, \end{aligned} \tag{4.2.12}$$

from which inverted relations are readily obtained

$$
\begin{aligned}
Z_\phi &= Z_4, & Z_{g_1} &= Z_1^{-3}, & Z_u &= Z_2 Z_1^{-1}, & Z_\nu &= Z_1, & Z_\alpha &= 1, \\
Z_{\phi'} &= Z_4^{-1}, & Z_{g_2} &= Z_6 Z_1^{-3}, & Z_{\tilde{v}} &= Z_3 Z_1^{-1}, & Z_c &= (Z_4 Z_5)^{1/2}, & Z_m &= 1.
\end{aligned}
\tag{4.2.13}
$$

Whereas the absence of the renormalization of α and m follows from the fact that non-local terms do not renormalize [22]. Also note, that no normalization of the fields v, v' is needed due to the absence of the normalization fo $v'\nabla_t v$. The full set of constants are found from divergent parts of all possible 1PI diagrams with amputated external propagators. The expressions for the 1PI functions in one loop approximation are then computed from (4.2.10) using (1.2.32)

$$
\Gamma^{v_i' v_j} = i\omega - \nu(\delta_{ij}k^2 - k_i k_j)Z_1 - u\nu k_i k_j Z_2 + \quad\text{}
\tag{4.2.14}
$$

$$
\Gamma^{\phi'\phi} = i\omega - \tilde{v}\nu k^2 Z_3 + \quad\text{} + \quad\text{}
\tag{4.2.15}
$$

$$
\Gamma^{v_i'\phi} = -ik_i Z_4 + \quad\text{}
\tag{4.2.16}
$$

$$
\Gamma^{\phi' v_i} = -ik_i c^2 Z_5 + \quad\text{} + \quad\text{} + \quad\text{}
\tag{4.2.17}
$$

$$
\Gamma^{v_i' v_j'} = g_1 \mu^y \nu^3 k^{4-d-y} \left(P_{ij}(\boldsymbol{k}) + \alpha Q_{ij}(\boldsymbol{k})\right) + g_2 \mu^\varepsilon \nu^3 \delta_{ij} Z_6 + \frac{1}{2} \quad\text{}
\tag{4.2.18}
$$

The explicit forms of divergent part of Feynman diagrams and renormalization constants can be found in appendices (B.1) and (C.2).

4.2.2   Renormalization of percolation field

Multiplicative renormalizability of model (4.1.8) was discussed in [18, 19], where the velocity field was modelled by Kraichnan (rapid-change) model (3.4.1) and in the latter by the incompressible NS model (3.4.13). In order to study turbulent reaction-diffusion processes, it is convenient to rescale the diffusion constant as $D_0 = w_0 \nu_0$ where the new dimensionless parameter w_0, an inverse of the Prantl number, has been introduced. The canonical dimensions of model (4.1.8) are shown in Tab. 4.3. We can see, that our model becomes logarithmic for $\varepsilon = 0$ and the formal index of UV divergence (1.3.44) for any vertex function is

$$
\delta_\Gamma = 6 - 3N_{v'} - N_v - 2(N_{\phi'} + N_\phi + N_\psi + N_{\psi'}) .
\tag{4.2.19}
$$

Vertex functions with non-negative UV exponents can be found in Tab. 4.4. We have also introduced a new coupling constant $g_{30} = \lambda_0^2$ since the actual expansion is λ_0^2 (see for example the normalization constants in Appendix C). Construction of the counterterms needs to consider additional facts [18, 19]:

Q	ψ'	ψ	λ_0	D_0	$g_{30} = \lambda_0^2$	$w_0 = D_0/\nu_0$	λ, a, a_0
d_Q^k	$d/2$	$d/2$	$\varepsilon/2$	-2	ε	0	0
d_Q^ω	0	0	0	1	0	0	0
d_Q	$d/2$	$d/2$	$\varepsilon/2$	0	ε	0	0

Table 4.3: Canonical dimensions of the bare fields and bare parameters for the model of directed percolation process

δ_Γ	3	2		1			0				
Γ	ψv	ψv^2	$\psi\phi$	ψv^3	$\psi^2 v$	$\psi\phi v$	ψv^4	$\psi\phi v^2$	$\psi\phi^2$	$\psi^2\phi$	ψ^3
	$\psi' v$	$\psi' v^2$	$\psi'\phi$	$\psi' v^3$	$\psi\psi' v$	$\psi'\phi v$	$\psi' v^4$	$\psi'\phi v^2$	$\psi'\phi^2$	$\psi\psi'\phi$	$\psi^2\psi'$
	ψ^2	$\psi\phi'$	$\psi v'$	$\psi'^2 v$	$\psi\phi' v$	$\psi v' v$	$\psi\phi' v^2$	$\psi\phi'\phi$	$\psi'^2\phi$	$\psi\psi'^2$	
	$\psi\psi'$	$\psi'\phi'$	$\psi' v'$		$\psi'\phi' v$	$\psi' v' v$	$\psi'\phi' v^2$	$\psi'\phi'\phi$	$\psi^2\phi'$	ψ'^3	
	ψ'^2								$\psi\phi'^2$	$\psi\psi'\phi'$	
									$\psi'\phi'^2$	$\psi'^2\phi'$	

Table 4.4: Vertex functions with non-negative UV exponent d_Γ for the model (4.1.8) and (4.1.9)

- Due to the structure of propagators, any vertex function that does not contain at least one field ψ and at least one field ψ' will contain a closed loop of retarded Green's functions and vanishes.

- As in the case of compressible NS mode, Galilean invariance implies that divergences in $\Gamma^{\psi'\psi}$ and $\Gamma^{\psi' v}$ can be eliminated by counterterms containing ∂^2, τ and ∇_t.

We conclude, that the necessary counterterms are

$$\psi'\partial_t\psi, \quad \psi'\partial^2\psi, \quad \tau\psi'\psi, \quad \psi'(v\partial)\psi, \quad \psi'(\partial v)\psi, \quad \psi'\psi^2, \quad \psi'^2\psi \,. \tag{4.2.20}$$

The fifth term has not been included in the original action functional, and therefore it is assigned with a dimensionless parameter a_0. In order to eliminate UV divergences, parameters and fields in (4.1.8) and (4.1.9) have to be renormalized as follows

$$g_{30} = g_3\mu^\varepsilon Z_{g_3}, \quad D_0 = D Z_D, \quad \tau_0 = \tau Z_\tau, \quad \psi_0 = Z_\psi\psi, \tag{4.2.21}$$

$$\lambda_0 = \lambda\mu^{\varepsilon/2} Z_\lambda, \quad w_0 = w Z_w, \quad a_0 = a Z_a, \quad \psi'_0 = Z_{\psi'}\psi', \tag{4.2.22}$$

where we have included the new coupling constant $g_3 = \lambda^2$. The full renormalized action functional for the advected DP process then attains the expected form

$$\mathcal{S}_R^{\mathrm{DP}}[\psi, \psi'] = \psi'\big\{Z_7\partial_t - Z_8 D\partial^2 + Z_9\tau\big\}\psi - \frac{D\lambda\mu^{\varepsilon/2}}{2}\big\{Z_{10}\psi' - Z_{11}\psi\big\}\psi'\psi, \tag{4.2.23}$$

$$\mathcal{S}_R^{\mathrm{Adv}}[\psi, \psi', \boldsymbol{v}] = \psi'\big\{Z_7 v_i\partial_i + Z_{12} a(\partial_i v_i)\big\}\psi, \tag{4.2.24}$$

where the relations between renormalization constants are

$$\begin{aligned}
Z_7 &= Z_{\psi'} Z_\psi, & Z_9 &= Z_{\psi'} Z_\psi Z_D Z_\tau, & Z_{11} &= Z_{\psi'} Z_\psi^2 Z_D Z_\lambda, \\
Z_8 &= Z_{\psi'} Z_\psi Z_D, & Z_{10} &= Z_{\psi'}^2 Z_\psi Z_D Z_\lambda, & Z_{12} &= Z_{\psi'} Z_\psi Z_a,
\end{aligned} \tag{4.2.25}$$

together with their inverses

$$\begin{aligned}
Z_\psi &= (Z_7 Z_{11} Z_{10}^{-1})^{1/2}, & Z_D &= Z_8 Z_7^{-1}, & Z_\lambda &= Z_8^{-1}(Z_7^{-1} Z_{10} Z_{11})^{1/2}, & Z_a &= Z_{12} Z_7^{-1}, \\
Z_{\psi'} &= (Z_7 Z_{11}^{-1} Z_{10})^{1/2}, & Z_\tau &= Z_9 Z_8^{-1}, & Z_w &= Z_D Z_\nu^{-1} = Z_8 Z_7^{-1} Z_1^{-1}, & Z_{g_3} &= Z_\lambda^2.
\end{aligned} \tag{4.2.26}$$

Note that the velocity field in (4.2.24) generally breaks down the duality symmetry (rapidity symmetry) (2.3.11). Renormalization constants are found from the following relations

for the vertex functions

$$\Gamma_{\psi'\psi} = i\omega Z_7 - Dk^2 Z_8 - D\tau Z_9 + \frac{1}{2} \quad + \quad \tag{4.2.27}$$

$$\Gamma_{\psi\psi'\psi'} = D\lambda\mu^{\frac{\varepsilon}{2}} Z_{10} + \quad + 2 \quad + 2 \quad \tag{4.2.28}$$

$$\Gamma_{\psi'\psi\psi} = - D\lambda\mu^{\frac{\varepsilon}{2}} Z_{11} + \quad + 2 \quad + 2 \quad \tag{4.2.29}$$

$$\Gamma_{\psi'\psi v_i} = - ip_i Z_7 - iq_i Z_{12} + \quad + \quad + \quad + \tag{4.2.30}$$

$$+ \quad + \quad + \quad \tag{4.2.31}$$

The explicit forms of the divergent parts of Feynman diagrams and renormalization constants calculated in the form of double expansion of y and ε can be found in appendices B.2 and C.2.

4.3 Asymptotic behaviour

The investigation of the large-scale behaviour requires analysis of the Green's functions at different scales. The Green's functions for the full model (4.1.1) are normalized in the following way (see section 1.3.3)

$$G(\{\boldsymbol{k}_i\}, \{\omega_i\}, e_0) = Z_\phi^{N_\phi}(g) Z_{\phi'}^{N_{\phi'}}(g) Z_\psi^{N_\psi}(g) Z_{\psi'}^{N_{\psi'}}(g) G(\{\boldsymbol{k}_i\}, \{\omega_i\}, e, \mu), \tag{4.3.1}$$

$$e_0 \equiv \{g_{10}, g_{20}, g_{30}, u_0, \tilde{v}_0, w_0, \nu_0, c_0, \tau_0\}, \tag{4.3.2}$$

$$e \equiv \{g_1, g_2, g_3, u, \tilde{v}, w, \nu, c, \tau\}, \tag{4.3.3}$$

$$g \equiv \{g_1, g_2, g_3, u, \tilde{v}, w\}, \tag{4.3.4}$$

where e_0, $e = e(\mu)$ are the full sets of unrenormalized and renormalized parameters and $g = g(\mu)$ is the full set of renormalized charges. Note the absence of the normalization constants Z_v and $Z_{v'}$ since they are equal to unity. By performing the partial derivative with respect to $\ln\mu$ (see section (1.2.4) and (1.3.3)) we obtain the basic RG equation

$$\{\mathcal{D}_{RG} + N_\phi\gamma_\phi + N_{\phi'}\gamma_{\phi'} + N_\psi\gamma_\psi + N_{\psi'}\gamma_{\psi'}\}G(\{\boldsymbol{k}_i\}, \{\omega_i\}, e, \mu) = 0 \ , \tag{4.3.5}$$

where $\mathcal{D}_{RG}$ is the operation $\tilde{\mathcal{D}}_\mu$ expressed in terms of renormalized variables:

$$\mathcal{D}_{RG} = \mathcal{D}_\mu + \beta_{g_1}\partial_{g_1} + \beta_{g_2}\partial_{g_2} + \beta_{g_2}\partial_{g_3} + \beta_u\partial_u + \beta_{\tilde{v}}\partial_{\tilde{v}} + \beta_w\partial_w$$
$$- \gamma_\nu\mathcal{D}_\nu - \gamma_c\mathcal{D}_c - \gamma_\tau\mathcal{D}_\tau \ . \tag{4.3.6}$$

The beta functions are found using relations between the renormalized and unrenormalized parameters (4.2.9) and (4.2.21) as

$$
\begin{aligned}
\beta_{g_1} &= \tilde{\mathcal{D}}_\mu g_1 = g_{10}\tilde{\mathcal{D}}_\mu \mu^{-y} Z_{g_1}^{-1} = g_1(-y - \gamma_{g_1}), & \beta_{g_3} &= \tilde{\mathcal{D}}_\mu g_3 = g_3(-\varepsilon - \gamma_{g_3}), \\
\beta_{g_2} &= \tilde{\mathcal{D}}_\mu g_2 = g_2(-\varepsilon - \gamma_{g_2}), & \beta_w &= \tilde{\mathcal{D}}_\mu w = w(-\gamma_w), \\
\beta_u &= \tilde{\mathcal{D}}_\mu u = u(-\gamma_u), & \beta_a &= \tilde{\mathcal{D}}_\mu a = a(-\gamma_a), \\
\beta_{\tilde{v}} &= \tilde{\mathcal{D}}_\mu \tilde{v} = \tilde{v}(-\gamma_{\tilde{v}}),
\end{aligned}
\tag{4.3.7}
$$

while the anomalous dimension γ_F for a quantity F is defined as

$$
\gamma_F = \tilde{\mathcal{D}}_\mu \ln Z_F \ .
\tag{4.3.8}
$$

The IR fixed point g^* is then defined by the vanishing values of the Beta functions $\beta_g(g^*) = 0$ and its stability is determined by the eigenvalues of the matrix

$$
\Omega_{ij} = \left. \frac{\partial \beta_{g_i}}{\partial g_j} \right|_{g=g^*} ,
\tag{4.3.9}
$$

which in the case of the IR stable point must be positive definite.

Anomalous dimensions are calculated from the normalization constants whose structure is found to be

$$
Z_F(y, \varepsilon, g) = 1 + c_F^{(1)} \frac{g_1}{y} + c_F^{(2)} \frac{g_2}{\varepsilon} + c_F^{(3)} \frac{g_3}{\varepsilon} + \frac{c_F^{(4)}}{2y - \varepsilon} \frac{g_1^2}{g_2} \ ,
\tag{4.3.10}
$$

where $c^{(i)}, i \in \{1, 2, 3, 4\}$ are some finite expressions that can depend only on parameters $u, \tilde{v}, w, a$ and α. The anomalous dimensions are found in a similar way as (1.2.74)

$$
\gamma_F = \left((\tilde{\mathcal{D}}_\mu g_1)\partial_{g_1} + (\tilde{\mathcal{D}}_\mu g_2)\partial_{g_2} + (\tilde{\mathcal{D}}_\mu g_3)\partial_{g_3} \right) \ln Z_F
\tag{4.3.11}
$$

$$
\approx - \left(g_1 c_F^{(1)} + g_2 c_F^{(2)} + g_3 c_F^{(3)} + \frac{g_1^2}{g_2} c_F^{(4)} \right) \ .
\tag{4.3.12}
$$

Eq. (4.2.13) and (4.2.26) then imply the following relations between the anomalous dimensions

$$
\begin{aligned}
\gamma_{v'} &= \gamma_v = \gamma_\alpha = \gamma_m = 0 \ , & \gamma_{g_3} &= -\gamma_7 + \gamma_{10} + \gamma_{11} - 2\gamma_8 \ , \\
\gamma_\phi &= -\gamma_{\phi'} = \gamma_4 \ , & \gamma_\psi &= (\gamma_7 + \gamma_{11} - \gamma_{10})/2 \ , \\
\gamma_c &= (\gamma_4 + \gamma_5)/2 \ , & \gamma_{\psi'} &= (\gamma_7 - \gamma_{11} + \gamma_{10})/2 \ , \\
\gamma_{\tilde{v}} &= \gamma_3 - \gamma_1 \ , & \gamma_w &= \gamma_8 - \gamma_7 + \gamma_1 \ , \\
\gamma_u &= \gamma_2 - \gamma_1 \ , & \gamma_\tau &= \gamma_9 - \gamma_8 \ , \\
\gamma_{g_2} &= \gamma_6 - 3\gamma_1 \ , & \gamma_D &= \gamma_8 - \gamma_7 \ , \\
\gamma_{g_1} &= -3\gamma_1 \ , & \gamma_a &= \gamma_{12} - \gamma_7 \ , \\
\gamma_\nu &= \gamma_1 \ .
\end{aligned}
\tag{4.3.13}
$$

4.3.1 Stable fixed points of compressible NS model

The explicit form of anomalous dimensions and beta functions can be found in appendices C.3 and C.4. This analysis was technically difficult and therefore programmatical

assistance was used to confirm the results [2]. Since in the one loop approximation the beta functions for the compressible NS model does not depend on the DP charges g_3, w, a, the stability can be treated individually. Direct analysis of the beta functions $\beta_{g_1}, \beta_{g_2}, \beta_u, \beta_{\tilde{v}}$ shows, that there are nine fixed points, shown in Tab. 4.4. The trivial (Gaussian) fixed point FPT^c has zero effective values for charges g_1^*, g_2^* while the parameters u^*, $\tilde{v}^*$ are not fixed. Another fixed point is FPI^c where the coupling constant describing non-local interactions g_1^* is effectively zero, the local interactions are nonzero $g_2^* \neq 0$ and the value of other parameters are $u^* = 1, \tilde{v}^* = 1$. This regime is absent in the 3D analysis of this model and it represents ubiquitous thermal fluctuations of the velocity field. The most interesting point is FPII^c where both local and non-local interactions are relevant. In contrast to the 3D case [21], in this regime the coupling constant g_1^* depends on the parameter α and the local interaction g_2^* emerges. However, it can be shown, that these differences modify only the Kolmogorov constant and the energy spectrum can be obtained in the same manner as in [21] (see Eq. (3.4.15)). This problem is beyond the purpose of this work and this problem is left for future studies. It is also interesting that for the purely transversal forcing $\alpha \to 0$ the coupling constant g_2^* vanishes while the charge g_1^* attains a value $g_1^* = 16/9y$. The limit for the purely longitudinal forcing requires slightly different investigation. In this case, the purely transversal forcing vanishes and therefore taking the bare limit $\alpha \to \infty$ is insufficient. Performing the following re-parametrization of the non-local part of the random force solves this problem

$$g_1(P_{ij}(\boldsymbol{k}) + \alpha Q_{ij}(\boldsymbol{k})) = g_1'(P_{ij}(\boldsymbol{k})/\alpha + Q_{ij}(\boldsymbol{k})), \qquad (4.3.14)$$

where the new parameter $g_1' = \alpha g_1$ has been introduced. This parameter must be taken fixed while performing this limit and therefore derivation of the new beta function is necessary

$$\beta_{g_1'} = \tilde{\mathcal{D}}_\mu(\alpha g_1) \qquad (4.3.15)$$
$$= \alpha \beta_{g_1}|_{g_1 \to g_1'/\alpha} . \qquad (4.3.16)$$

The resulting beta functions can be found in the Appendix C.4 and the corresponding IR fixed point FPII$^c_{\alpha \to \infty}$ is shown on the Tab. 4.4.

In order to obtain the full set of fixed points we must also consider the limit cases $u \to \infty$ and $\tilde{v} \to \infty$. As in the case of purely longitudinal random force, the structure of the beta functions is inconvenient for taking this limit. In the first case, one must introduce a new parameter $t = 1/u$ and modify beta functions in the following way

	$g_1^*(g_1'^*)$	g_2^*	u^*	$\tilde{v}^*$
FPT^c	0	0	NF	NF
FPI^c	0	$\frac{8}{3}\varepsilon$	1	1
FPII^c	$\frac{16y(2y-3\varepsilon)}{9((\alpha+2)y-3\varepsilon)}$	$\frac{16\alpha y^2}{9((\alpha+2)y-3\varepsilon)}$	1	1
FPII$^c_{\alpha=0}$	$\frac{16y}{9}$	0	1	1
FPII$^c_{\alpha\to\infty}$	$\frac{16}{9}(2y-3\epsilon)$	$\frac{16}{9}y$	1	1
FPIII^c	0	$\frac{8}{3}\varepsilon$	∞	C
FPIV^c	$\frac{8}{3}y$	0	∞	C
FPV^c	0	$\frac{8}{3}\varepsilon$	1	∞
FPVI^c	$\frac{16y(2y-3\varepsilon)}{9((\alpha+2)y-3\varepsilon)}$	$\frac{16\alpha y^2}{9((\alpha+2)y-3\varepsilon)}$	1	∞
FPVII^c	0	$\frac{8}{3}\varepsilon$	∞	∞
FPVIII^c	$\frac{8}{3}y$	0	∞	∞

Figure 4.4: Table of fixed points for the bare compressible NS model. The constant $C = (\sqrt{13}-1)/2$ and NF stands for "not fixed".

$$\beta_t = -t^{-2}\beta_u|_{u\to t} , \quad \beta_g \to \beta_g|_{u\to 1/t} , \qquad (4.3.17)$$

---

where g is the set of all coupling constants except u. The limit $u \to \infty$ then corresponds to $t \to 0$. The resulting fixed points are FPIII^c and FPIV^c in the Tab. 4.4. In the first case, the non-local random force is irrelevant and the universality class is determined by the local random force. Note, that this regime is not present in the original formulation of incompressible NS turbulence [12]. The latter regime represents the incompressible fixed point, which is in agreement with previous works [12] up to the value of $\tilde{v}^*$. The limit $\tilde{v} \to \infty$ can be obtained in a similar manner as $u \to \infty$. Introducing $f = 1/\tilde{v}$ and modifying beta functions similarly to (4.3.17) one obtains fixed points FPV^c and FPVI^c. Note that these fixed points are identical to FPI^c and FPII^c up to the value $\tilde{v}^*$. This is caused by fact that $\tilde{v}$ is present only in the $\beta_{\tilde{v}}$ function and this limit does not affect effective values of other coupling constants (see Appendix C.4). The same situation occurs for the $(u, \tilde{v}) \to \infty$ limit, where fixed points FPVII^c and FPVIII^c are identical to FPIII^c and FPIV^c (up to the value $\tilde{v}^*$).

The stability matrix (4.3.9) has the following form in the case of compressible NS

$$\mathbf{\Omega}^{\mathrm{cNS}} = \begin{pmatrix} \partial_{g_1}\beta_{g_1} & \partial_{g_2}\beta_{g_1} & \partial_u\beta_{g_1} & \partial_{\tilde{v}}\beta_{g_1} \\ \partial_{g_1}\beta_{g_2} & \partial_{g_2}\beta_{g_2} & \partial_u\beta_{g_2} & \partial_{\tilde{v}}\beta_{g_2} \\ \partial_{g_1}\beta_u & \partial_{g_2}\beta_u & \partial_u\beta_u & \partial_{\tilde{v}}\beta_u \\ \partial_{g_1}\beta_{\tilde{v}} & \partial_{g_2}\beta_{\tilde{v}} & \partial_u\beta_{\tilde{v}} & \partial_{\tilde{v}}\beta_{\tilde{v}} \end{pmatrix}\Bigg|_{g=g^*}, \tag{4.3.18}$$

and the resulting eigenvalues for different fixed points are shown in Tab. 4.5. The Gaussian FP^c is stable for $y < 0$ and $\varepsilon < 0$ while the local fixed point FPI^c is stable for $\varepsilon > 0$ and $3\varepsilon > 2y$. The fixed points FPIII^c, FPIV^c, FPV^c, FPVII^c and FPVIII^c are clearly unstable for any values of (y, ε). The stability of FPII^c was found by also taking into account, that charges g_1^* and g_2^* must be positive. As a result, this regime is stable for $y > 0$ and $3\varepsilon < 2y$. The last fixed point FPVI^c is due to the minus sign in λ_4 unstable for any (y, ε). The resulting phase portrait is shown in the Fig. 4.5. The point representing physical values of parameters $(y, \varepsilon) = (4, 1)$ lies in the region FPII^c which belongs to the

	λ_1	λ_2	λ_3	λ_4
FPT^c	$-y$	$-\varepsilon$	0	0
FPI^c	$\frac{1}{2}(3\varepsilon - 2y)$	ε	$\frac{7}{18}\varepsilon$	$\frac{5}{6}\varepsilon$
FPII^c	$\frac{A+\sqrt{B}}{C}$	$\frac{A-\sqrt{B}}{C}$	D	$\frac{y((4\alpha+6)y-(\alpha+9)\epsilon)}{6((\alpha+2)y-3\epsilon)}$
FPII$^c_{\alpha=0}$	y	$\frac{1}{3}(2y - 3\varepsilon)$	$\frac{11}{54}y$	$\frac{1}{2}y$
FPII$^c_{\alpha\to\infty}$	$\frac{1}{3}(y + \sqrt{y(9\varepsilon - 5y)})$	$\frac{1}{3}(y - \sqrt{y(9\varepsilon - 5y)})$	$\frac{1}{54}(20y - 9\varepsilon)$	$\frac{1}{6}(4y - \varepsilon)$
FPIII^c	$\varepsilon - y$	ε	$-\frac{1}{3}\varepsilon$	$\frac{2(\sqrt{13}+13)}{3(\sqrt{13}+1)^2}\varepsilon$
FPIV^c	y	$y - \varepsilon$	$-\frac{1}{3}y$	$\frac{2(\sqrt{13}+13)}{3(\sqrt{13}+1)^2}\varepsilon$
FPV^c	$\frac{1}{2}(3\varepsilon - 2y)$	ε	$\frac{7}{18}\varepsilon$	$-\frac{1}{2}\varepsilon$
FPVI^c	$\frac{A+\sqrt{B}}{C}$	$\frac{A-\sqrt{B}}{C}$	D	$-\frac{1}{3}\varepsilon$
FPVII^c	$\varepsilon - y$	ε	$-\frac{1}{3}\varepsilon$	$-\frac{1}{3}\varepsilon$
FPVIII^c	y	$y - \varepsilon$	$-\frac{1}{3}y$	$-\frac{1}{3}y$

Table 4.5: Table of the fixed points eigenvalues for the compressible NS model. Expressions A, B, C and D are found in the Appendix (C.1).
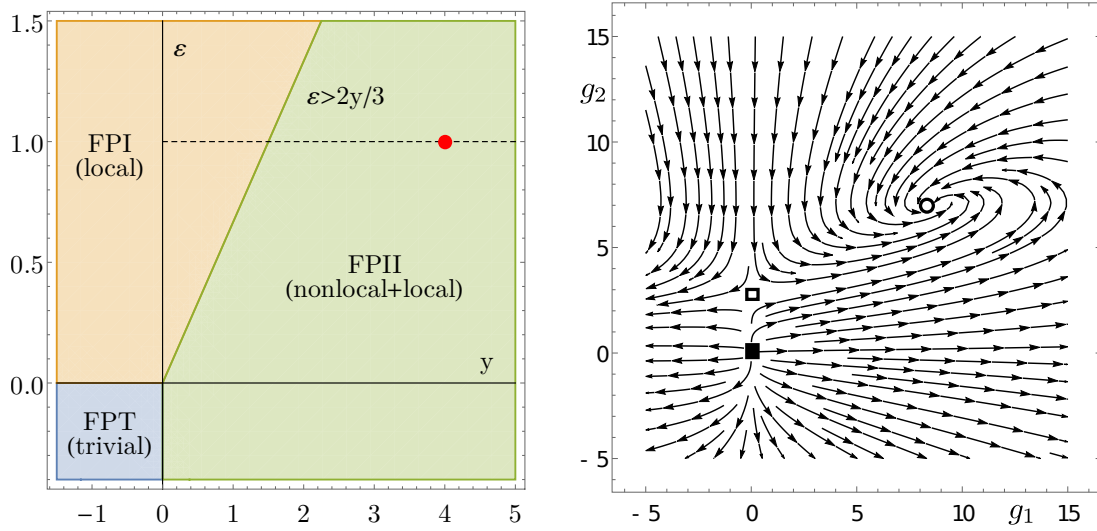
Figure 4.5: Left: Phase portrait for the compressible NS model in the y-ε plane. Different regions are denoted by different colors. The dashed line represents the physical value of the parameter $\varepsilon = 1(d = 3)$ and the physical point $(y, \varepsilon) = (4, 1)$ is denoted by the red dot. Only the FPT^c, FPI^c and FPII^c are present, while other fixed points are unstable. Right: RG flow for the charges g_1 and g_2 for the case $(y, \varepsilon, \alpha) \to (4, 1, \infty)$. Full square – FPT^c, empty square – FPI^c, empty circle – FPII^c.

universality class of FDT with relevant local and non-local fluctuations. These results differ from the ones obtained by performing RG analysis around $d = 3$ [21], where the g_2^* was not present at all.

4.3.2 Stable fixed points of advected DP process

Here we present the first part of the main results of this thesis - the IR behaviour of the DP process advected by compressible turbulent flow. Critical scaling and comparison with previous works will be discussed in the next section. The IR fixed points g^* for this model are determined by vanishing beta functions $\beta_{g_3}, \beta_w, \beta_a$ together with fixed points obtained from the compressible NS model. Together, eleven fixed points have been found, whose final form is listed in Tab. 4.6.

First, let us consider only those compressible NS fixed points, that are not completely unstable. Six regimes with different effective values of parameters are found. The first is the Gaussian (trivial) fixed point FPT where the velocity and DP field are irrelevant, while parameters $u^*, \tilde{v}^*, w^*, a^*$ remain not fixed. The second fixed point FPI describes the pure DP process where the velocity field is irrelevant. The value $a^* = 1/2$ is interesting, since it is connected to the velocity field. FPII represents the DP process advected by the thermal fluctuations of the velocity field. In this case, parameters w^* and a^* do not attain a fixed value, but rather may represent the whole line of fixed points whose length may be determined by the stability of this fixed point. This is due to the structure of β_a, that also vanishes for $g_3 = 0$ and therefore only the β_w function determines the values of w^* and a^* (see Appendix C.4). The next fixed point FPIII belongs to the universality class of DP process advected by thermal fluctuations of the velocity field. In this case, fixed points g_3^* and w^* are calculated numerically. The most interesting fixed points are FPIV and FPV, where both non-local and local interactions of the velocity field are relevant. In

the first case, percolation triple interactions are irrelevant and this regime belongs to the universality class of turbulent diffusion (advected by compressible NS equations). This regime also shows a non-universal behaviour with respect to the parameter a^* as in the case of FPII. The most non-trivial fixed point is FPV which describes the DP process advected by compressible NS turbulence. The special case $\alpha \to 0$ of these fixed points are also shown in the table. It seems that in the case of FPIV this leads to the fixation of $w^* = 1$ while a^* remains unfixed. The limit case $\alpha \to \infty$ was not possible to solve in analytical fashion and therefore a numerical simulation is necessary (see below).

The complete set of fixed points is closed with the limit cases $u^*, \tilde{v}^*, w^* \to \infty$. Fixed points for $u^* \to \infty$ with other parameters finite are FPVI-FPIX. The first two, FPVI and FPVII represent the advection of the passive scalar by the local interactions, while the latter one the DP process advected by thermal fluctuations of the velocity field. FPVIII and FPIV describe similar processes, but advected solely by the non-local term. This fixed point represents the incompressible limit case that will be compared later with [19]. It is also important to note the apparent similarity between $\text{FPIV}_{\alpha \to 0}$ and FPIX. Fixed points with $\tilde{v} \to \infty$ are not present, since in the one-loop calculation they differ from already mentioned fixed points only in the value of the $\tilde{v}^*$ (and they are all unstable). The last fixed point is FPX with $w = D/\nu \to \infty$ and any compressible NS fixed point. Straightforward analysis of DP Feynman diagrams (see Appendix B) shows, that in this limit the contributions from the velocity field to the DP process vanish. On the other hand, diagrams that do not contain velocity field remain unchanged. Hence all fixed points with $w^* \to \infty$ belong to the universality class of the bare DP process.

Stability of the above fixed points is again determined by the analysis of the eigenvalues

	g_1^*	g_2^*	u^*	$\tilde{v}^*$	g_3^*	w^*	a^*
FPT	0	0	NF	NF	0	NF	NF
FPI	0	0	NF	NF	$\frac{4}{3}\varepsilon$	0	$\frac{1}{2}$
FPII	0	$\frac{8}{3}\varepsilon$	1	1	0	NF	NF
FPIII	0	$\frac{8}{3}\varepsilon$	1	1	$0.3505(0)\varepsilon$	$1.0819(2)$	$\frac{1}{2}$
FPIV	$\frac{16y(2y-3\varepsilon)}{9((\alpha+2)y-3\varepsilon)}$	$\frac{16\alpha y^2}{9((\alpha+2)y-3\varepsilon)}$	1	1	0	NF	NF
FPV	$\frac{16y(2y-3\varepsilon)}{9((\alpha+2)y-3\varepsilon)}$	$\frac{16\alpha y^2}{9((\alpha+2)y-3\varepsilon)}$	1	1	$g_3^*(y,\varepsilon,\alpha)$	$w^*(y,\varepsilon,\alpha)$	$\frac{1}{2}$
$\text{FPIV}_{\alpha\to0}$	$\frac{16y}{9}$	0	1	1	0	1	NF
$\text{FPV}_{\alpha\to0}$	$\frac{16y}{9}$	0	1	1	$\frac{8}{15}(3\epsilon-2y)$	$\frac{1}{2}\left(\sqrt{1-\frac{40y}{\epsilon-4y}}-1\right)$	$\frac{1}{2}$
FPVI	0	$\frac{8\epsilon}{3}$	∞	C	0	C	NF
FPVII	0	$\frac{8\epsilon}{3}$	∞	C	$\frac{8\epsilon}{15}$	$\frac{1}{6}\left(\sqrt{129}-3\right)$	$\frac{1}{2}$
FPVIII	$\frac{8y}{3}$	0	∞	C	0	C	NF
FPIX	$\frac{8y}{3}$	0	∞	C	$\frac{8}{15}(3\epsilon-2y)$	$\frac{1}{2}\left(\sqrt{1-\frac{40y}{\epsilon-4y}}-1\right)$	$\frac{1}{2}$
FPX	any from FPT^c-FPVIII^c				$\frac{4}{3}\varepsilon$	∞	$\frac{1}{2}$

Table 4.6: List of fixed points, where $C = (\sqrt{13}-1)/2$ and NF - not fixed. The description is given in the text above.

	$\lambda_1,\ \lambda_2, \lambda_3, \lambda_4$	λ_5	λ_6	λ_7
FPT	FPT^c $(y < 0 \wedge \varepsilon < 0)$	$-\varepsilon$	0	0
FPI	FPT^c $(y < 0 \wedge \varepsilon < 0)$	ε	$-\frac{1}{12}\varepsilon$	$\frac{1}{6}\varepsilon$
FPII	FPI^c $(3\varepsilon > 2y \wedge \varepsilon > 0)$	0	$\lambda_6^{\mathrm{II}}(a^*, \varepsilon)$	$\lambda_7^{\mathrm{II}}(a^*, \varepsilon)$
FPIII	FPI^c $(3\varepsilon > 2y \wedge \varepsilon > 0)$	$0.0438(1)\varepsilon$	$0.2165(2)\varepsilon$	$0.8083(8)\varepsilon$
FPIV	FPII^c $(3\varepsilon < 2y \wedge y > 0)$	$\lambda_5^{\mathrm{IV}}(a^*, \Delta)$	$\lambda_6^{\mathrm{IV}}(a^*, \Delta)$	$\lambda_7^{\mathrm{IV}}(a^*, \Delta)$
FPV	FPII^c $(3\varepsilon < 2y \wedge y > 0)$	$\lambda_5^{\mathrm{V}}(\Delta)$	$\lambda_6^{\mathrm{V}}(\Delta)$	$\lambda_5^{\mathrm{V}}(\Delta)$
FPIV$_{\alpha \to 0}$	FPII^c $(3\varepsilon < 2y \wedge y > 0)$	$\frac{1}{3}(2y - 3\varepsilon)$	$\frac{y}{2}$	0
FPV$_{\alpha \to 0}$	FPII^c $(3\varepsilon < 2y \wedge y > 0)$	$\frac{1}{15}(3\varepsilon - 2y)$	$\lambda_6^{\mathrm{V_0}}(\Delta)$	$\lambda_7^{\mathrm{V_0}}(\Delta)$
FPX	FPI^c $(y < 0 \wedge \varepsilon < 0)$	ε	$\frac{1}{12}\varepsilon$	$\frac{1}{6}\varepsilon$
FPX	FPI^c $(3\varepsilon > 2y \wedge \varepsilon > 0)$	ε	$-\frac{19}{60}\varepsilon$	$\frac{1}{6}\varepsilon$
FPX	FPII^c $(3\varepsilon < 2y \wedge y > 0)$	ε	$\frac{1}{12}(\varepsilon - 4y)$	$\frac{1}{6}\varepsilon$

Table 4.7: List of fixed points where $\Delta = \{y, \varepsilon, \alpha\}$, $C = (\sqrt{13} - 1)/2$ and NF – not fixed. Fixed points FPVI-FPVIII and FPX with other compressible NS fixed points are not present, since the corresponding compressible NS fixed points are already unstable for all y and ε. The structure of some eigenvalues is rather lengthy and therefore they are not displayed.

of the following matrix

$$\boldsymbol{\Omega}^{\mathrm{Per}} = \begin{pmatrix} \partial_{g_3}\beta_{g_3} & \partial_w\beta_{g_3} & \partial_a\beta_{g_3} \\ \partial_{g_3}\beta_w & \partial_w\beta_w & \partial_a\beta_w \\ \partial_{g_3}\beta_a & \partial_w\beta_a & \partial_a\beta_a \end{pmatrix}\Bigg|_{g=g^*}, \qquad (4.3.19)$$

together with eigenvalues obtained for the bare velocity field (Tab. 4.5). The results are shown in Tab. 4.7. As one can notice, the Gaussian fixed point FPT is stable for $\varepsilon < 0$ and $y < 0$ (as expected) and the pure DP process is unstable everywhere. The asymptotic cases $u^*, \tilde{v}^* \to \infty$ are not displayed, since they are generally unstable even for the bare velocity field (see Tab. 4.5). The limit case $w^* \to \infty$ represented by fixed points FPX-FPXIII are clearly unstable for all (y, ε). The most interesting fixed points are FPII-FPV. Here, only FPIII has a trivial structure which tells us that it is a stable fixed point for $\varepsilon > 0$ and 2ε and $2y$. The stability of the fixed points FPIV and FPV is trivial only in the limit $\alpha \to 0$. In this case FPIV$_{\alpha \to 0}$ is stable for $3\varepsilon < 2y$ and $y > 0$ while FPV remains unstable everywhere. For nonzero values of α, the stability is too complicated and therefore a numerical solution is called for.

The physically most interesting fixed points FPII, FPIV and FPV show difficult structure of eigenvalues. In addition the FPII and PFIV to be also non-universal and the final form of the eigenvalues depends on the parameter a^*. In order to solve this problem, we have performed a numerical solution of Gell-Mann's equations. This can be done by re-parametrizing the arbitrary introduced mass scale as $\mu(l) = \mu l$ and solving the resulting beta functions in the limit $l \to 0$ (see section 1.2.4). By doing this, one obtains the fixed points values g_3^* shown on the Fig. 4.6. In these figures, g_3^* is plotted in the (y, ε) plane for the values $\alpha = \{0, 1, \infty\}$. The solid and the dashed grey lines represent the lines $y = 0, \varepsilon = 0$ and the physical line $\varepsilon = 1(d = 3)$.

The most realistic value $(y, \varepsilon) = (4, 1)$ is marked by the red dot. Here, several regimes denoted by different planes separated by solid black lines. The FPT is presented in the $y < 0$ and $\varepsilon < 0$ area and the FPIII is present for the values $\varepsilon > 0$ and $3\varepsilon > 2y$. These regimes do not change by varying α. The fixed point FPII is not not present at all. For $\alpha = 0$ only the FPIV is present, while FPV is unstable everywhere. By increasing of value α the most non-trivial regime emergences - FPV - the compressible turbulent advection of the DP process. However, this regime remains small even for the limits $\alpha \to \infty$. In the limit of the purely longitudinal random force, i.e. $\alpha \to \infty$ the boundary between FPIV and FPV does not cross the physical point $(y, \varepsilon) = (4, 1)$. The realistic point therefore corresponds to the universality class of passive compressible turbulent advection for all values of α. In this regime however, the values of w^* and a^* remain un-fixed and the they depend on the initial values of in the RG flow.

In order to visualise the situation occurring for $(y, \varepsilon) = (4, 1)$, we plot the RG flow in the (a, w, g_3) plane for the various values of α. The results can be seen in Fig. 4.7. These plots have been obtained by numerically solving the DP beta function, $\beta_{g_3}, \beta_w, \beta_a$ at the fixed point FPII^c for $\alpha = \{0, 1, \infty\}$. One can see, that in all cases, the DP is irrelevant, i.e. $g_3^* = 0$. In the case $\alpha = 0$, the fixed point value $w^* = 1$ (dashed line) which matches with the analytical solutions (see Tab. 4.6). The value a^* depends on the initial value a and there is no restriction about the fixed point value from the stability matrix (see Tab. 4.7). By increasing α, the value $w^* \neq 1$ and a different line of stability emerges (second dashed line). In addition, the parameter a^* is being attracted to the "centre"

Figure 4.6: Results of the numerical solution for the coupling constant g_3^* at the (y, ε) for the limits $\alpha \to \{0, 1, \infty\}$ (from top to the bottom).

represented by the line $a^* = 1/2, g_3^* = 0$. Note that this graph is symmetric along the plane $a = 1/2$. In the limit $\alpha \to \infty$, the graph becomes quantitatively more different. The points close to $g_3^* = 0$ and $a^* \in \{0, 1\}$ are obviously unstable, since only a small perturbation drives the RG flow away from the g_3^* plane but then attracts it back close to $a = 1/2$. We conclude that the line of fixed points is therefore shrinking with increasing α. The similar result has been obtained by considering Kraichnan model for the velocity field [18], where the line of stability becomes a fixed point $a^* = 1/2$ for the limit $\alpha \to \infty^3$. The fixed point value is in this case shifted away from $w^* = 1$. This situation might change in the higher-loop approximation.

---

[3] One should keep in mind, that in the Kraichnan model the α represents the degree of compressibility.
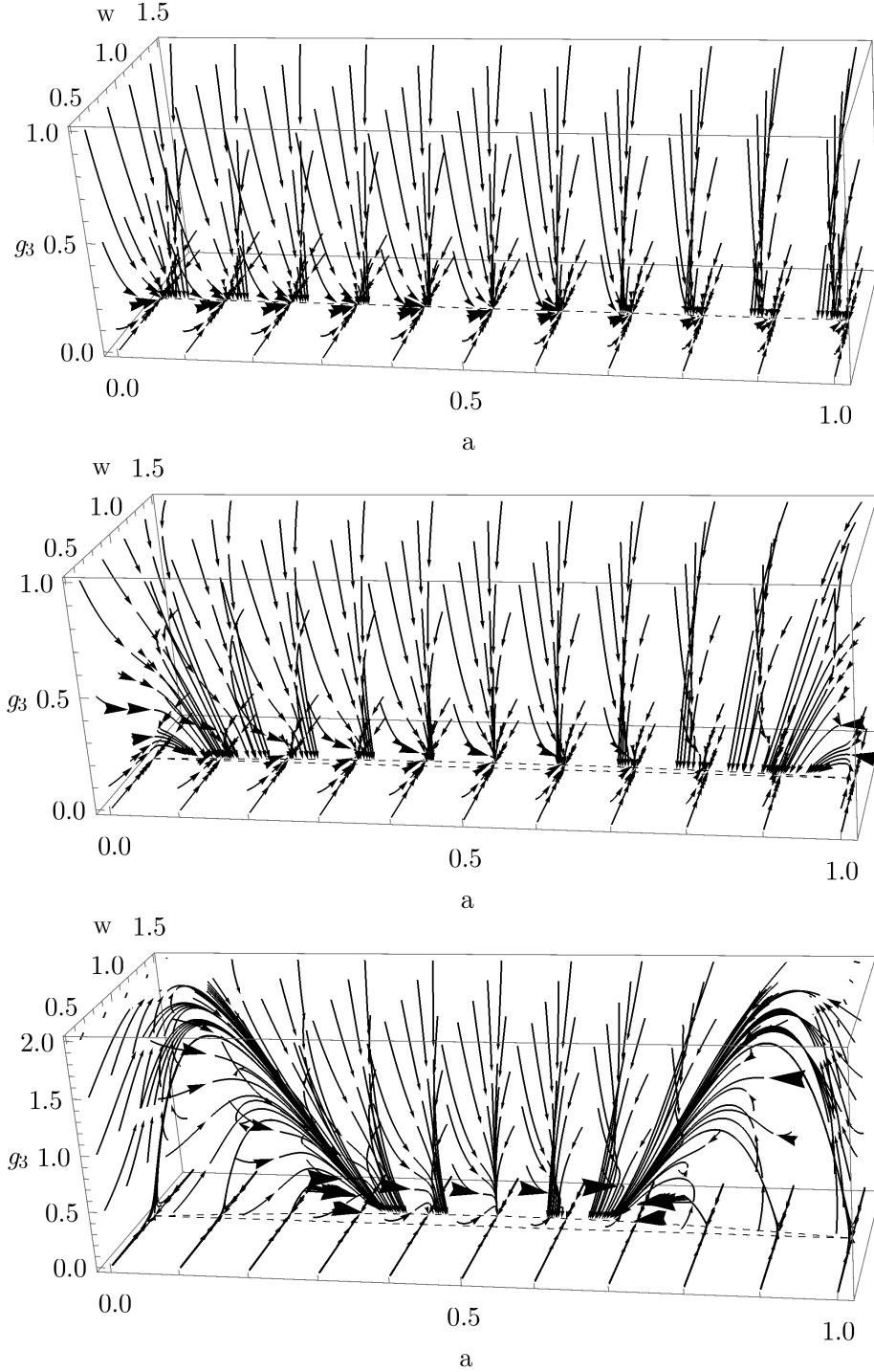
Figure 4.7: The RG flow for the parameters (g_3, w, a) for the values $(y, \varepsilon) = (4, 1)$ evaluated at the FPII^c. From top to the bottom: the limits $\alpha \to \{0, 1, \infty\}$. In all cases percolation is irrelevant $g_3^* = 0$ and parameters w^*, a^* represent a whole line of stability. In the case $\alpha \to 0$ the fixed point values are $w^* = 1$ and a^* remains unfixed. This is represented by dashed line in the upper Figure. By increasing the value of α the line of stable points shifts from $w^* = 1$ to slightly larger values and it becomes curved (second dashed line). In the limit $\alpha \to \infty$, the points close to $a \in \{0, 1\}$ becomes unstable and they are driven closer to $a^* = 1/2$. The diagram is symmetric around $a = 1/2$.

The above results allow us to construct a schematic phase diagram in the (y, ε) plane. This can be seen in Fig. 4.8 where we have also plotted results obtained by other authors. The upper diagram corresponds to our model. As stated before, only 4 regimes are present. The Gaussian fixed point (FPT) is stable for $0 < \varepsilon \wedge 0 < y$. In addition, for $\alpha = 0$ only DP process advected by thermal fluctuations of the velocity field (FPIII) and passive compressible turbulent advection (FPIV) are present. Their stability is denoted by the green and orange areas separated by the line $\varepsilon = 2y/3$. By increasing value of α, the regime for the compressible turbulent advection of DP process (FPV) is present, denoted by red area. Dashed lines represent the limits $\alpha \in \{0, 1, \infty\}$. For $\alpha \to \infty$, the area stops growing and the boundary with passive advection does not cross the physical fixed point $(y, \varepsilon) = (4, 1)$ represented by the red dot. The bare DP process is not present at all.

In the middle panel of Fig. 4.8 results obtained using incompressible model of NS equation are displayed [19]. Here, the bare DP process is present for $\varepsilon > 4y$. The DP process advected by incompressible turbulent mixing is present in the region $\varepsilon < 4y$ and $\varepsilon > 2y/3$. The passive incompressible turbulent advection is present in the same region as for our model in the case $\alpha \to 0$.

The last panel describes results obtained by using the compressible Kraichnan model for the velocity field instead of NS equations [18] (see section 3.4). Here, the expansion parameter is ξ instead of y and the physical value is $\xi = 4/3$ which leads to the Kolmogorov spectrum. The phase portrait has been rescaled for our purposes. For the limit $\alpha \to 0$ one can see that, even though the values of the parameters are quantitatively different, the graph is qualitatively the same as in the case of incompressible NS model (middle panel). This is a reasonable result, since the parameter α in this model describes the degree of compressibility and thus the limit $\alpha \to 0$ represents an incompressible limit (represented by dashed line in the Figure).

The increasing value of α leads to a crossover between the universality class of the
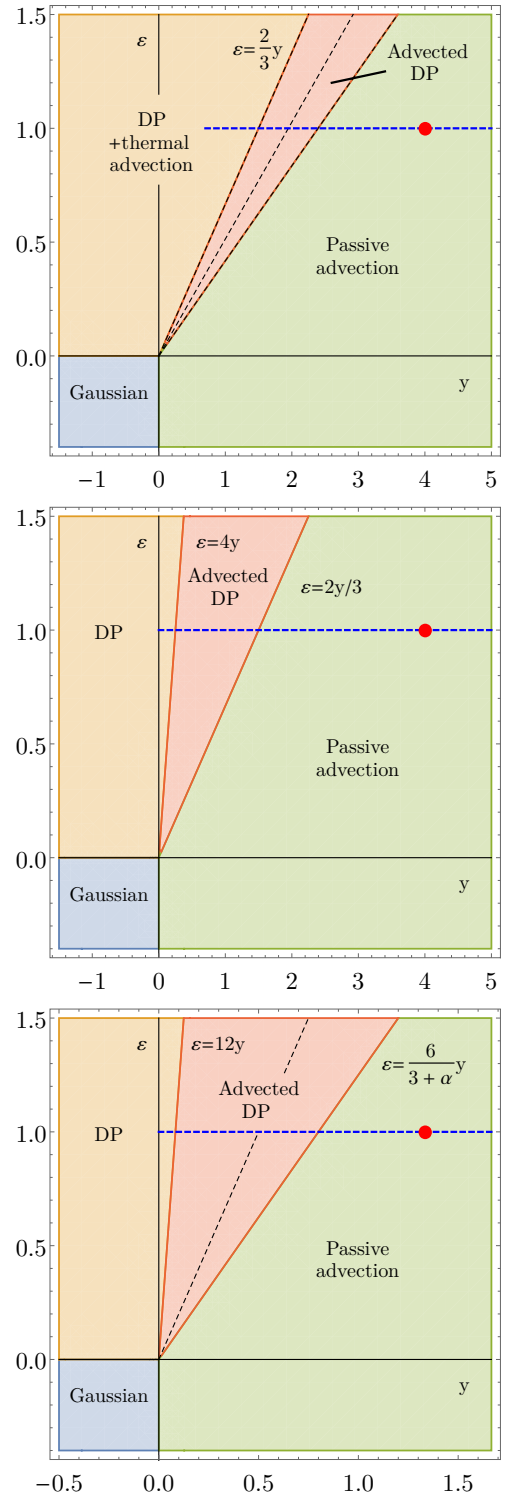
Figure 4.8: Phase portraits: top - our mode, middle - incompressible NS model [19], bottom - Kraichnan model [18].

passive turbulent advection and the turbulent advection of the DP process. This occurs for $\alpha = 5$ and it is in contrast to our results, since we don't observe any crossover in our model.

4.3.3   Critical scaling

In this final section we discuss universal properties of the DP process advected by compressible turbulent flow. However, algebraic solutions of some of the fixed points are too complicated or they depend on the non-universal parameter a^*. Therefore, we do not express their final form. This applies also for the physical point $(y, \varepsilon) = (4, 1)$.

    Anomalous dimensions obtained for this model are displayed in Tab. (4.8). In the case of the Gaussian fixed point they are zero (as expected) while anomalous dimensions for the bare DP process FPI are in agreement with the results obtained in [38]. The fixed point FPII, which is generally unstable for all y and ε has a non-universal value depending on the parameter a^*. Anomalous dimensions for the FPIII have been calculated numerically. The most interesting fixed points FPIV and FPV also show a non-universal behaviour. The passive advection FPIV that is stable for physical values of parameters is non-universal in the sense that it depends on the parameter α and the final value a^* in the RG flow (see Fig. 4.7). This situation might change in the higher-loop approximation. The most non-trivial fixed point FPV shows only the non-universality with the parameter α. Similar non-universality has been obtained in [18].

    The complete set of anomalous dimensions is given by calculating also the limit cases $u^*, w^* \to \infty$ (the limit $v^* \to \infty$ collides with other fixed points, see section 4.3.1). In the incompressible limit u^* fixed points FPVI and FPVII are not presented in [19]. The results for FPVIII and FPIX that correspond to passive advection and advection of the

	γ_ψ^*	$\gamma_{\psi'}^*$	γ_τ^*	γ_D^*
FPT	0	0	0	0
FPI	$-\frac{1}{12}\varepsilon$	$-\frac{1}{12}\varepsilon$	$-\frac{1}{4}\varepsilon$	$\frac{1}{12}\varepsilon$
FPII	$\gamma_\psi^{*\mathrm{II}}(a^*)$	$\gamma_{\psi'}^{*\mathrm{II}}(a^*)$	$\gamma_\tau^{*\mathrm{II}}(a^*)$	$\gamma_D^{*\mathrm{II}}(a^*)$
FPIII	-0.0603583ε	-0.0603583ε	-0.543813ε	0.5ε
FPIV	$\gamma_\psi^{*\mathrm{IV}}(a^*, \Delta)$	$\gamma_{\psi'}^{*\mathrm{IV}}(a^*, \Delta)$	$\gamma_\tau^{*\mathrm{IV}}(a^*, \Delta)$	$\gamma_D^{*\mathrm{IV}}(a^*, \Delta)$
FPV	$\gamma_\psi^{*\mathrm{V}}(\Delta)$	$\gamma_{\psi'}^{*\mathrm{V}}(\Delta)$	$\gamma_\tau^{*\mathrm{V}}(\Delta)$	$\gamma_D^{*\mathrm{V}}(\Delta)$
$\mathrm{FPIV}_{\alpha \to 0}$	0	0	$-\frac{1}{3}y$	$-\frac{1}{3}y$
$\mathrm{FPV}_{\alpha \to 0}$	$\frac{1}{30}(2y - 3\varepsilon)$	$\frac{1}{30}(2y - 3\varepsilon)$	$-\frac{1}{5}(y + \varepsilon)$	$\frac{1}{3}y$
FPVI	0	0	$\frac{1}{3}\varepsilon$	$\frac{1}{3}\varepsilon$
FPVII	$-\frac{1}{30}\varepsilon$	$-\frac{1}{30}\varepsilon$	$-\frac{2}{5}\varepsilon$	$\frac{1}{3}\varepsilon$
FPVIII	0	0	$-\frac{1}{3}y$	$-\frac{1}{3}y$
FPIX	$\frac{1}{30}(2y - 3\varepsilon)$	$\frac{1}{30}(2y - 3\varepsilon)$	$-\frac{1}{5}(y + \varepsilon)$	$\frac{1}{3}y$

Table 4.8: Anomalous dimensions for fixed points 4.6 ($\Delta = \{y, \varepsilon, \alpha\}$). Some gamma functions are not displayed due to their complicated structure. In the most of the cases $\gamma_\psi^* = \gamma_{\psi'}^*$, since it does not depend on the non-universal parameter a^*. Anomalous dimensions for FPX are not displayed, since they are identical to FPI. Note that $\mathrm{FPIV}_{\alpha \to 0}$ and $\mathrm{FPV}_{\alpha \to 0}$ coincide with FPVIII and FPIX .

DP process in the incompressible limit are in agreement with the previous work obtained in [19]. Note also that anomalous dimensions $FPIV_{\alpha \to 0}$, $FPV_{\alpha \to 0}$ are identical to FPVIII and FPIX. This is a very interesting result, because the limit $\alpha \to 0$ does not generally correspond to the incompressible case. The results for FPX-FPXIII are not present, since they are generally identical to FPI.

One may also notice another important result. Anomalous dimensions for the γ_ψ^* and $\gamma_{\psi'}^*$ are identical for all fixed points except FPII and FPIV. This is also due to the fact, that these anomalous dimensions are identical for the value $a^* = 1/2$ (see Appendix C.3). In the case FPII and FPIV the fixed point value a^* depends on the initial condition of the RG flow, but the anomalous dimensions γ_ψ^* and $\gamma_{\psi'}^*$ are symmetric arround $a^* = 1/2$, i.e. symmetric with respect to the transformation

$$a \to (1-a) \ . \tag{4.3.20}$$

As stated in [38], these anomalous dimensions are identical if the rapidity symmetry is satisfied (see section 2.2.1). This is an interesting result, because our model is generally not invariant with respect to the symmetry (2.3.11). This is due to the fact, that the velocity field introduced by the compressible NS model (4.1.2) generally breaks down this symmetry.

A similar result has been obtained by authors in [18], where the velocity field has been modelled by the compressible Kraichnan model (3.4.1). It has also been shown, that their model is invariant with respect to the transformation

$$\psi(\boldsymbol{x}, t) \leftrightarrow \psi'(-\boldsymbol{x}, -t), \quad v_i(\boldsymbol{x}, t) \to v_i(-\boldsymbol{x}, -t), \quad a_0 \to (1 - a_0), \quad \lambda_0 \to -\lambda_0 \ , \tag{4.3.21}$$

where the parameter a_0 has the same meaning as it does in our case. The transformation of λ_0 is unimportant here, since it enters the counterterms as λ_0^2. Due to the transformation (4.3.21), anomalous dimensions possessed the symmetry (4.3.20) which implied that the critical exponents δ and δ' were identical. It is unclear why our anomalous dimensions are also invariant with respect to the transformation (4.3.20), since our model does not posses the symmetry (4.3.21).

In [19], where the incompressible NS model of the velocity field was used, authors have claimed, that the DP action functional (4.1.8) is invariant with respect to the transformation

$$\psi(\boldsymbol{x}, t) \leftrightarrow \psi'(-\boldsymbol{x}, -t), \quad \lambda_0 \to -\lambda_0 \ . \tag{4.3.22}$$

This is of course true, but their NS model for the velocity field breaks down this symmetry. In fact, authors have not discussed the transformation of the velocity field at all. However, invalidity of this symmetry does not change the process of renormalization (the construction of the counterterms and so on) and therefore their results seem to be correct. Anomalous dimensions for the fields ψ and ψ' were also identical, which implies the reduction of the critical exponents to three. Their argumentation is, in our opinion unsatisfactory.

Critical exponents derived for this model can be seen in Fig. 4.9. The values of α and δ are identical for all fixed points except FPII and FPIV. Therefore in these cases there are only three independent critical exponents describing the universal properties of the DP phase transition. However, as stated before, the most realistic fixed point $(y, \varepsilon) = (4, 1)$ corresponds to the FPIV which is non-universal with respect to the values α and a^*. The similar non-universality was obtained in the previous work [18]. The coincidence of the

	$\tilde{z}$	Θ	$\delta,\ \delta'$
FPT	1	0	$1-\frac{1}{4}\varepsilon$
FPI	$1+\frac{1}{14}\varepsilon$	$\frac{1}{12}\varepsilon$	$1-\frac{1}{4}\varepsilon$
FPII	$\tilde{z}^{\mathrm{II}}(a^*)$	$\Theta^{\mathrm{II}}(a^*)$	$\delta^{\mathrm{II}}(a^*)\neq\delta'^{\mathrm{II}}(a^*)$
FPIII	$1+0.0109532\varepsilon$	0.0219064ε	$1-\frac{1}{4}\varepsilon$
FPIV	$\tilde{z}^{\mathrm{IV}}(a^*,\Delta)$	$\Theta^{\mathrm{IV}}(a^*,\Delta)$	$\delta^{\mathrm{IV}}(a^*,\Delta)\neq\delta'^{\mathrm{IV}}(a^*,\Delta)$
FPV	$\tilde{z}^{\mathrm{V}}(\Delta)$	$\Theta^{\mathrm{V}}(\Delta)$	$\delta^{\mathrm{V}}(\Delta)=\delta'^{\mathrm{V}}(\Delta)$
FPIV$_{\alpha\to0}$	$1+\frac{1}{6}y$	0	$1-\frac{1}{4}\varepsilon+\frac{1}{24}(4-\varepsilon)y$
FPV$_{\alpha\to0}$	$1+\frac{1}{6}y$	$\frac{1}{10}\varepsilon-\frac{1}{30}(4-\varepsilon)y$	$1-\frac{3}{10}\varepsilon+\frac{1}{20}(4-\varepsilon)y$
FPVI	$1+\frac{1}{6}\varepsilon$	0	$1-\frac{1}{12}\varepsilon$
FPVII	$1+\frac{1}{6}\varepsilon$	$\frac{1}{30}\varepsilon$	$1-\frac{1}{10}\varepsilon$
FPVIII	$1+\frac{1}{6}y$	0	$1-\frac{1}{4}\varepsilon+\frac{1}{24}(4-\varepsilon)y$
FPIX	$1+\frac{1}{6}y$	$\frac{1}{10}\varepsilon-\frac{1}{30}(4-\varepsilon)y$	$1-\frac{3}{10}\varepsilon+\frac{1}{20}(4-\varepsilon)y$

Table 4.9: Critical exponents for various fixed points ($\Delta=\{y,\varepsilon,\alpha\}$). As one can see, α and δ are identical in most of the cases (except FPII and FPV) because they don't depend on the non-universal parameter a^*. Critical exponents for FPX is not displayed since they are identical to FPI.

limits FPIV$_{\alpha\to0}$,FPV$_{\alpha\to0}$ and FPVIII, FPIX remains unclear. It seems that in the one loop approximation the limit $\alpha\to0$ shows the same universal properties as the incompressible limit. This situation might change in the higher loop approximation.

Chapter 5

Conclusion

In this thesis we have studied the influence of the compressible turbulent mixing on the DP phase transition. First we introduced all methods that have been used. Then we described the basic properties of the DP process and following the standard literature [23] we have derived a field-theoretic formulation using Doi-Peliti action functional. In the following chapter we described the basic properties of the fully developed turbulence and discussed the differences between the incompressible and compressible turbulence. The field-theoretic formulation was later derived in terms of De Dominicis-Janssen action functional. In contrast to the previous works, compressibility was modelled by an additional scalar field related to the density.

In order to study the turbulent advection of the DP process, we have coupled the velocity field to the percolation field by introducing the generalized covariant derivative. We have shown that the model is multiplicatively renormalizable by renormalizing all vertex functions with a non-negative degree of divergence. Since the DP model has the upper critical dimension $d_c = 4$, the velocity field was also renormalized around $d = 4$. In contrast to the 3D case, an additional divergences was present in the two-point velocity field correlator. This divergence was eliminated by introducing the local term to the random force correlator which, from the physical point of view, can be related to the thermal fluctuations of the fluid. The regularization was done by performing the double expansion in terms of parameters y and ε, where the former corresponds to the analytical regularization of the non-local part of the random force correlator and the latter to the dimensional regularization around the upper critical dimension $\varepsilon = 4 - d$. The renormalization process then consisted of the calculation of the divergent parts of twenty two Feynman diagrams, where for the practical calculations the MS scheme was used. The large scale and long time properties was found by analysing the IR limit of the beta functions describing the running coupling constant.

Since in the one-loop approximation there was no contribution from the DP field to the velocity field, the IR behaviour of the latter could be investigated separately. Eight non-trivial fixed points were found, where only three were stable in some region of the parameter space y, ε, α. Most non-trivial fixed points, where both local and non-local parts of the random force were relevant, were found to be stable for the physical values of parameters $(y, \varepsilon) = (4, 1)$. These results have been calculated independently and published recently in [70].

The main part of our work was the IR behaviour of the DP process advected by the compressible velocity field. Here ten non-trivial fixed points were found, four of which appeared to be stable in the parameter space (y, ε). We showed that the bare DP process

is completely unstable, which is in contrast to previous works [18, 19]. Several new universality classes were found, such as passive scalar and DP process advected by thermal fluctuations and the DP process advected by compressible turbulent mixing. The advection of the passive scalar by the compressible turbulent mixing was also obtained. This regime together with the DP advected by compressible turbulence shows non-universal properties, i.e. they both depend on the parameter α which describes the structure of the random force correlator. The boundary between these two regimes seems to vary with respect to α. The regime of the turbulent advection of the DP process ceases to exist in the limit of purely transversal force $\alpha \to 0$ and only the advection of the passive scalar is present.

Similar non-universalities have been found in previous works, where authors were using Kraichnan model of the velocity field. In their work, the parameter α describes the degree of compressibility and the limit $\alpha \to 0$ represents the incompressible limit. In our case the situation is different, since the parameter α describes the structure of the random force correlator. However, in the limit $\alpha \to 0$ we have obtained scaling behaviour of the DP process that was obtained in previous work using the incompressible NS model.

The physical point $(y, \varepsilon) = (4, 1)$ belongs to the universality class of passive turbulent advection of the scalar field and no crossover between different regimes has been found. In the limit $\alpha \to \infty$ the boundary between turbulent advection of the passive scalar and the advected DP process is still far away from the physical point. This is in contrast to the results obtained in [18], where a certain value of α showed the crossover between these two regimes. One should keep in mind that in our case the parameter α does not necessary describe the degree of compressibility.

Another important fact is that the physical regime shows a non-universality with respect to the coupling constant a. Only in the limit $\alpha \to 0$ the scaling properties do not depend on this parameter and they are in agreement with the results obtained in [70]. This means that for a nonzero value of α, this regime is qualitatively different from the classical universality class of the passive scalar advection obtained in [70], where the parameter was fixed $a = 1$ and did not renormalize.

We have also discussed the violation of the rapidity symmetry. Even though this symmetry is generally violated by introducing the turbulent mixing, most of the regimes we found seem to have scaling properties as if it would be satisfied. It is unclear why this is the case. We have also mentioned that the modified reflection symmetry introduced by authors in [19] is generally not satisfied. However, this fact does not influence the results obtained in their work.

We therefore conclude that the model (4.1.1) for the compressible velocity field has interesting properties. Even though the limit $\alpha \to 0$ does not describe the incompressible limit, the resulting scaling properties of the advected DP field show behaviour identical to the incompressible limit. This is also supported by the fact that the energy spectrum of the compressible turbulence obeys the Kolmogorov power law when $\alpha \to 0$ (see Eq. (3.4.15)). Investigation of the current problem in higher-loop approximations is necessary. However, this is beyond the scope this thesis and is left as a subject for possible future work.

Appendices

Appendix A

Derivation of propagators and vertices

A.1 Propagators

In this thesis, the following convention for the Fourier transformation has been used

$$f(\boldsymbol{x}, t) = \int \frac{\mathrm{d}^d k \mathrm{d}\omega}{(2\pi)^{d+1}} \, f(\boldsymbol{k}, \omega) \mathrm{e}^{i(\boldsymbol{k}.\boldsymbol{x} - \omega t)} \tag{A.1.1}$$

$$f(\boldsymbol{k}, \omega) = \int \mathrm{d}^d x \mathrm{d}t \, f(\boldsymbol{x}, t) \mathrm{e}^{-i(\boldsymbol{k}.\boldsymbol{x} - \omega t)} \tag{A.1.2}$$

Compressible NS propagators

Propagators for the model (4.1.2) can be found as an inverse of the action functional[1]

$$\begin{aligned}
\mathcal{S}_0^{\mathrm{cNS}}[\Phi] = \; & -\frac{1}{2} v_i' D_{ij}^f v_j' + v_i' \{\partial_t v_i - \nu[\delta_{ij}\partial^2 - \partial_i\partial_j]v_j - u\nu\partial_i\partial_j v_j + \partial_i\phi + e\partial_i\psi\} \\
& + \phi'\{\partial_t\phi - v\nu\partial^2\phi + c^2(\partial_i v_i)\},
\end{aligned} \tag{A.1.3}$$

where $\Phi = (v_i' \; v_i \; \phi' \; \phi)^\dagger$ and

$$D_{ij}^f = d_1^f P_{ij} + d_2^f Q_{ij}, \quad d_1^f = \alpha g_1 k^{4-d-y} + g_2, \quad d_2^f = g_1 k^{4-d-y} + g_2 \tag{A.1.4}$$

In order to invert the expressions (A.1.3), we need to rewrite them into more suitable matrix form

$$\mathcal{S}_0^{\mathrm{cNS}}[\Phi] = \frac{1}{2}\Phi^\dagger M \Phi = \frac{1}{2}
\begin{pmatrix} v_i' \\ v_i \\ \phi' \\ \phi \end{pmatrix}^\dagger
\begin{pmatrix}
T_{ij}^{11} & T_{ij}^{12} & V_i^{13} & V_i^{14} \\
T_{ij}^{21} & T_{ij}^{22} & V_i^{23} & V_i^{24} \\
V_j^{31} & V_j^{32} & S^{33} & S^{34} \\
V_j^{41} & V_j^{42} & S^{43} & S^{44}
\end{pmatrix}
\begin{pmatrix} v_j' \\ v_j \\ \phi' \\ \phi \end{pmatrix} \tag{A.1.5}$$

where T_{ij}^{mn} represents a $d \times d$ dimensional block matrix, V_i^{mn} are d dimensional vectors and S^{mn} are scalars. Together, M is a $(2d + 2)$ dimensional matrix. Using Fourier

---

[1]We skip the subscripts "0" for the unrenormalized quantities for the simplicity.

transformation (A.1.1) and $\delta_{ij} = P_{ij} + Q_{ij}$, we can rewrite (A.1.3) as

$$
\begin{aligned}
\mathcal{S}_0^{\text{cNS}}[\Phi] =& \frac{1}{2} v_i' D_{ij}^f v_j' + v_i'\{i\omega(P_{ij}^k + Q_{ij}^k)v_j - \nu k^2 P_{ij}^k v_j - u\nu k^2 Q_{ij}^k v_j - ik_i\phi - eik_i\psi\} \\
&+ \phi'\{i\omega\phi - v\nu k^2\phi - c^2 ik_i v_i\} + \psi'\{i\omega - D(k^2+\tau)\}\psi \\
=& -\frac{1}{2}\{v_i'(-D_{ij}^f)v_j' + 2v_i'[\epsilon_1 P_{ij}^k + \epsilon_2 Q_{ij}^k)\}v_j + 2ik_i v_i'\phi + 2\epsilon_3\phi'\phi + 2ik_i c^2\phi'v_i \\
& 2iek_i v_i'\psi + 2\psi' L\psi] \ ,
\end{aligned}
$$
$$(A.1.6)$$

where the following labelling was used

$$
\epsilon_1 = -i\omega + \nu k^2, \qquad \epsilon_2 = -i\omega + \nu u k^2, \tag{A.1.7}
$$
$$
\epsilon_3 = -i\omega + \nu v k^2, \quad L = -i\omega + D(k^2+\tau). \tag{A.1.8}
$$

Using the fact, that $2\phi'\epsilon_i\phi = \phi'\epsilon_i\phi + (\phi\epsilon_i^*\phi')^\dagger$, we find that the matrix M has the form

$$
M = \begin{pmatrix}
-d_1^f P_{ij} - d_2^f Q_{ij} & \epsilon_1 P_{ij} + \epsilon_2 Q_{ij} & 0 & ik_i \\
\epsilon_1^* P_{ij} + \epsilon_2^* Q_{ij} & 0 & -ic^2 k_i & 0 \\
0 & ic^2 k_j & 0 & \epsilon_3 \\
-ik_j & 0 & \epsilon_3^* & 0
\end{pmatrix} . \tag{A.1.9}
$$

The inverse of the matrix M is a matrix Δ for which the following relation holds

$$
\Delta M = 1 \ , \tag{A.1.10}
$$

where

$$
1 = \begin{pmatrix}
P_{ij} + Q_{ij} & 0 & 0 & 0 \\
0 & P_{ij} + Q_{ij} & 0 & 0 \\
0 & 0 & 1 & 0 \\
0 & 0 & 0 & 1
\end{pmatrix} . \tag{A.1.11}
$$

It is reasonable to expect the matrix Δ to be in the form

$$
\Delta = \begin{pmatrix}
a_{11} P_{ij} + b_{11} Q_{ij} & a_{12} P_{ij} + b_{12} Q_{ij} & a_{13} k_i & a_{14} k_i \\
a_{21} P_{ij} + b_{21} Q_{ij} & a_{22} P_{ij} + b_{22} Q_{ij} & a_{23} k_i & a_{24} k_i \\
a_{31} k_j & a_{32} k_j & a_{33} & a_{34} \\
a_{41} k_j & a_{42} k_j & a_{43} & a_{44}
\end{pmatrix} . \tag{A.1.12}
$$

After expanding (A.1.10) and comparing terms with P_{ij}, Q_{ij} and k_i, we arrive at

$$
\Delta = \begin{pmatrix}
0 & \dfrac{1}{\epsilon_1^*}P_{ij} + \dfrac{\epsilon_3^*}{R^*}Q_{ij} & 0 & \dfrac{ic^2 k_i}{R^*} \\
\dfrac{1}{\epsilon_1}P_{ij} + \dfrac{\epsilon_3}{R}Q_{ij} & \dfrac{d_1^f}{|\epsilon_1|^2}P_{ij} + \dfrac{d_2^f|\epsilon_3|^2}{|R|^2}Q_{ij} & -\dfrac{ik_j}{R} & -\dfrac{ic^2 k_i d_2^f \epsilon_3}{|R|^2} \\
0 & \dfrac{ik_j}{R^*} & 0 & \dfrac{\epsilon_2^*}{R^*} \\
-\dfrac{ic^2 k_j}{R} & \dfrac{ic^2 k_j d_2^f \epsilon_3^*}{|R|^2} & \dfrac{\epsilon_2}{R} & \dfrac{c^4 k^2 d_2^f}{|R|^2}
\end{pmatrix} , \tag{A.1.13}
$$

where $R = \epsilon_2\epsilon_3 + c^2k^2$. From the matrix above, one identifies propagators for compressible NS:

$$G_0^{v_iv_j}(\boldsymbol{k},\omega) \equiv \langle v_iv_j \rangle_0 = \frac{d_1^f}{|\epsilon_1|^2}P_{ij} + d_2^f\left|\frac{\epsilon_3}{R}\right|^2 Q_{ij}\ , \quad G_0^{\phi\phi}(\boldsymbol{k},\omega) \equiv \langle \phi\phi \rangle_0 = \frac{c^4k^2}{|R|^2}d_2^f\ ,$$

$$G_0^{v_i'v_j}(\boldsymbol{k},\omega) \equiv \langle v_i'v_j \rangle_0 = \frac{1}{\epsilon_1^*}P_{ij} + \frac{\epsilon_3^*}{R^*}Q_{ij}\ , \qquad G_0^{\phi'\phi}(\boldsymbol{k},\omega) \equiv \langle \phi'\phi \rangle_0 = \frac{\epsilon_2^*}{R^*}\ ,$$

$$G_0^{v_i'\phi}(\boldsymbol{k},\omega) \equiv \langle v_i'\phi \rangle_0 = \frac{ic^2k_i}{R^*}\ , \qquad\qquad G_0^{v_i\phi}(\boldsymbol{k},\omega) \equiv \langle v_i\phi \rangle_0 = \frac{ic^2\epsilon_3k_i}{|R|^2}d_2^f\ ,$$

$$G_0^{v_i\phi'}(\boldsymbol{k},\omega) \equiv \langle v_i\phi' \rangle_0 = \frac{-ik_i}{R}\ ,$$

$$\text{(A.1.14)}$$

with their conjugated propagators. All other propagators are zero.

Percolation propagators

Propagators for the percolation model (4.1.8) are identical to model A, Eq. 1.3.29, with $\tilde{D} = 0$ and with τ being the deviation from the percolation criticality.

A.2 Vertices

Vertex (4.1.6)

By performing Fourier transformation (A.1.1) we obtain

$$V_1[\boldsymbol{v}',\boldsymbol{v}] = -\int d^dkd^dk'd^dk''\delta(\boldsymbol{k}+\boldsymbol{k}'+\boldsymbol{k}'')\ v_m'(\boldsymbol{k})v_n(\boldsymbol{k}')k_n''v_m(\boldsymbol{k}'').\qquad\text{(A.2.1)}$$

Variational differentiations then yields

$$\frac{\delta V_1[\phi',\phi,\boldsymbol{v}]}{\delta v_l(\boldsymbol{p})} = -\int d^dkd^dk''\ \delta(\boldsymbol{k}+\boldsymbol{p}+\boldsymbol{k}'')v_m'(\boldsymbol{k})ik_l''v_m(\boldsymbol{k}'')-\qquad\text{(A.2.2)}$$

$$-\int d^dkd^dk'\ \delta(\boldsymbol{k}+\boldsymbol{k}'+\boldsymbol{p})v_l'(\boldsymbol{k})v_n(\boldsymbol{k}')ip_n,\qquad\text{(A.2.3)}$$

$$\frac{\delta^2 V_1[\boldsymbol{v}',\boldsymbol{v}]}{\delta v_j(\boldsymbol{q})\delta v_l(\boldsymbol{p})} = -\int d^dk\ \delta(\boldsymbol{k}+\boldsymbol{p}+\boldsymbol{q})i\left(v_j'(\boldsymbol{k})q_l + v_l'(\boldsymbol{k})p_j\right),\qquad\text{(A.2.4)}$$

$$\frac{\delta^3 V_1[\boldsymbol{v}',\boldsymbol{v}]}{\delta v_i'(\boldsymbol{r})\delta v_j(\boldsymbol{q})\delta v_l(\boldsymbol{p})} = \underbrace{-i\left(\delta_{ij}q_l + \delta_{il}p_j\right)}_{V_{ijl}^{\text{cNS}}}\delta(\boldsymbol{r}+\boldsymbol{p}+\boldsymbol{q}),\qquad\text{(A.2.5)}$$

where the δ function ensures the momentum conservation at the vertex.

Vertex (4.1.7)

By performing Fourier transformation we obtain

$$V_2[\phi',\phi,\boldsymbol{v}] = -\int d^dkd^dk'd^dk''\delta(\boldsymbol{k}+\boldsymbol{k}'+\boldsymbol{k}'')\ \phi'(\boldsymbol{k})v_m(\boldsymbol{k}')ik_m''\phi(\boldsymbol{k})\ .\qquad\text{(A.2.6)}$$

Variational differentiations then yields

$$\frac{\delta^3 V_2[\phi',\phi,\boldsymbol{v}]}{\delta\phi'(\boldsymbol{r})\delta v_i(\boldsymbol{q})\delta\phi(\boldsymbol{p})} = \underbrace{-ip_i}_{V_i^{\text{cNS}}}\delta(\boldsymbol{r}+\boldsymbol{p}+\boldsymbol{q})\ .\qquad\text{(A.2.7)}$$

Vertex (4.1.12)

By performing Fourier transformation we obtain

$$V_3[\psi', \psi, \boldsymbol{v}] = -\int \mathrm{d}^d k \mathrm{d}^d k' \mathrm{d}^d k'' \delta(\boldsymbol{k} + \boldsymbol{k}' + \boldsymbol{k}'') \ \psi'(\boldsymbol{k})\{v_m(\boldsymbol{k}')k_m'' + a_0 k_m' v_m(\boldsymbol{k}')\}\psi(\boldsymbol{k}') \ .$$

(A.2.8)

Variational differentiations then yields

$$\frac{\delta^3 \mathrm{V}_3[\boldsymbol{v}', \boldsymbol{v}]}{\delta \psi'(\boldsymbol{r})\delta v_i(\boldsymbol{q})\delta \psi(\boldsymbol{p})} = \underbrace{-i(p_i + a q_i)}_{V_i^{\mathrm{Per}}} \delta(\boldsymbol{r} + \boldsymbol{p} + \boldsymbol{q}) \ .$$

(A.2.9)

Appendix B

Explicit form of Feynman diagrams

Feynman diagrams have been calculated by hand and the results have been checked using Mathematica. For the source code see this link.

B.1 Feynman diagrams for the compressible NS model

$$= (-ik_i c^2) \times \frac{\overline{S}_d(v-u)}{2du(u+v)^3} \left(\frac{\alpha g_1 m^{-y}}{y} + \frac{g_2 m^{-\varepsilon}}{\varepsilon} \right) \tag{B.1.1}$$

$$= (-ik_i c^2) \times \frac{-\overline{S}_d}{2du(u+v)^2} \left(\frac{\alpha g_1 m^{-y}}{y} + \frac{g_2 m^{-\varepsilon}}{\varepsilon} \right) \tag{B.1.2}$$

$$= (-ip_1 c^2) \times \frac{\overline{S}_d}{d(u+v)^3} \left(\frac{g_1 \alpha m^{-y}}{y} + \frac{g_2 m^{-\varepsilon}}{\varepsilon} \right) \tag{B.1.3}$$

$$= (-ik_i) \times \frac{\overline{S}_d(1-d)}{2d(1+u)(1+v)} \left(\frac{g_1 m^{-y}}{y} + \frac{g_2 m^{-\varepsilon}}{\varepsilon} \right) \tag{B.1.4}$$

$$= (-v\nu k^2) \times \frac{\overline{S}_d}{2dv} \left(\frac{d-1}{1+v} \left(\frac{g_1 m^{-y}}{y} + \frac{g_2 m^{-\varepsilon}}{\varepsilon} \right) + \tag{B.1.5} \right.$$

$$\left. + \frac{u-v}{u(u+v)^2} \left(\frac{\alpha g_1 m^{-y}}{y} + \frac{g_2 m^{-\varepsilon}}{\varepsilon} \right) \right) \tag{B.1.6}$$

$$= 0, \quad \text{(UV finite, proportional to } c^2) \tag{B.1.7}$$

$$\frac{1}{2} \qquad = (\nu^3 g_2 \delta_{ij}) \times \frac{\overline{S}_d(d-1)}{2du(1+u)} \left(\frac{\alpha g_1^2 m^{\varepsilon-2y}}{(2y-\varepsilon)g_2} + \frac{(\alpha+1)g_1 m^{-y}}{y} + \frac{g_2 m^{-\varepsilon}}{\varepsilon} \right) \tag{B.1.8}$$

$$= -\nu(\delta_{ij}k^2 - k_i k_j)I_\perp - u\nu k_1 k_2 I_\parallel \tag{B.1.9}$$

$$I_\perp = -\overline{S}_d \left(\frac{u^2 d(1-d) + u(8-2d-2d^2) - d(d+3)}{4d(d+2)(u+1)^2} \left(\frac{g_1 m^{-y}}{y} + \frac{g_2 m^{-\varepsilon}}{\varepsilon} \right) + \tag{B.1.10} \right.$$

$$\left. + \frac{(1-u)}{2du(1+u)^2} \left(\frac{\alpha g_1 m^{-y}}{y} + \frac{g_2 m^{-\varepsilon}}{\varepsilon} \right) \right) \tag{B.1.11}$$

$$I_\parallel = \frac{\overline{S}_d(d-1)}{2u} \frac{u^2(d-1) + u(d+4) + 1}{d(d+2)(u+1)^2} \left(\frac{g_1 m^{-y}}{y} + \frac{g_2 m^{-\varepsilon}}{\varepsilon} \right) \tag{B.1.12}$$

B.2   Diagrams for the DP model

$$\frac{1}{2} \quad = -\frac{g_3 \overline{S}_d}{8} \left(+i\Omega - Dp^2 \frac{d-2}{d} - 2D\tau \right) \frac{m^{-\varepsilon}}{\varepsilon}, \tag{B.2.1}$$

$$= \frac{\overline{S}_d a(a-1)}{2u(u+w)^2} (i\Omega - \tau D) \left(g_1 \alpha \frac{m^{-y}}{y} + g_2 \frac{m^{-\varepsilon}}{\varepsilon} \right) \tag{B.2.2}$$

$$+ Dp^2 \left(P \left(g_1 \frac{m^{-y}}{y} + g_2 \frac{m^{-\varepsilon}}{\varepsilon} \right) + Q \left(g_1 \alpha \frac{m^{-y}}{y} + g_2 \frac{m^{-\varepsilon}}{\varepsilon} \right) \right),$$

$$P = \frac{\overline{S}_d (1-d)}{2w(1+w)d}, \tag{B.2.3}$$

$$Q = \frac{\overline{S}_d}{2u(u+w)^2} \left(\frac{w-u}{dw} + \frac{a(a-1)w}{u+w} \left(\frac{4}{d} - \frac{u}{w} - 1 \right) \right), \tag{B.2.4}$$

$$= \lambda D \frac{(1-a)^2 \overline{S}_d}{2uw(u+w)} \left(\frac{\alpha g_1 m^{-y}}{y} + \frac{g_2 m^{-\varepsilon}}{\varepsilon} \right), \tag{B.2.5}$$
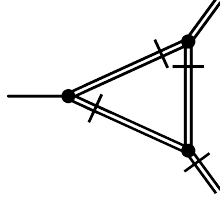
$$2 \quad = \lambda D \frac{-g_3 \overline{S}_d}{2} \frac{m^{-\varepsilon}}{\varepsilon}, \tag{B.2.6}$$

$$2 \quad = \lambda D \frac{a(a-1)\overline{S}_d}{u(u+w)^2} \left(\frac{\alpha g_1 m^{-y}}{y} + \frac{g_2 m^{-\varepsilon}}{\varepsilon} \right), \tag{B.2.7}$$

$$= -\lambda D \frac{a^2 \overline{S}_d}{2uw(u+w)} \left(\frac{\alpha g_1 m^{-y}}{y} + \frac{g_2 m^{-\varepsilon}}{\varepsilon} \right), \tag{B.2.8}$$
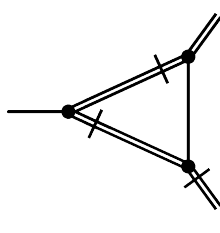
$$2 \quad = -\lambda D \frac{-g_3 \overline{S}_d}{2} \frac{m^{-\varepsilon}}{\varepsilon}, \tag{B.2.9}$$

$$2 \quad = -\lambda D \frac{a(a-1)\overline{S}_d}{u(u+w)^2} \left(\frac{\alpha g_1 m^{-y}}{y} + \frac{g_2 m^{-\varepsilon}}{\varepsilon} \right), \tag{B.2.10}$$
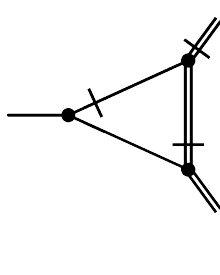
$$= (-i) \left(\frac{d(1-a)-3}{4da} aq_i - \frac{1}{2d} p_i \right) \overline{S}_d \frac{g_3 m^{-\varepsilon}}{\varepsilon}; \quad \psi(p), v_i(q), \qquad \text{(B.2.11)}$$

$$= \overline{S}_d \left(\frac{g_1 \alpha m^{-y}}{y} + \frac{g_2 m^{-\varepsilon}}{\varepsilon} \right) (-i)(p_i A + aq_i B); \quad \psi(p), v_i(q),$$

$$A = \frac{1}{2u(u+w)^2} \left(-\frac{1}{d} + a(a-1) + \frac{4wa(1-a)}{(u+w)d} \right),$$
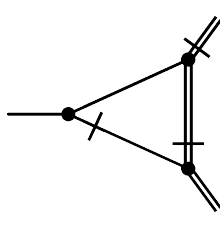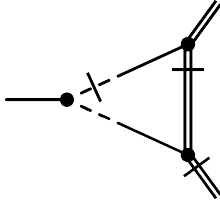
$$B = \frac{1}{2u(u+w)^2} \left(-\frac{1}{d} + a(a-1) + \frac{2w(1-a)}{(u+w)d} \right), \qquad \text{(B.2.12)}$$

$$= \overline{S}_d \left(\frac{g_1 \alpha m^{-y}}{y} + \frac{g_2 m^{-\varepsilon}}{\varepsilon} \right) (-i)(p_i C + aq_i D); \quad \psi(p), v_i(q),$$

$$C = \frac{1}{2du^2(u+w)^2} \left(\frac{wa(a-1)(5u+w)}{u+w} + \frac{3u+w}{2} \right),$$
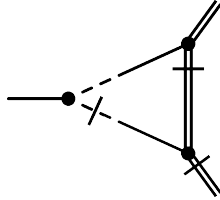
$$D = \frac{1}{2du^2(u+w)^2} \left(\frac{(2a-1)(3u+w)}{2} + \frac{(1-a)(7u^2+4uw+w^2)}{2(u+w)} \right),$$

$$\text{(B.2.13)}$$

$$= \overline{S}_d \left(\frac{g_1 \alpha m^{-y}}{y} + \frac{g_2 m^{-\varepsilon}}{\varepsilon} \right) (-i)(p_i E + aq_i F); \quad \psi(p), v_i(q),$$

$$E = \frac{1}{4du^2(u+w)} \left(-1 + \frac{2wa(1-a)}{u+w} \right),$$

$$F = \frac{1}{4du^2(u+w)} \left(\frac{(1-a)(u+3w)}{u+w} + 2a - 3 \right), \qquad \text{(B.2.14)}$$

$$= 0, \quad \text{(UV finite, proportional to } c^2 \text{)}, \qquad \text{(B.2.15)}$$

$$= 0, \quad \text{(UV finite, proportional to } c^2 \text{)}. \qquad \text{(B.2.16)}$$

Note.

In the whole section we denote $\overline{S}_d \equiv \frac{S_d}{(2\pi)^d}$, where $S_d = 2\pi^{d/2}/\Gamma(d/2)$ is the surface of d-dimensional unit sphere and we suppress the subscript "0" for the non-renormalized quantities.

Appendix C

Explicit results

C.1   Some formulas

Formulas from Tab. 4.5

$$A = 2\left(\alpha^2 + 7\alpha + 10\right)y^3 - 9(3\alpha + 8)y^2\varepsilon + 9(\alpha + 9)y\varepsilon^2 - 27\varepsilon^3, \tag{C.1.1}$$

$$B = -((\alpha + 2)y - 3\varepsilon)^2\left(4\left(5\alpha^2 + 14\alpha - 1\right)y^4 - 12\left(3\alpha^2 + 17\alpha + 1\right)y^3\varepsilon + \right.$$
$$\left. + 9(20\alpha + 3)y^2\varepsilon^2 + 54y\varepsilon^3 - 81\varepsilon^4\right), \tag{C.1.2}$$

$$C = 6((\alpha + 2)y - 3\varepsilon)^2, \tag{C.1.3}$$

$$D = \frac{y((20\alpha + 22)y - 3(3\alpha + 11)\epsilon)}{54((\alpha + 2)y - 3\varepsilon)}, \tag{C.1.4}$$

C.2   Renormalization constants

Renormalization constants for the compressible NS field

$$Z_1 = 1 + \frac{u^2 d(1 - d) + u(8 - 2d - 2d^2) - d(d + 3)}{4d(d + 2)(u + 1)^2}\left(\frac{g_1}{y} + \frac{g_2}{\varepsilon}\right) + \tag{C.2.1}$$

$$+ \frac{(1 - u)}{2du(1 + u)^2}\left(\frac{\alpha g_1}{y} + \frac{g_2}{\varepsilon}\right), \tag{C.2.2}$$

$$Z_2 = 1 + (1 - d)\frac{u^2(d - 1) + u(d + 4) + 1}{2d(d + 2)u(u + 1)^2}\left(\frac{g_1}{y} + \frac{g_2}{\varepsilon}\right), \tag{C.2.3}$$

$$Z_3 = 1 - \frac{1}{2vd}\left(\frac{d - 1}{1 + v}\left(\frac{g_1}{y} + \frac{g_2}{\varepsilon}\right) + \frac{u - v}{u(u + v)^2}\left(\frac{\alpha g_1}{y} + \frac{g_2}{\varepsilon}\right)\right) \tag{C.2.4}$$

$$Z_4 = 1 + \frac{d - 1}{2d(1 + u)(1 + v)}\left(\frac{g_1}{y} + \frac{g_2}{\varepsilon}\right), \tag{C.2.5}$$

$$Z_5 = 1, \tag{C.2.6}$$

$$Z_6 = 1 + \frac{1 - d}{4du(1 + u)}\left(\frac{\alpha g_1^2}{g_2(2y - \varepsilon)} + \frac{(\alpha + 1)g_1}{y} + \frac{g_2}{\varepsilon}\right), \tag{C.2.7}$$

Renormalization constants for the DP field

$$Z_7 = 1 + \frac{a(1-a)}{2u(u+w)^2}\left(\frac{\alpha g_1}{y} + \frac{g_2}{\varepsilon}\right) + \frac{1}{8}\frac{g_3}{\varepsilon}, \tag{C.2.8}$$

$$Z_8 = 1 + (P + \alpha Q)\frac{g_1}{y} + (P + Q)\frac{g_2}{\varepsilon} + R\frac{g_3}{\varepsilon}, \tag{C.2.9}$$

$$P = \frac{(1-d)}{2w(1+w)d}, \quad R = \frac{d-2}{8d}, \tag{C.2.10}$$

$$Q = \frac{1}{2u(u+w)^2}\left(\frac{w-u}{dw} + \frac{a(a-1)w}{u+w}\left(\frac{4}{d} - \frac{u}{w} - 1\right)\right), \tag{C.2.11}$$

$$Z_9 = 1 - \frac{a(a-1)}{2u(u+w)^2}\left(\frac{\alpha g_1}{y} + \frac{g_2}{\varepsilon}\right) + \frac{1}{4}\frac{g_3}{\varepsilon}, \tag{C.2.12}$$

$$Z_{10} = 1 - \left(\frac{(1-a)^2}{2uw(u+w)} + \frac{a(a-1)}{u(u+w)^2}\right)\left(\frac{\alpha g_1}{y} + \frac{g_2}{\varepsilon}\right) + \frac{1}{2}\frac{g_3}{\varepsilon}, \tag{C.2.13}$$

$$Z_{11} = 1 - \left(\frac{a^2}{2uw(u+w)} + \frac{a(a-1)}{u(u+w)^2}\right)\left(\frac{\alpha g_1}{y} + \frac{g_2}{\varepsilon}\right) + \frac{1}{2}\frac{g_3}{\varepsilon}, \tag{C.2.14}$$

$$Z_{12} = 1 + \frac{a(1-a)}{2u(u+w)^2}\left(\frac{\alpha g_1}{y} + \frac{g_2}{\varepsilon}\right) + \frac{3+d(a-1)}{4ad}\frac{g_3}{\varepsilon}, \tag{C.2.15}$$

C.3   Anomalous dimensions

Anomalous dimensions for the compressible NS field

$$\gamma_\phi = -\frac{3(g_1 + g_2)}{8(u+1)(v+1)}, \tag{C.3.1}$$

$$\gamma_{\phi'} = \frac{3(g_1 + g_2)}{8(u+1)(v+1)}, \tag{C.3.2}$$

$$\gamma_{g_1} = \frac{3(1-u)(\alpha g_1 + g_2)}{8u(u+1)^2} - \frac{(g_1 + g_2)(3u^2 + 8u + 7)}{8(u+1)^2}, \tag{C.3.3}$$

$$\gamma_{g_2} = \frac{3(1-u)(\alpha g_1 + g_2)}{8u(u+1)^2} - \frac{(g_1 + g_2)(3u^2 + 8u + 7)}{8(u+1)^2}, \tag{C.3.4}$$

$$+ \frac{3}{8u(u+1)}\left(\alpha\frac{g_1^2}{g_2} + (\alpha + 1)g_1 + g_2\right), \tag{C.3.5}$$

$$\gamma_u = \frac{(1-u)(\alpha g_1 + g_2)}{8u(u+1)^2} - \frac{(6u^3 + 7u^2 - 10u - 3)(g_1 + g_2)}{48u(u+1)^2}, \tag{C.3.6}$$

$$\gamma_v = \frac{3(g_1 + g_2)}{8v(v+1)} - \frac{(u-1)(\alpha g_1 + g_2)}{8u(u+1)^2} + \frac{(u-v)(\alpha g_1 + g_2)}{8uv(u+v)^2} - \tag{C.3.7}$$

$$- \frac{(3u^2 + 8u + 7)(g_1 + g_2)}{24(u+1)^2}, \tag{C.3.8}$$

$$\gamma_\nu = \frac{(3u^2 + 8u + 7)(g_1 + g_2)}{24(u+1)^2} + \frac{(u-1)(\alpha g_1 + g_2)}{8u(u+1)^2}, \tag{C.3.9}$$

$$\gamma_c = -\frac{3(g_1 + g_2)}{16(u+1)(v+1)}, \tag{C.3.10}$$

$$\tag{C.3.11}$$

Anomalous dimensions for the DP field

$$\gamma_\psi = \left(\frac{(a-1)a}{2u(u+w)^2} + \frac{2a-1}{2uw(u+w)} \right) (\alpha g_1 + g_2) - \frac{g_3}{8}, \tag{C.3.12}$$

$$\gamma_{\psi'} = \left(\frac{(a-1)a}{2u(u+w)^2} + \frac{1-2a}{2uw(u+w)} \right) (\alpha g_1 + g_2) - \frac{g_3}{8}, \tag{C.3.13}$$

$$\gamma_{g_3} = \left(\frac{3(a-1)a}{2u(u+w)^2} + \frac{2(a-1)a+1}{2uw(u+w)} - \frac{4(a-1)auw + u^2 - w^2}{4uw(u+w)^3} \right) \times$$
$$\times (\alpha g_1 + g_2) - \frac{3(g_1+g_2)}{4w(w+1)} - \frac{3g_3}{4}, \tag{C.3.14}$$

$$\gamma_w = \left(\frac{u^2 - (1-2a)^2 w^2}{8uw(u+w)^3} + \frac{1-u}{8u(u+1)^2} \right) (\alpha g_1 + g_2) +$$
$$+ \left(\frac{3}{8w(w+1)} - \frac{3u^2 + 8u + 7}{24(u+1)^2} \right) (g_1 + g_2) + \frac{g_3}{16}, \tag{C.3.15}$$

$$\gamma_a = \frac{(1-2a)g_3}{16a}, \tag{C.3.16}$$

$$\gamma_D = \frac{(u^2 - (1-2a)^2 w^2)}{8uw(u+w)^3} (\alpha g_1 + g_2) + \frac{3(g_1+g_2)}{8w(w+1)} + \frac{g_3}{16}, \tag{C.3.17}$$

$$\gamma_\tau = \frac{((1-2a)^2 w^2 - u^2)}{8uw(u+w)^3} (\alpha g_1 + g_2) - \frac{3(g_1+g_2)}{8w(w+1)} - \frac{3g_3}{16}. \tag{C.3.18}$$

C.4 Beta functions

C.4.1 Beta functions for compressible NS

$$\beta_{g_1} = -g_1 \left(y + \frac{3(1-u)(\alpha g_1 + g_2)}{8u(u+1)^2} - \frac{(3u^2 + 8u + 7)(g_1+g_2)}{8(u+1)^2} \right), \tag{C.4.1}$$

$$\beta_{g_2} = -g_2 \left(\varepsilon + \frac{3(1-u)(\alpha g_1 + g_2)}{8u(u+1)^2} - \frac{(3u^2 + 8u + 7)(g_1+g_2)}{8(u+1)^2} + \right.$$
$$\left. + \frac{3\left(\frac{\alpha g_1^2}{g_2} + (\alpha+1)g_1 + g_2 \right)}{8u(u+1)} \right), \tag{C.4.2}$$

$$\beta_u = -u \left(\frac{(1-u)(\alpha g_1 + g_2)}{8u(u+1)^2} - \frac{(6u^3 + 7u^2 - 10u - 3)(g_1+g_2)}{48u(u+1)^2} \right), \tag{C.4.3}$$

$$\beta_v = -v \left(\left(\frac{3}{v(v+1)} - \frac{3u^2 + 8u + 7}{3(u+1)^2} \right) \frac{(g_1+g_2)}{8} + \right.$$
$$\left. + \left(\frac{u-v}{v(u+v)^2} - \frac{u-1}{(u+1)^2} \right) \frac{(\alpha g_1 + g_2)}{8u} \right). \tag{C.4.5}$$

The limit $\alpha \to \infty$

Introducing $g_1' = \alpha g_1$, beta functions are found

$$\beta_{g_1'}|_{\alpha \to \infty} = \alpha \beta_{g_1}|_{\alpha \to \infty}^{g_1 \to g_1'/\alpha} = -g_1'\left(y + \frac{3(1-u)\,(g_1'+g_2)}{8u(u+1)^2} - \frac{(3u^2+8u+7)\,g_2}{8(u+1)^2}\right), \quad \text{(C.4.6)}$$

$$\beta_{g_2}|_{\alpha \to \infty}^{g_1 \to g_1'/\alpha} = -g_2\left(\varepsilon + \frac{3(1-u)\,(g_1'+g_2)}{8u(u+1)^2} - \frac{(3u^2+8u+7)\,g_2}{8(u+1)^2} + \frac{3\,(g_1'+g_2)}{8u(u+1)}\right), \quad \text{(C.4.7)}$$

$$\beta_u|_{\alpha \to \infty}^{g_1 \to g_1'/\alpha} = -u\left(\frac{(1-u)\,(g_1'+g_2)}{8u(u+1)^2} - \frac{(6u^3+7u^2-10u-3)\,g_2}{48u(u+1)^2}\right), \quad \text{(C.4.8)}$$

$$\beta_v|_{\alpha \to \infty}^{g_1 \to g_1'/\alpha} = -v\left(\left(\frac{3}{v(v+1)} - \frac{3u^2+8u+7}{3(u+1)^2}\right)\frac{g_2}{8} + \right. \quad \text{(C.4.9)}$$

$$\left. + \left(\frac{u-v}{v(u+v)^2} - \frac{u-1}{(u+1)^2}\right)\frac{(g_1'+g_2)}{8u}\right). \quad \text{(C.4.10)}$$

The limits $u \to \infty$

In order to perform this limit we preform a substitution $u = 1/t$ and then take the limit $t \to 0$. Beta functions are then

$$\beta_{g_1}|_{t \to 0}^{u \to 1/t} = -g_1\left(y - \frac{3}{8}(g_1+g_2)\right), \quad \text{(C.4.11)}$$

$$\beta_{g_2}|_{t \to 0}^{u \to 1/t} = -g_2\left(\varepsilon - \frac{3}{8}(g_1+g_2)\right), \quad \text{(C.4.12)}$$

$$\beta_t|_{t \to 0} = -t^2 \beta_u|_{t \to 0}^{u \to 1/t} = 0, \quad \text{(C.4.13)}$$

$$\beta_v|_{t \to 0}^{u \to 1/t} = \frac{(v^2+v-3)\,(g_1+g_2)}{8(v+1)}. \quad \text{(C.4.14)}$$

$$\text{(C.4.15)}$$

The limit $v \to \infty$

The limit $v \to \infty$ affects only the β_v function. In order to perform this limit we substitute again make $v = 1/f$ which changes the beta function as

$$\beta_f|_{f \to 0} = -f^2 \beta_v|_{f \to 0}^{v \to 1/f} = 0. \quad \text{(C.4.16)}$$

$$\text{(C.4.17)}$$

C.4.2 Beta functions for DP

$$\beta_{g_3} = -g_3 \left(\varepsilon + \left(\frac{3(a-1)a}{2u(u+w)^2} + \frac{2(a-1)a+1}{2uw(u+w)} - \frac{4(a-1)auw+u^2-w^2}{4uw(u+w)^3} \right) \times \right. \tag{C.4.18}$$

$$\left. \times (\alpha g_1 + g_2) - \frac{3(g_1+g_2)}{4w(w+1)} - \frac{3g_3}{4} \right), \tag{C.4.19}$$

$$\beta_w = -w \left(\left(\frac{u^2-(1-2a)^2w^2}{8uw(u+w)^3} + \frac{1-u}{8u(u+1)^2} \right) (\alpha g_1 + g_2) + \right. \tag{C.4.20}$$

$$\left. + \left(\frac{3}{8w(w+1)} - \frac{3u^2+8u+7}{24(u+1)^2} \right)(g_1+g_2) + \frac{g_3}{16} \right). \tag{C.4.21}$$

$$\beta_a = g_3 \frac{2a-1}{16} \tag{C.4.22}$$

The limit $\alpha \to 0$ in FPII^c

$$\beta_{g_3} = -g_3 \left(\varepsilon - \frac{4y}{3w(w+1)} - \frac{3}{4}g_3 \right), \tag{C.4.23}$$

$$\beta_w = \frac{16(w^2+w-2)y - 3g_3w(w+1)}{48(w+1)}, \tag{C.4.24}$$

$$\beta_a - \text{does not change.} \tag{C.4.25}$$

The limit $u \to \infty$ in FPII^c

$$\beta_{g_3} = -g_3 \left(\varepsilon - \frac{3(g_1+g_2)}{4w(w+1)} - \frac{3g_3}{4} \right), \tag{C.4.26}$$

$$\beta_w = -\frac{w}{8} \left(\left(\frac{3}{w(w+1)} - 1 \right)(g_1+g_2) + \frac{g_3}{2} \right), \tag{C.4.27}$$

$$\beta_a - \text{does not change.} \tag{C.4.28}$$

The limit $w \to \infty$ in FPII^c

$$\beta_{g_3}|_{m\to 0}^{w\to 1/m} = -g_3 \left(\varepsilon - \frac{3}{4}g_3 \right), \tag{C.4.29}$$

$$\beta_m|_{m\to 0} = -m^{-2}\beta_w|_{m\to 0}^{w\to 1/m} = 0, \tag{C.4.30}$$

$$\beta_a - \text{does not change.} \tag{C.4.31}$$

Bibliography

[1] P. A. M. Dirac. "The quantum theory of the electron". In: *Proc. R. Soc. A* 117.778 (1928), pp. 610–624. ISSN: 1364-5021. URL: http://rspa.royalsocietypublishing.org/content/117/778/610.

[2] J. Zinn-Justin. *Quantum field theory and critical phenomena*. Vol. 85. Clarendon, 1993, pp. 1–996. ISBN: 9780198509233. DOI: 10.1093/acprof:oso/9780198509233.001.0001..

[3] D. V. Bogoliubov, N. N. Shirkov. *Introduction to the theory of quantized fields*. Interscience Publishers, 1959. ISBN: 0470086130.

[4] K. G. Wilson. "Renormalization group and critical phenomena. I. Renormalization group and the Kadanoff scaling picture". In: *Physical Review B* 4.9 (1971), pp. 3174–3183. ISSN: 01631829. DOI: 10.1103/PhysRevB.4.3174.

[5] K. G. Wilson. "Renormalization group and critical phenomena. II. Phase-space cell analysis of critical behavior". In: *Physical Review B* 4.9 (1971), pp. 3184–3205. ISSN: 01631829. DOI: 10.1103/PhysRevB.4.3184.

[6] P. C. Martin, E. D. Siggia, and H. A. Rose. "Statistical dynamics of classical systems". In: *Physical Review A* 8.1 (1973), pp. 423–437. ISSN: 10502947. DOI: 10.1103/PhysRevA.8.423.

[7] C. De Dominicis. "Techniques De Renormalisation De La Théorie Des Champs Et Dynamique Des Phénomènes Critiques". In: *Le Journal de Physique Colloques* 37.C1 (1976), pp. C1–247–C1–253. ISSN: 0449-1947. DOI: 10.1051/jphyscol:1976138.

[8] H. W. Wyld. "Formulation of the theory of turbulence in an incompressible fluid". In: *Annals of Physics* 14 (1961), pp. 143–165. ISSN: 0003-4916. DOI: 10.1016/0003-4916(61)90056-2.

[9] D. Forster, D. R. Nelson, and M. J. Stephen. "Long-time tails and the large-eddy behavior of a randomly stirred fluid". In: *Physical Review Letters* 36.15 (1976), pp. 867–870. ISSN: 00319007. DOI: 10.1103/PhysRevLett.36.867.

[10] D. Forster, D. R. Nelson, and M. J. Stephen. "Large-distance and long-time properties of a randomly stirred fluid". In: *Physical Review A* 16.2 (1977), pp. 732–749. ISSN: 10502947. DOI: 10.1103/PhysRevA.16.732.

[11] C. De Dominicis and P. C. Martin. "Energy spectra of certain randomly-stirred fluids". In: *Physical Review A* 19.1 (1979), pp. 419–422. ISSN: 10502947. DOI: 10.1103/PhysRevA.19.419.

[12] L. T. Adzhemyan, N. V. Antonov, and A. N. Vasiliev. *The Field Theoretic Renormalization Group in Fully Developed Turbulence*. 1. CRC Press, 1999, p. 208. ISBN: 9789056991456.

[13]   M. Doi. "Stochastic theory of diffusion-controlled reaction". In: *Journal of Physics
        A: Mathematical and General* 9.9 (1976), pp. 1479–1495. ISSN: 0305-4470. DOI: 10.
        1088/0305-4470/9/9/009.

[14]   L. Peliti. "Path integral approach to birth-death processes on a lattice". In: *Journal
        de Physique* 46.9 (1985), pp. 1469–1483. ISSN: 0302-0738. DOI: 10.1051/jphys:
        019850046090146900.

[15]   H.-K. Janssen et al. "Lévy-flight spreading of epidemic processes leading to perco-
        lating clusters". In: *The European Physical Journal B* 7.1 (1999), pp. 137–145. ISSN:
        1434-6028. DOI: 10.1007/s100510050596.

[16]   U. C. Täuber. *Critical Dynamics: A Field Theory Approach to Equilibrium and
        Non-Equilibrium Scaling Behavior.* Cambridge University Press, 2014. DOI: 10.
        1017/CBO9781139046213.

[17]   N. Sarkar. "Active-to-absorbing-state phase transition in an evolving population
        with mutation". In: *Physical Review E - Statistical, Nonlinear, and Soft Matter
        Physics* 92.4 (2015), p. 42110. ISSN: 15502376. DOI: 10.1103/PhysRevE.92.042110.

[18]   N. V. Antonov and A. S. Kapustin. "Effects of turbulent mixing on critical behaviour
        in the presence of compressibility: renormalization group analysis of two models".
        In: *Journal of Physics A: Mathematical and Theoretical* 43.40 (2010), p. 405001.
        ISSN: 1751-8113. DOI: 10.1088/1751-8113/43/40/405001.

[19]   N. V. Antonov, A. S. Kapustin, and A. V. Malyshev. "Effects of turbulent transfer on
        critical behavior". In: *Theoretical and Mathematical Physics* 169.1 (2011), pp. 1470–
        1480. ISSN: 00405779. DOI: 10.1007/s11232-011-0123-x.

[20]   N. V. Antonov et al. "Directed percolation process in the presence of velocity fluc-
        tuations: Effect of compressibility and finite correlation time". In: *Physical Review
        E - Statistical, Nonlinear, and Soft Matter Physics* 93.1 (2016), p. 12151. ISSN:
        15502376. DOI: 10.1103/PhysRevE.93.012151.

[21]   N. V. Antonov, M. Y. Nalimov, and A. A. Udalov. "Renormalization group in the
        problem of fully developed turbulence of a compressible fluid". In: *Theoretical and
        Mathematical Physics* 110.3 (1997), pp. 305–315. ISSN: 1573-9333. DOI: 10.1007/
        BF02630456.

[22]   A. N. Vasilev. *The Field Theoretic Renormalization Group in Critical Behavior
        Theory and Stochastic Dynamics.* Chapman Hall/CRC, Boca Raton, FL, 2004. DOI:
        10.1201/9780203483565.

[23]   U. C. Täuber, M. Howard, and B. P. Vollmayr-Lee. "Applications of Field-Theoretic
        Renormalization Group Methods to Reaction-Diffusion Problems". In: *Journal of
        Physics A: Mathematical and General* 38.February 2008 (2005), R79–R129. ISSN:
        0305-4470. DOI: 10.1088/0305-4470/38/17/R01.

[24]   T. Lancaster and S. J. Blundell. *Quantum Field Theory for the Gifted Amateur.*
        Oxford university press, 2014. ISBN: 9780199699339.

[25]   M. Hnatič, J. Honkonen, and T. Lučivjanský. "Advanced field-theoretical meth-
        ods in stochastic dynamics and theory of developed turbulence". In: *Acta Physica
        Slovaca* 66.2 (2016), pp. 69–264. ISSN: 0323-0465. arXiv: 1611.06741.

[26]   N. G. Van Kampen. *Stochastic processes in Physics and Chemistry.* North-Holland,
        1984. ISBN: 9780444529657.

[27] L. D. Landau, E. M. Lifšic, and L. P. Pitaevskij. *Statistical physics*. Pergamon, 1996. ISBN: 9780750626361. DOI: SKUSNAJSTDOI.

[28] D. J. Amit. *Field Theory; The Renormalization Group and Critical Phenomena*. World Scientific Publishing Company, 2005. ISBN: 978-981-256-109-1.

[29] N Goldenfeld. *Lectures on Phase Transitions and the Renormalization Group*. Vol. 85. Addison-Wesley, 1992, p. 258. ISBN: 0201554097.

[30] C. G. Bollini and J. J. Giambiagi. "Dimensional Renormalization: The number of dimensions as a regularizing parameter". In: *Il Nuovo Cimento* 12.1 (1972), pp. 20–26. ISSN: 1826-9877. DOI: 10.1007/BF02895558.

[31] G. t'Hooft. "Dimensional Regularization and the Renormalization Group". In: *Nuclear Physics B61* 61 (1973), pp. 455–468. ISSN: 0550-3213. DOI: 10.1016/0550-3213(73)90376-3.

[32] H.-K. Janssen. "On a Lagrangean for classical field dynamics and renormalization group calculations of dynamical critical properties". In: *Zeitschrift für Physik B Condensed Matter and Quanta* 23.4 (1976), pp. 377–380. ISSN: 0340224X. DOI: 10.1007/BF01316547.

[33] M. Hnatič, J. Honkonen, and T. Lučivjanský. "Field-theoretic technique for irreversible reaction processes". In: *Physics of Particles and Nuclei* 44.2 (2013), pp. 316–348. ISSN: 1531-8559. DOI: 10.1134/S1063779613020160.

[34] B. P. Lee and J. Cardy. "Renormalization group study of the $A + A \to \emptyset$ diffusion-limited reaction". In: *Journal of Statistical Physics* 80.5-6 (1995), pp. 971–1007. ISSN: 0022-4715. DOI: 10.1007/BF02179861.

[35] M. Henkel, H. Hinrichsen, and S. Lübeck. *Non-Equilibrium Phase Transitions: Volume 1-Absorbing Phase Transitions*. Springer, 2008. ISBN: 978-1-4020-8765-3. DOI: 10.1007/978-1-4020-8765-3.

[36] P. Grassberger and A. De La Torre. "Reggeon Field Theory (Schlogl's First Model) on a Lattice: Monte Carlo Calculations of Critical Behaviour". In: *Annals of Physics* 396.2 (1979), pp. 373–396. ISSN: 0003-4916. DOI: 10.1016/0003-4916(79)90207-0.

[37] J. F. F. Mendes, R. Dickman, and M. Henkel. "Generalized scaling for models with multiple absorbing states". In: *Journal of Physics A:* 27.9 (1994), pp. 3019–3028. ISSN: 0305-4470, 1361-6447. DOI: 10.1088/0305-4470/27/9/017.

[38] H.-K. Janssen and U. C. Täuber. "The field theory approach to percolation processes". In: *Annals of Physics* 315.1 (2005), pp. 147–192. ISSN: 00034916. DOI: 10.1016/j.aop.2004.09.011.

[39] F. Van Wijland. "Field theory for reaction-diffusion processes with hard-core particles". In: *Physical Review E - Statistical, Nonlinear, and Soft Matter Physics* 63.2 I (2001), pp. 0221011–0221014. ISSN: 15393755. DOI: 10.1103/PhysRevE.63.022101.

[40] J. L. Cardy and R. L. Sugar. "Directed percolation and Reggeon field theory". In: *Journal of Physics A: Mathematical and General* 13.12 (1980), p. L423. ISSN: 0305-4470. DOI: 10.1088/0305-4470/13/12/002.

[41] H.-K. Janssen. "Survival and percolation probabilities in the field theory of growth models". In: *Journal of Physics: Condensed Matter* 17.20 (2005), S1973–S1993. ISSN: 0953-8984. DOI: 10.1088/0953-8984/17/20/021.

[42] G. Lemoult et al. "Directed percolation phase transition to sustained turbulence in Couette flow". In: *Nature Physics* 12.March (2016), pp. 254–258. ISSN: 1745-2473. DOI: 10.1038/nphys3675.

[43] M. Sano and K. Tamai. "A Universal Transition to Turbulence in Channel Flow". In: *Nature Physics* 12.March (2016), pp. 249–254. ISSN: 1745-2473. DOI: 10.1038/NPHYS3659.

[44] P. Rupp, R. Richter, and I. Rehberg. "Critical exponents of directed percolation measured in spatiotemporal intermittency." In: *Physical review. E, Statistical, nonlinear, and soft matter physics* 67.3 Pt 2 (2003), p. 036209. ISSN: 1063-651X. DOI: 10.1103/PhysRevE.67.036209.

[45] K. A. Takeuchi et al. "Directed Percolation Criticality in Turbulent Liquid Crystals". In: *Physical Review Letters* 99.23 (2007), p. 234503. ISSN: 0031-9007. DOI: 10.1103/PhysRevLett.99.234503.

[46] G. K. Batchelor. *An Introduction to Fluid Dynamics*. Cambridge University Press, 1967. ISBN: 0-521-66396-2. DOI: 10.1063/1.3060769.

[47] L. D. Landau and E. M. Lifshitz. *Fluid Mechanics: Landau and Lifshitz: Course of Theoretical Physics, Volume 6*. zv. 6. Elsevier Science, 1987, pp. 84–88. ISBN: 0-08-033932-8.

[48] L. D. Landau and E. M. Lifshitz. *Theory of Elasticity*. Pergamon, 1980. ISBN: 9780750626330.

[49] G. G. Stokes. "On the theories of the internal friction of cluids in motion". In: *Transactions of the Cambridge Philosophical Society* 8 (1845), pp. 287–305. URL: https://books.google.se/books?id=tQYFAAAAQAAJ.

[50] U. Frisch. *Turbulence: the legacy of A.N. Kolmogorov*. Cambridge University Press, 1995. ISBN: 9780521457132.

[51] A. N. Kolmogorov. "The local structure of turbulence in incompressible viscous fluid for very large Reynolds numbers". In: *Proceedings of the Royal Society of London. Series A-Mathematical and Physical Sciences* 434.1890 (1991), pp. 9–13. ISSN: 1364-5021. DOI: 10.1098/rspa.1991.0075.

[52] L. F. Richardson. *Weather prediction by numerical methods*. Cambridge Mathematical Library. Cambridge University Press, 1922. ISBN: 9780521680448. URL: https://archive.org/details/weatherpredictio00richrich.

[53] K. R. Sreenivasan. "On the universality of the Kolmogorov constant". In: *Physics of Fluids* 7.11 (1995), pp. 2778–2784. ISSN: 10706631. DOI: 10.1063/1.868656.

[54] A. S. Monin and A. M. Yaglom. *Statistical Fluid Mechanics Volume 1*. MIT Press, 1971, p. 769. ISBN: 978-0-486-45883-0.

[55] S. Banerjee. "Compressible turbulence in space and strophysical plasmas: Analytical approach and in-situ data analysis for the solar wind". Theses. Université Paris Sud - Paris XI, 2014. URL: https://tel.archives-ouvertes.fr/tel-01087024.

[56] P. Sagaut and C. Cambon. *Homogeneous Turbulence Dynamics*. Cambridge University Press, 2008, p. 481. ISBN: 9780521855488. DOI: 10.1017/CBO9780511546099.

[57] M. J. Lighthill. "On Sound Generated Aerodynamically. I. General Theory". In: *Proceedings of the Royal Society A: Mathematical, Physical and Engineering Sciences* 211.1107 (1952), pp. 564–587. ISSN: 1364-5021. DOI: 10.1098/rspa.1952.0060.

[58] S. Galtier and S. Banerjee. "Exact relation for correlation functions in compressible isothermal turbulence". In: *Physical Review Letters* 107.13 (2011), p. 134501. ISSN: 00319007. DOI: 10.1103/PhysRevLett.107.134501.

[59] A. G. Kritsuk et al. "The Statistics of Supersonic Isothermal Turbulence". In: *Apj* 665.1 (2007), pp. 0–0. ISSN: 0004-637X. DOI: 10.1086/519443.

[60] C. Federrath et al. "Comparing the statistics of interstellar turbulence in simulations and observations: Solenoidal versus compressive turbulence forcing". In: *Astronomy and Astrophysics* 512 (2010), p. 28. ISSN: 0004-6361. DOI: 10.1051/0004-6361/200912437.

[61] L. T. Adzhemyan, M. Y. Nalimov, and M. M. Stepanova. "Renormalization-group approach to the problem of the effect of compressibility on the spectral properties of developed turbulence". In: *Theoretical and Mathematical Physics* 104.2 (1995), pp. 971–979. ISSN: 15739333. DOI: 10.1007/BF02065977.

[62] D. Porter, A. Pouquet, and P. Woodward. "Measures of intermittency in driven supersonic flows". In: *Physical Review E - Statistical, Nonlinear, and Soft Matter Physics* 66.2 (2002), p. 26301. ISSN: 15393755. DOI: 10.1103/PhysRevE.66.026301.

[63] N. V. Antonov. "Renormalization group, operator product expansion and anomalous scaling in models of turbulent advection". In: *Journal of Physics A: Mathematical and General* 39.25 (2006), p. 7825. DOI: 10.1088/0305-4470/39/25/S04.

[64] R. Kraichnan. "Small-Scale Structure of a Scalar Field Convected by Turbulence". In: *Physics of Fluids* 11.5 (1968), p. 945. ISSN: 00319171. DOI: 10.1063/1.1692063.

[65] N. V. Antonov. "Anomalous scaling regimes of a passive scalar advected by the synthetic velocity field". In: *Phys. Rev. E* 60.6 (1999), pp. 6691–6707. ISSN: 1063651X. DOI: 10.1103/PhysRevE.60.6691.

[66] L. T. Adzhemyan, N. V. Antonov, and A. N. Vasil'ev. "Infrared divergences and the renormalization group in the theory of fully developed turbulence". In: *Zhurnal Eksperimentalnoi i Teoreticheskoi Fiziki* 95 (1989), pp. 1272–1278. URL: http://jetp.ac.ru/cgi-bin/dn/e_068_04_0733.pdf.

[67] D. Y. Volchenckov and M. Y. Nalimov. "Corrections to fully developed turbulent spectra due to compressibility of the fluid". In: *Theoretical and Mathematical Physics* 106.3 (1996), pp. 307–318. ISSN: 0040-5779. DOI: 10.1007/BF02071475.

[68] I. Staroselsky et al. "Long-time, large-scale properties of a randomly stirred compressible fluid". In: *Physical Review Letters* 65.2 (1990), pp. 171–174. ISSN: 00319007. DOI: 10.1103/PhysRevLett.65.171.

[69] N. V. Antonov and M. M. Kostenko. "Anomalous scaling in magnetohydrodynamic turbulence: Effects of anisotropy and compressibility in the kinematic approximation". In: *Physical Review E - Statistical, Nonlinear, and Soft Matter Physics* 92.5 (2015), p. 53013. ISSN: 15502376. DOI: 10.1103/PhysRevE.92.053013.

[70] N. V. Antonov et al. "Turbulent compressible fluid: Renormalization group analysis, scaling regimes, and anomalous scaling of advected scalar fields". In: *Physical Review E - Statistical, Nonlinear, and Soft Matter Physics* 95.3 (2017). ISSN: 15502376. DOI: 10.1103/PhysRevE.95.033120.

[71] L. T. Adzhemyan et al. "Improved ε expansion for three-dimensional turbulence: Two-loop renormalization near two dimensions". In: *Physical Review E - Statistical, Nonlinear, and Soft Matter Physics* 71.3 (2005), p. 36305. ISSN: 15393755. DOI: 10.1103/PhysRevE.71.036305.